7-2020

Phenotypic Plasticity of Japanese Medaka Gill in Response to Changing Salinities

Laura V. Ellis
University of Arkansas, Fayetteville

Phenotypic Plasticity of Japanese Medaka Gill in Response to Changing Salinities

A dissertation submitted in partial fulfillment
of the requirements for the degree of
Doctor of Philosophy in Biology

by

Laura V. Ellis
University of North Carolina Asheville
Bachelor of Science in Ecology and Evolutionary Biology 2014
Appalachian State University
Master of Science in Biological Sciences, 2016

July 2020
University of Arkansas

This dissertation is approved for recommendation to the Graduate Council.

_____
Christian Tipsmark, Ph.D.
Chair

_____
Mack Ivey, Ph.D.
Committee Member

_____
Steven Beaupre, Ph.D.
Committee Member

_____
Wayne Kuenzel, Ph.D.
Committee Member

Abstract

Japanese medaka (*Oryzais latipes*) are euryhaline fish, meaning they are capable of surviving in a variety of salinities from fresh water to seawater. The ability to maintain an internal osmotic concentration stems from the phenotypic plasticity of the osmoregulatory organs, the gill, kidney, intestine, and integument. The gill is the main site of osmotic and ionic regulation in fish due to the three-dimensional structure, the direct contact with the outside environment, and the composition of the gill cells. Fish gills are multifunctional as they regulate water movement, acid/base exchange, nitrogenous waste excretion, and ion fluctuations. In freshwater environments, fish are challenged with a passive osmotic gain and ion loss. While the reverse is true in seawater, with passive ion gain and osmotic water loss. Salinity changes and the endocrine system drive regulation of cell type composition and activity.

This dissertation focuses on the Japanese medaka, osmotic regulation patterns in response to salinity fluctuations. Investigation into regulatory patterns of gill aquaporins and claudins were measured in response to exposure to freshwater, seawater, and ion poor water. Hormone *in vitro* experiments were conducted to understand the effects of prolactin and cortisol on the regulation of aquaporin 1 and aquaporin 3 in the gill. Function and regulation of claudin 30c within the gill in response to salinity was investigated and preliminary experiments for a loss of function study was conducted.

Aquaporin 3 was significantly increased in initial ion poor water exposure. Hormone studies demonstrated the stimulatory effect of prolactin on aquaporin 3, both alone and in combination with cortisol. Aquaporin 1 remained constitutively expressed in all salinities and under hormone exposure. Claudin 30C mRNA was significantly increased in response to ion poor water conditions, and protein expression significantly decreased in seawater versus fresh

water. Localization studies showed claudin 30C in the tight junctions of hatchling medaka skin. The work performed in this thesis shows the regulatory patterns of osmoregulatory proteins in medaka, which will aid functional studies within other vertebrate system, as well as show that medaka are a suitable knock down model.

Acknowledgements

To my parents, you have always believed in my dreams, no matter how crazy or long term they may be. You taught me that I can do anything I want in life and I cannot thank you both enough for your support and love. I would not be here without you.

To Gary, thank you for believing in me enough to survive four very long years, eight hours apart. You may never know how much it means to me that we made it through all of this. The long drives were terrible, but this is why we did it. Now we get to have mail to Dr Ellis and Mr Pandolfi and I'm so excited for this next chapter.

To Dr. Steffen Madsen, thank you for being the expert I needed, the push to work those very long days in the lab, and the reason behind my largest publication. I cannot thank you enough for all that you have taught me.

To my lab mates, Julie Starling and Dr. Rebecca Bollinger. To say I wouldn't have survived without you both is an understatement. From long coffee chats about grad school, to teaching me all the techniques you knew, to hours spent in the fish room, I would not be writing this without you both.

To Dr. Sue Edwards, you may not have been my advisor this time around, but you are the guiding example I set for becoming a professor, researcher, and a woman of science. I can't thank you enough for pushing me during my Masters, this set me up for my PhD in ways I never knew.

To Dr. Christian Tipsmark, thank you for taking a chance on the very excited girl who loves science. You have allowed me to grow into a better scientist, learn about things I thought I would never understand, and guided me through countless research endeavors.

Table of Contents

List of Figures

Arrows marks aspartic acids (D55 and D64), found to be important for cation and water pore function of CLDN15 (Günzel and Fromm, 2012; Günzel and Yu, 2013; Alberini et al., 2018; Samanta et al., 2018). Mouse CLDN3 has been classified as a barrier protein and included as a reference. Sequences used: Human CLDN15: Acc. No. NP_001172009; Mouse CLDN15: Acc. No. NP_068365; Mouse CLDN3: NP_034032; Medaka Cldn15a: XP_004079873; Medaka Cldn15b: XP_004076514; Zebrafish Cldn15a: NP_956698; Zebrafish Cldn15b: NP_001035404……125

List of Published Chapters

Chapter Two:

Ellis, L. V., Bollinger, R. J., Weber, H. M., Madsen, S. S., & Tipsmark, C. K. (2019). Differential Expression and Localization of Branchial AQP1 and AQP3 in Japanese Medaka (Oryzias latipes). *Cells*, *8*(5), 422.

Supplemental:

Tipsmark, C.K., Nielsen, A.M., Bossus, M.C., Ellis, L.V., Baun, C., Andersen, T.L., Dreier, J., Brewer, J.R. & Madsen, S.S., 2020. Drinking and water handling in the medaka intestine: A possible role of claudin-15 in paracellular absorption?. *International Journal of Molecular Sciences*, *21*(5), p.18

Chapter 1 Introduction

1.1 Medaka

Japanese medaka (*Oryzias latipes*) are small fish found predominately in rice patties across Asia (Whittbrodt et al., 2002; Iwamatsu 2004; Shima and Mitani, 2004; Naruse et al., 2004). The medaka, which in Japanese means tiny fish with big eyes, is a common fish in Japan and now genomic studies (Whittbrodt et al., 2002). Since the beginning of the 2000s, medaka has shown itself as a suitable model for diverse biological studies (Sakamoto et al., 2001; Kirchmaier et al., 2015). They are an ideal laboratory fish as they breed readily in captivity, have a fully sequenced genome, transparent embryos, and can be used with genetic tools such as morpholino and CRISPR/ Cas9 (Sakamoto et al., 2001; Kasahara et al., 2007; Kirchmaier et al., 2015). Medaka have been used in a range of studies to investigate ontogenesis, toxicology, osmoregulation (Gray and Metcalfe, 1999; Sakamoto et al., 2001; Bossus et al., 2015; Bossus et al., 2017; Zimmer et al., 2019); and are an ideal organism to study vertebrate osmoregulation due to their euryhaline capabilities (Sakamoto et al., 2001).

1.2 Euryhaline Fish

Euryhaline teleost fish have maintained their ability to exist and thrive in a range of salinities, ranging from dilute to highly concentrated. These fluctuations in salinity can be tidal or seasonal, with unique challenges associated with both types of environments. Euryhaline fish maintain an internal osmotic concentration of 300-350 mOsm while freshwater (FW) is around 1 mOsm, seawater (SW) is 1050mOsm (Evans et al., 2005; McCormick et al., 2013, Bossus et al., 2015). In SW, fish are challenged with a hyperosmotic environment and passively gain ions and lose water (Figure 1.1). Conversely in dilute hypoosmotic environments, such as FW, fish face passive ion loss and water gain (Figure 1.1). The ability to live in varying environments stems

from the plasticity of the main osmoregulatory organs, the gills, intestine, and the kidney (Evans, 2008).

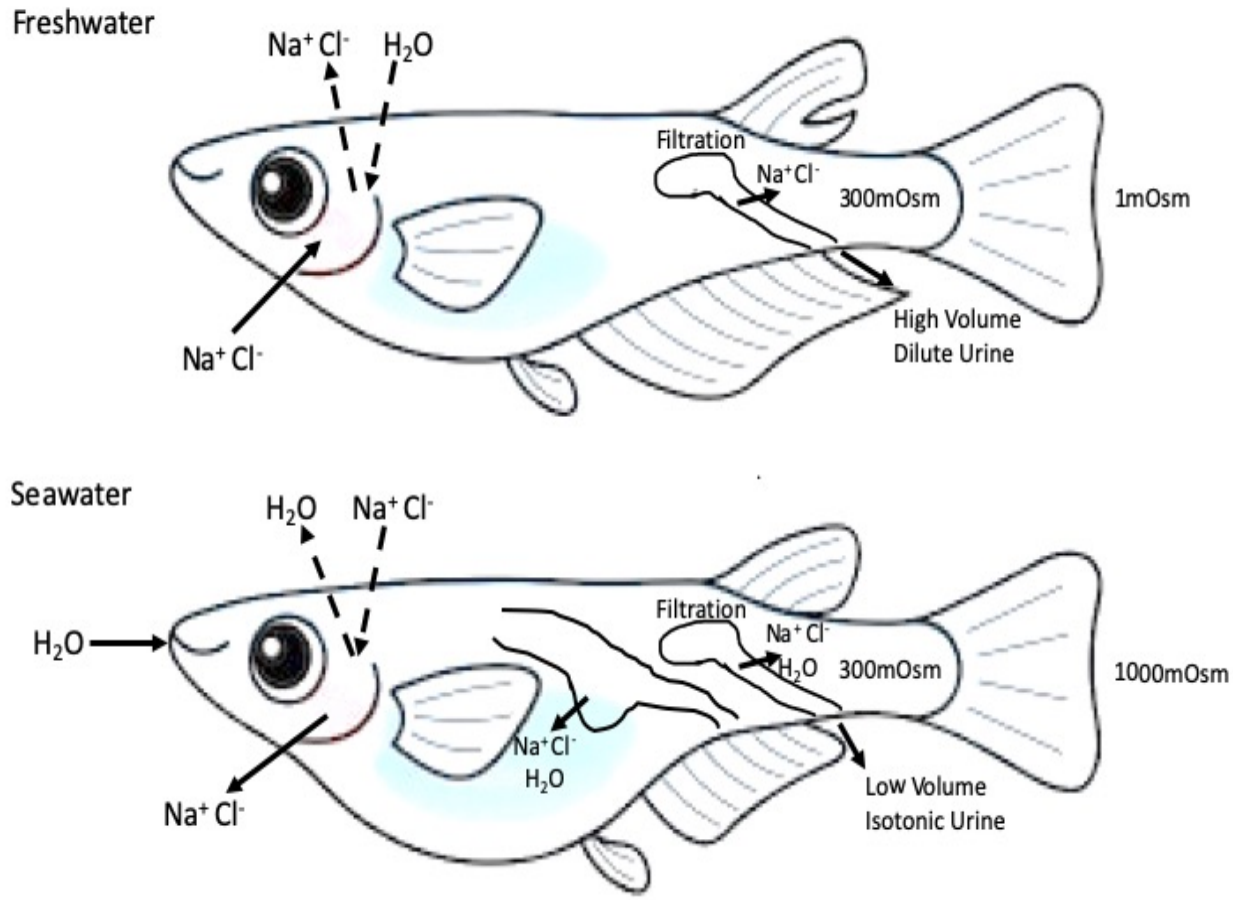

Figure 1.1 Movement of water and ions in freshwater (FW) and seawater (SW) fish (adapted from Evans 2008). Passive movement denoted by hatched arrows, while active movement is denoted by solid arrows. FW fish actively take up ions at the gill, reabsorb ions from the primary filtrate in the kidney and produce large amount of dilute urine, while passively losing ions and gaining water at the gills. SW fish actively drink water, excrete monovalent ions at the gill, absorb ions and water in the intestine and rid divalent ions in the kidney, and produce small amounts of isotonic urine, while passively gaining ions and losing water at the gills.

1.3 Gill Function

The gills of teleost fish are ideally adapted to allow the movement of gases, ions, and nitrogenous waste from the internal to external environments and vice versa (Evans et al. 2005). The gill is a multidimensional structure with high vascularization and organization to facilitate the movement of ions and waste. The paired cartilaginous gill arches have filaments extending perpendicular to them with vascularized lamellae extending off the filaments. The blood flow moves counter current to the water flow. The surface area of an adult fish is comprised 90% of the gill, which directly interacts with the external water.

The gill is composed of several cell types, pavement, pillar, mitochondrion-rich, accessory, mucous, and neuroepithelial cells (Edwards 2000) (Figure 1.2). Mucous cells are localized throughout the gill and secrete mucous (Edwards 2000). Neuroepithelial cells are localized along the edge of the gill and have been theorized to be involved in osmosensing (Zachar and Jonz 2012). Pavement and pillar cells, are found on the lamellae of the fish gills and are primarily involved in gas exchange (Wilson and Laurent, 2002; Evans et al., 2005). Mitochondrion Rich Cells, MRCs have an abundance of mitochondria that supply the necessary ATP to support active ionic secretion pathways (Evans et al. 2005). Accessory cells form junctions with MRC's and these are regulated to either allow or disallow ion movement (Laurent and Dunel 1980; Evans et al., 2005). MRCs and accessory cells are localized to the filament on the fish gill (Evans et al., 2005).

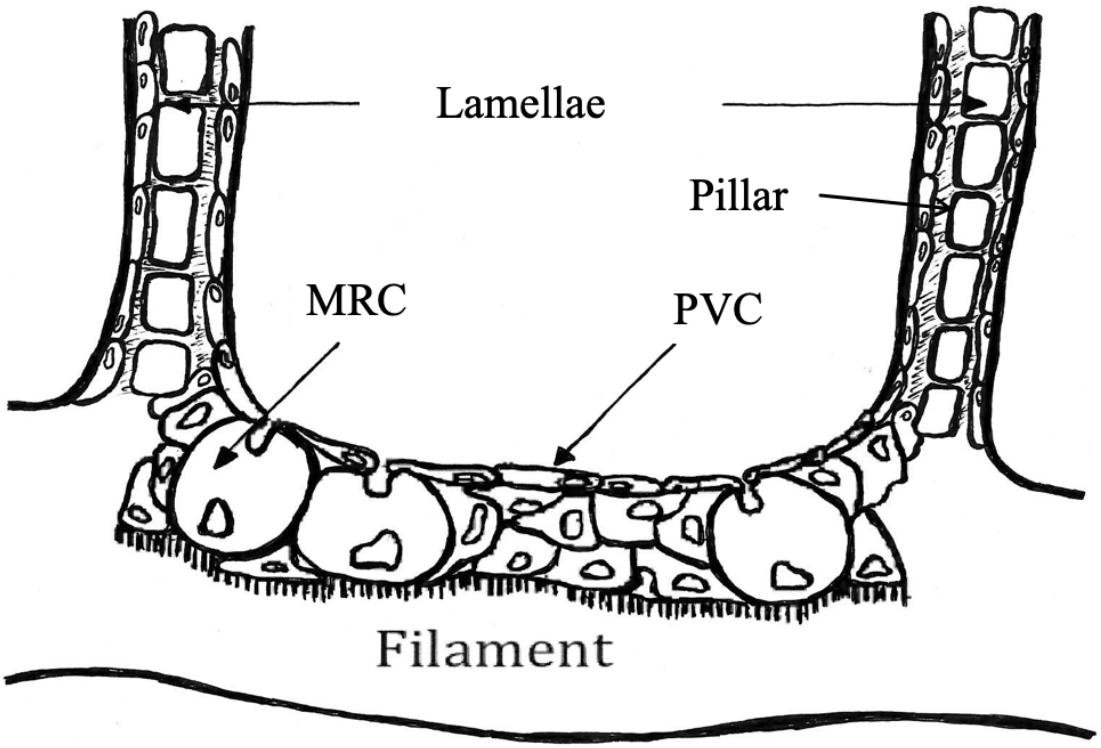

Figure 1.2 Cell types within the fish gill filament and lamellae. Pavement cells (PVC) and mitochondrion-rich cells (MRC) are localized to the filament, while pillar and PVCs are found on the lamellae (Adapted from Edwards 2000).

1.3.1 Gill Ion Transporters

The active transport of ions, sodium, potassium, chloride, and calcium, occurs across the fish gill via specialized transporters. These transporters include Na^+,K^+-ATPase, NKA, Na^+,K^+,$2Cl^-$ cotransporter, NKCC, Epithelial Calcium Channel, ECaC, H^+ ATPase, HAT, Na^+/H^+ exchanger, NHE, and the chloride channel Cystic Fibrosis Transmembrane conductance Regulator, CFTR (Evans et al., 2005; Edwards and Marshall, 2013; Brix et al., 2015; Catches et al., 2006). NKA plays a pivotal role in the regulation and maintenance of ionic homeostasis. NKA is responsible for moving three sodium ions out of the cell in exchange for two potassium ions into the cell while using one ATP (Evans et al., 2005). In salmonids and tilapia, NKA isoforms and

enzymatic activity change depend on the environment the fish gill is exposed to, NKAα1a isoform is found predominately in FW adapted fish, while NKAα1b isoform is predominately found in SW adapted fish (Richards et al., 2003; Tipsmark et al., 2011). The regulatory switch mechanism between the isoforms is still being investigated and appear only to occur in some euryhaline fish species, apparently not including medaka (Bollinger et al., 2015). NKCC is a SW ion transporter found in MRC's in the fish gill and transports one Na^+, one K^+ and two Cl^- from the internal environment across the cell membrane into the cell and thus utilize the NKA generated Na^+ gradient to conduct chloride transport from the serosa to the cytosol (Hiroi and McCormick, 2007). CFTR is located apically on the MRC in SW adapted fish and allows the movement of Cl^- out into the external environment (Evans et al., 2005; Evans 2010). ECaC is located apically on the FW MRC in the gill and is responsible for uptake of Ca^{2+} from the external environment. HAT is a catalytic pump that moves H^+ ions out into the surrounding waters, which helps create the acidic boundary layer found around freshwater adapted fish gills (Scott et al., 2005, Claiborne et al., 1999). NHE is an electrical neutral exchanger, which exchanges H^+ ions for the uptake of Na^+ (Edwards et al., 2005).

In medaka there are multiple types of MRCs, which are specified by their function and the ion transporters localized to them (Figure 1.3). In all named MRC types, there is a basolateral NKA, maintaining the Na^+ gradient and cell membrane potential. In FW MRCs there are three predominant cell types, which are named for the ion transporter specifically localized to them. The NCC cell, named after the apical sodium chloride transporter, is coupled with both a basolateral NKA, and HAT, which are catalytic exchangers and pumps (Hsu et al. 2014). The NCC cells are responsible for predominately Na^+ and Cl^- movement, from the external

environment into the blood (Hsu et al. 2014). The ECaC cell is named after the apical calcium channel, facilitating the movement of calcium across the cell. The NHE cell in FW medaka has a large complex of transporters and exchangers localized in its membranes, including the removal pathway of the metabolic waste product ammonia. Apically there is an NHE and a Rhesus Glycoprotein C paralog, which are theorized to aid in the movement of ammonia and ammonium waste out of the cell. Localized on the basolateral membrane in addition to NKA, there are an NKCC, an anion exchanger (AE), which exchanges HCO3- for Cl- , and the Rhesus Glycoprotein B paralog.

In SW, the MRC is one singular type that interacts with the adjacent accessory cell. The SW type cell has apical CFTR, NHE, and rhesus glycoprotein C, while the basolateral membrane has NKA, NKCC, and the rhesus glycoprotein b paralog. The SW type cell is responsible for NaCl secretion, fighting the passive ion gain due to the external environment. The basolateral Na^+ gradient maintained by the NKA drives the secretion of Cl^- across the apical membrane coupled with paracellular Na^+ extrusion.

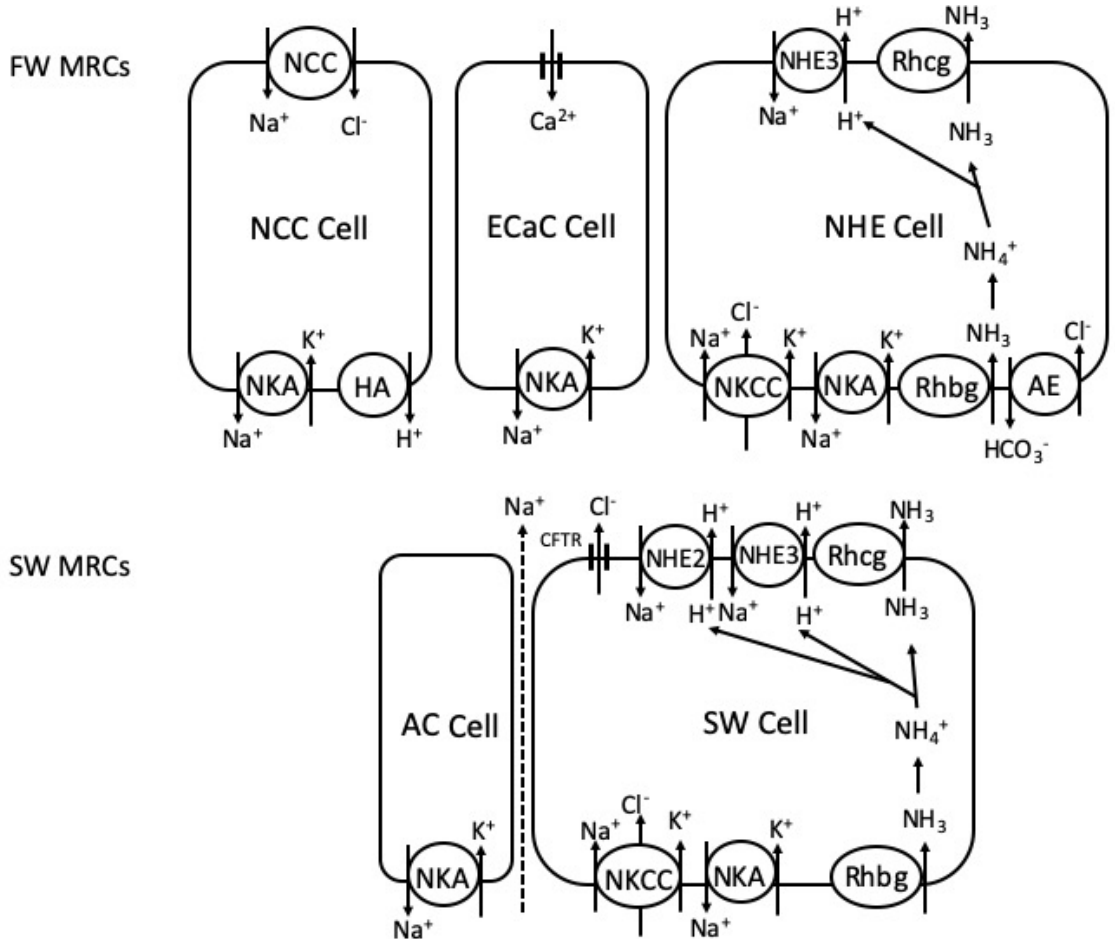

Figure 1.3 Proposed model of Freshwater (FW) and seawater (SW) type cells in the medaka gill (Adapted from Hsu et al. 2014). FW Mitochondria Rich Cells, MRCs, are Sodium Chloride Cotransporter (NCC), Epithelial Calcium Channel (ECaC) cells, and Sodium Hydrogen Exchanger (NHE) cells, named based on the transporters localized to their membranes. SW MRC and accessory cells (AC) form junctions and the paracellular and transcellular movement of ions is shown with associated transporters.

1.3.2 Tight Junctions within the Gill

The tight junction (TJ) complex between epithelial cells is composed of four types of proteins, claudins, occludins, tricellulins, and junctional adhesion molecules (Kwong and Perry, 2013; Günzel and Yu, 2013) (Figure 1.4). These four proteins form a complex that acts as a barrier to regulate the paracellular movement of solutes and water (Chasiotis et al., 2012). Each protein varies in function and location, claludins and occludins form the bridge to close the gap between

cells, while claudins can specifically form or seal pores to regulate ions (Chasiotis et al., 2012; Rosenthal et al., 2020). Zonula Occludens 1 (ZO1) is a member of the tight junction associated domain proteins, which bind to actin to anchor the tight junctions within the cell (Günzel and Yu, 2013).

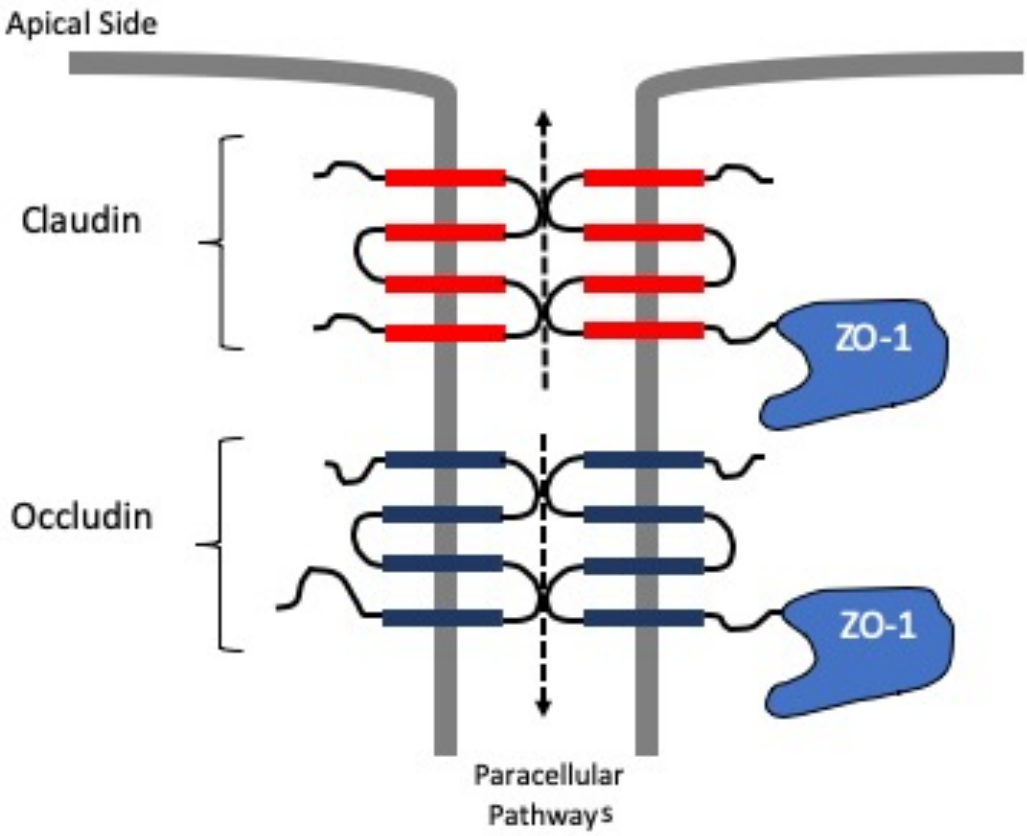

Figure 1.4 The proposed model of tight junctions between epithelial gill cells and the proteins associated with the formation and signaling of the cellular pathways (adapted from Chasiotis et al. 2012). Claudin and occludin proteins span the intracellular space and regulate the paracellular pathway. Zonula Occludens 1 (ZO-1) anchors the tight junction to the cytoskeleton.

The composition, structure, and permeability of the TJs change depending upon environmental salinity (Sardet et al., 1979; Chasiotis et al., 2012). In SW, the tight junction is shallow between accessory cells and MRCs and considered “leaky” as increased permeability across the gill

epithelium is linked to the movement of Na^+. The deeper TJs between MRCs and accessory cells and pavement cells are not as leaky (Chasiotis et al., 2012). The permeability of the TJ complex can aid in the ionic regulation when challenged with salinity fluctuations (Gilmour and Perry 2018).

1.3.3 Aquaporins

In addition to ion transporters in the membranes, there are other associated proteins that aid in regulation of osmotic and ionic homeostasis. Aquaporins, AQPs, are integral plasma membrane proteins that form water pores responsible for the regulation and movement of water (Ishibashi et al. 2009; Madsen et al. 2015). In the gills AQPs are capable of movement of water on both the mucosal and serosal sides of the cells. Japanese medaka have 11 paralogs of AQPs, compared to 13 mammalian paralogs (Madsen et al. 2014). Two AQPs are localized to the gill and found in highest abundance, AQP1 and AQP3, and are theorized to play a role in branchial water homeostasis (Madsen et al. 2014). AQP1 is a water selective aquaporin, while AQP3 is an aquaglyceroporin, which are capable of transporting glycerol and urea as well as water (Ishibashi et al. 2009).

The earliest report of aquaporins in fish was the isolation of aqp3ab from European eel and when exposed to SW, expression levels decreased within the gill (Cutler and Cramb 2000). Since this discovery, AQP3 has been studied and a decrease in expression due to SW exposure has been seen in European seabass, Mozambique tilapia, Atlantic salmon, to name a few (Watanabe et al., 2005; Giffard-Mena et al., 2007; Tipsmark et al., 2009). The regulation pattern of AQP1 and its paralogs are varied, some fish such as Atlantic salmon have aqp1aa and aqp1ab and aqp1aa is downregulated upon SW acclimation while aqp1ab increases (Tipsmark et al. 2010). Aquaporins

play a key role in cell volume regulation as well as osmotic homeostasis, and metalloid homeostasis (Ishibashi et al., 2009). Transcellular pathways for water movement on the superficial layer of the gill epithelium would be detrimental to osmotic homeostasis and thus it may be expected that apical permeability and aquaporin abundance would be low while basolateral aquaporins could safeguard cell volume (Ellis et al., 2019).

1.4 Intestine

The intestine of the medaka is organized with an esophagus, anterior, and posterior intestine. Medaka are agastric, meaning they lack a defined stomach for the degradation of food. The role of the intestine is absorption and secretion of water, nutrients, and ions. In FW the intestines regulate ion absorption and digestion, while conversely in SW the intestine is reabsorbing water from drinking (Madsen et al., 2014). Absorption of Na^+ and Cl^- across the intestinal epithelium is driven by the apical NKCC and basolateral NKA and creates the osmotic drive for compensatory water uptake (Marshall and Grossel, 2005; Esbaugh and Cutler, 2016). Water uptake in the posterior section of the SW intestine is partially driven by the drop is osmolality associated with precipitation of Ca^{2+} and Mg^{2+} carbonates (Marshall and Grossel, 2005).

1.5 Kidney

The kidney of the medaka is essential for filtration of the blood, reuptake of essential nutrients, and regulation of blood pressure and ion composition (Marshall and Grossel, 2005). The teleost kidney is composed of nephrons, with either glomerular filtration or aglomerular secretion, and are the basic unit of the kidney. Teleost fish kidneys lack a Loop of Henle, which means they are incapable of the generation of hypertonic urine (Marshall and Grossel, 2005). In FW the kidneys

are responsible for the generation of large amounts of highly dilute urine, to combat the passive water gain. In SW, the kidney produces isotonic urine in small quantities to limit water loss while specifically excreting divalent ions.

1.6 Integument

The larval fish skin is capable of osmoregulation and have been extensively used as a model for gill function (Marshall and Bellamy, 2010). The larval integument of medaka are highly vascularized and contain MRCs, meaning it is capable of compensatory ion transport sufficient during this stage. The yolk sac has been shown to have NCC cells similar to the gill (Marshall and Bellamy, 2010). Hatchling medaka have NCC, NKA, HAT, ECaC, CFTR and NHE transporters on their epithelium, demonstrating the ability to regulate ion concentrations without the use of the gill (Hsu et al. 2014). If the hatched medaka embryos are subjected to salinity challenges during development, varying expression patterns of transporters on the epithelium are observed associated with typical gill expression patterns in salinity challenges (Hsu et al. 2014). Developing larvae are thus capable of both gas exchange and ion transport across the yolk sac epithelium before the gill develop and become functional (Marshall and Grossel, 2005).

1.7 Endocrine System's Role in Osmotic and Ionic Regulation

The endocrine system is a series of organs associated through either direct neuronal contact or loosely associated through the blood stream, that regulates osmotic and ionic homeostasis through the release of hormones. It includes the anterior pituitary, posterior pituitary, gastrointestinal tract, gonads, hypothalamus, thyroid gland, and pancreas (Hill, Wyse, and Anderson, 2012). The hormones secreted by endocrine glands affect not only the release of other

hormones, but also impact the salinity tolerance of the fish (McCormick et al. 2005) as well as other key components of their physiology.

Endocrine factors prolactin, growth hormone (GH), insulin-like growth factor 1 (IGF-1), and cortisol all have effects on the regulation of ionic and osmotic homeostasis (Figure 5). Prolactin is considered the FW adapting hormone; it can both decrease the amount of secretory MRCs, as well as increase attributes that lead to an increase in ion uptake (Takei and McCormick, 2013). Increased amount of prolactin leads to the decrease in IGF-1 in the liver, which decreases salt secretion (Manzon, 2002; McCormick, 2001). GH and IGF-1, are intrinsically linked due to GH causing the release of endocrine IGF-1 from the liver.

In SW, increased GH levels cause an increase in circulating and localized production of IGF-1 (Takei and McCormick, 2013). IGF-1 stimulates an increase in NKA activity in the gill directly, which can aid in SW adaptation. Increased levels of GH receptors in key osmoregulatory organs in euryhaline fishes, as well as high affinity IGF-1 receptors, could be partially responsible for the ability to adjust with salinity changes (Tipsmark et al., 2007; Breves et al., 2010).

Cortisol can play multiple roles within the gill to aid in adjusting to both FW and SW. Cortisol can act synergistically with prolactin to increase the stimulatory effect of prolactin to aid in FW acclimation (Ellis et al., 2019). Other studies have shown the addition of cortisol blocks the effect of prolactin (Breves et al., 2016). Cortisol can also aid in SW adjustment as it interacts with GH and IGF-1 to promote salt excretion. Cortisol and GH combined increases salinity tolerance as well as gill NKA activity, which is a synergistic potentiation, meaning a greater magnitude than either of the hormones on their own.

1.7.1 Endocrine Regulation of Ion Transporters

The endocrine system and hormones play direct roles in the regulation of specific ion transporters (Figure 1.5). GH and IGF-1 specifically increase NKAα1b, NKCC, and CFTR, which are all found in higher abundance in SW acclimated fish (Edwards and Marshall, 2013). Prolactin has been shown to decrease the transcription of liver IGF1 and increase ion uptake MRCs (McCormick 2001; Tipsmark and Madsen, 2009). Cortisol has the ability to increase ion uptake or secretion, dependent upon fish species. Additionally, in some species a FW paralog, NKAα1a are upregulated by prolactin, while NKAα1b isoforms are downregulated (Takei and McCormick, 2013; Tipsmark and Madsen, 2009; Tipsmark et al., 2011).

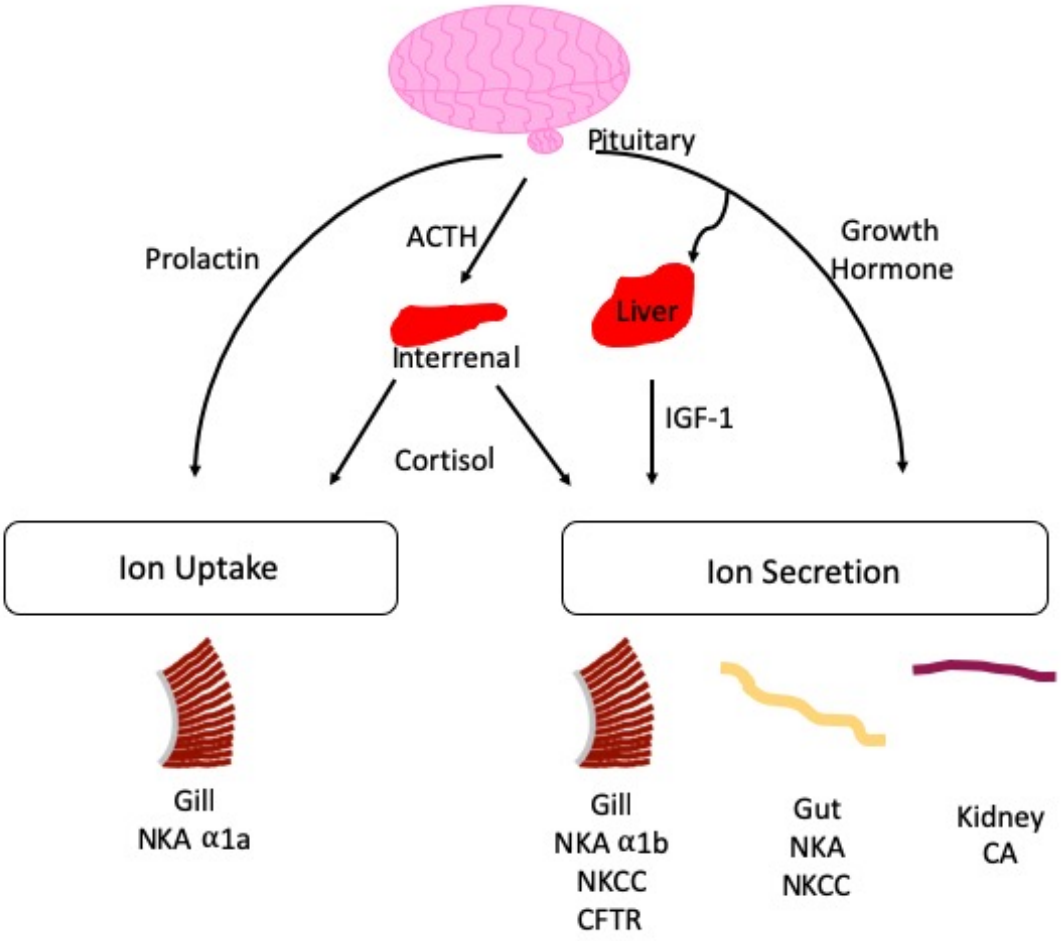

Figure 1.5 The endocrine system's role in ion regulation, though the activated cascade from the pituitary down to osmoregulatory organs (Adapted from Takei and McCormick 2012). Endocrine factors, prolactin, cortisol, IGF-1, and growth hormone are responsible for the regulation of ion uptake and secretion in multiple organs associated with osmotic and ionic regulation. Prolactin stimulates the sodium potassium ATPase (NKA) α1a isoform. The pituitary secretes Adrenocorticotropic hormone (ACTH) to stimulate the release of cortisol, which directly affect NKAα1b expression in the gill. Growth hormone and insulin like growth factor 1 (IGF-1) lead to ion secretion, stimulating gill NKAα1b, sodium potassium chloride cotransporter (NKCC) and cystic fibrosis transmembrane conductance regulator (CFTR), Gut NKA and NKCC, and kidney carbonic anhydrase (CA).

1.8 Synopsis

Teleost fish have a fascinating physiology while being a valuable alternative model for biological and biomedical research. The osmoregulatory organs have similar genes to humans and can be easily used to understand physiological systems. Euryhaline Japanese medaka, in

particular, are ideal vertebrate osmoregulatory model animals as the plasticity of their transport epithelia in response to salinity changes can be extensively studied. In comparison to other model species, these fish are easy to maintain, rear, and keep in the laboratory, while being cost effective. Japanese medaka are a useful tool in the pursuit in the understanding of how vertebrate systems can be regulated, fluctuate, and respond to a variety of stressors.

1.9 Dissertation Outline

This dissertation follows research on mechanisms within the gill of Japanese medaka *(Oryzais latipes*) which allow for osmotic and ionic homeostasis during salinity pressures. Chapter 2 characterizes the differences between aquaporin 1 and aquaporin 3, which are key water pores involved in the regulation of water transport within the gill. Chapter 3 investigates the role of claudin 30c with in the gill in response to changing salinities and the localization within the gill.

1.10 References

Bollinger, R.J., S.S. Madsen, M.C. Bossus, and C.K. Tipsmark. 2016. Does Japanese medaka ++ (Oryzias latipes) exhibit a gill Na /K -ATPase isoform switch during salinity change? Journal of Comparative Physiology B-Biochemical Systemic and Environmental Physiology. 186:485-501.

Bossus, M.C., S.S. Madsen, and C.K. Tipsmark. 2015. Functional dynamics of claudin expression in Japanese medaka (Oryzias latipes): Response to environmental salinity. Comparative Biochemistry and Physiology. Part A, Physiology. 187:74-85.

Bossus, M.C., R.J. Bollinger, P.J. Reed, and C.K. Tipsmark. 2017. Prolactin and cortisol regulate branchial claudin expression in Japanese medaka. General and Comparative Endocrinology. 240:77-83. 21

Breves, J.P., S. Watanabe, T. Kaneko, T. Hirano, and E.G. Grau. 2010. Prolactin restores branchial mitochondrion-rich cells expressing Na^+/Cl^- cotransporter in hypophysectomized Mozambique tilapia. American Journal of Physiology-Regulatory Integrative and Comparative Physiology. 299:R702-R710.

Breves, J.P.; McCormick, S.D.; Karlstrom, R.O. Prolactin and teleost ionocytes: New insights into cellular and molecular targets of prolactin in vertebrate epithelia. *Gen. Comp. Endocrinol.* 2014, *203*, 21–28, doi:10.1016/j.ygcen.2013.12.014.

Breves, J.; Inokuchi, M.; Yamaguchi, Y.; Seale, A.P.; Hunt, B.; Watanabe, S.; Lerner, D.; Kaneko, T., Grau, G. Hormonal regulation of aquaporin 3: Opposing actions of prolactin and cortisol in tilapia gill. *J. Endocrinol.* 2016, doi:10.1530/JOE-16-0162.

Brix KV, Esbaugh AJ, Mager EM, Grosell M (2015). Comparative evaluation of Na+ uptake in Cyprinodon variegatus variegatus (Lacepede) and Cyprinodon variegatus hubbsi (Carr)(Cyprinodontiformes, Teleostei): Evaluation of NHE function in high and low Na+ freshwater. Comp Biochem Phys A 185: 115-124. Doi:10.1016/j.cbpa.2015.04.002

Catches JS, Burns JM, Edwards SL, Claiborne JB (2006) Na+/H+ antiporter, V-H+- ATPase and Na+/K+-ATPase immunolocalization in a marine teleost (Myoxocephalus octodecemspinosus). Journal of Experimental Biology 209(17): 3440-3447.

Chasiotis, H., D. Kolosov, P. Bui, and S.P. Kelly. 2012. Tight junctions, tight junction proteins and paracellular permeability across the gill epithelium of fishes: A review. Respiratory Physiology & Neurobiology. 184:269-281.

Claiborne, J.B., Blackston, C.R., Choe, K.P., Dawson, D.C., Harris, S.P., Mackenzie, L.A. and Morrison-Shetlar, A.I., 1999. A mechanism for branchial acid excretion in marine fish: identification of multiple Na+/H+ antiporter (NHE) isoforms in gills of two seawater teleosts. *Journal of Experimental Biology*, *202*(3), pp.315-324.

Cutler, C.P.; Cramb, G. Branchial expression of an aquaporin 3 (AQP-3) homologue is downregulated in the European eel *Anguilla anguilla* following seawater acclimation. *J. Exp. Biol.* 2002, *205*, 2643–2651, doi:0022-0949.Edwards, S.L. (2000). Identification of NHEs in the gills of fishes. Doctoral Dissertation, Deakin University, Geelong Victoria, Australia.

Edwards SL, Wall BP, Morrison-Shetlar A, Sligh S, Weakley JC, Claiborne JB. (2005) The effect of environmental hypercapnia and salinity on the expression of NHE-like isoforms in the gills of a euryhaline fish (Fundulus heteroclitus). J Exp Zool 303A(6) : 464–475. doi:10.1002/jez.a.175

Edwards, S.L., and W.S. Marshall. 2013. Euryhaline Fishes: Principles and Patterns of Osmoregulation and Euryhalinity in Fishes. Elsevier. 1-44 pp.

Ellis, L.V., Bollinger, R.J., Weber, H.M., Madsen, S.S. and Tipsmark, C.K., 2019. Differential Expression and Localization of Branchial AQP1 and AQP3 in Japanese Medaka (Oryzias latipes). *Cells*, *8*(5), p.422.

Esbaugh, A.J. and Cutler, B., 2016. Intestinal Na+, K+, 2Cl− cotransporter 2 plays a crucial role in hyperosmotic transitions of a euryhaline teleost. *Physiological reports*, *4*(22), p.e13028.

Evans, D.H. 2002. Cell signaling and ion transport across the fish gill epithelium. Journal of Experimental Zoology. 293:336-347.

Evans, D.H. 2008. Teleost fish osmoregulation: what have we learned since August Krogh, Homer Smith, and Ancel Keys. American Journal of Physiology-Regulatory Integrative and Comparative Physiology. 295:R704-R713.

Evans DH (2010) A brief history of fish osmoregulation: the central role of the Mt. Desert Island Biological Laboratory. Front Physio 1:1-10. Doi:10.3389/Fphys.2010.00013

Evans, D.H., P.M. Piermarini, and K.P. Choe. 2005. The multifunctional fish gill: Dominant site of gas exchange, osmoregulation, acid-base regulation, and excretion of nitrogenous waste. Physiological Reviews. 85:97-177. 24

Giffard-Mena, I.; Boulo, V.; Aujoulat, F.; Fowden, H.; Castille, R.; Charmantier, G.; Cramb, G. Aquaporin molecular characterization in the sea-bass (*Dicentrarchus labrax*): The effect of salinity on AQP1 and AQP3 expression. *Comp. Biochem. Phys. A* 2007, *148*, 430–444, doi:10.1016/j.cbpa.2007.06.002.

Günzel, D. and Yu, A.S., 2013. Claudins and the modulation of tight junction permeability. *Physiological reviews*, *93*(2), pp.525-569.

Gray, M.A. and Metcalfe, C.D., 1999. Toxicity of 4-tert-octylphenol to early life stages of Japanese medaka (Oryzias latipes). *Aquatic toxicology*, *46*(2), pp.149-154.

Hill RW, Wyse GA, Anderson. M. (2012) Animal Physiology. Sunderland, MA: Sinauer Associates.

Hiroi, J., and S.D. McCormick. 2007. Variation in salinity tolerance, gill Na /K -ATPase, $Na^{+}/K^{+}/2Cl^{(-)}$ cotransporter and mitochondria-rich cell distribution in three salmonids Salvelinus namaycush, Salvelinus fontinalis and Salmo salar. Journal of Experimental Biology. 210:1015-1024.

Hsu, H.H., L.Y. Lin, Y.C. Tseng, J.L. Horng, and P.P. Hwang. 2014. A new model for fish ion regulation: identification of ionocytes in freshwater- and seawater-acclimated medaka (Oryzias latipes). Cell Tissue Res. 357:225-243.

Ishibashi, K.; Hara, S.; Kondo, S. Aquaporin water channels in mammals. *Clin. Exp. Nephrol.* 2009, *13*, 107–117, doi:10.1007/s10157-008-0118-6.

Iwamatsu, T., 2004. Stages of normal development in the medaka Oryzias latipes. *Mechanisms of development*, *121*(7-8), pp.605-618.

Kasahara, M., Naruse, K., Sasaki, S., Nakatani, Y., Qu, W., Ahsan, B., Yamada, T., Nagayasu, Y., Doi, K., Kasai, Y. and Jindo, T., 2007. The medaka draft genome and insights into vertebrate genome evolution. *Nature*, *447*(7145), pp.714-719.

Kirchmaier, S., Naruse, K., Wittbrodt, J. and Loosli, F., 2015. The genomic and genetic toolbox of the teleost medaka (Oryzias latipes). *Genetics*, *199*(4), pp.905-918.

Kwong, R.W. and Perry, S.F., 2013. The tight junction protein claudin-b regulates epithelial permeability and sodium handling in larval zebrafish, Danio rerio. *American Journal of Physiology-Regulatory, Integrative and Comparative Physiology*, *304*(7), pp.R504-R513.

Laurent, P. and Dunel, S., 1980. Morphology of gill epithelia in fish. *American Journal of Physiology-Regulatory, Integrative and Comparative Physiology*, *238*(3), pp.R147-R159.

Marshall, W.S. and Bellamy, D., 2010. The 50 year evolution of in vitro systems to reveal salt transport functions of teleost fish gills. *Comparative Biochemistry and Physiology Part A: Molecular & Integrative Physiology*, *155*(3), pp.275-280.

Marshall, W.S.; Grosell, M. Ion transport, osmoregulation, and acid -base regulation. In *The Physiology of Fishes;* Evans, D.H., Clairborne, J.B., Eds.; Taylor and Francis Group: Boca Raton, FL, USA, 2006; pp. 177–210, ISBN 978-0849380426.

Manzon, L.A. 2002. The role of prolactin in fish osmoregulation: A review. General and Comparative Endocrinology. 125:291-310.

McCormick, S.D. 2001. Endocrine control of osmoregulation in teleost fish. American Zoologist. 41:781-794.

McCormick, S.D., Farrell, A.P. and Brauner, C.J. eds., 2013. *Fish physiology: euryhaline fishes*. Academic Press.

McCormick, S.D., O'Dea, M.F., Moeckel, A.M., Lerner, D.T. and Björnsson, B.T., 2005. Endocrine disruption of parr-smolt transformation and seawater tolerance of Atlantic salmon by 4-nonylphenol and 17β-estradiol. *General and comparative endocrinology*, *142*(3), pp.280-288.

Naruse, K., Tanaka, M., Mita, K., Shima, A., Postlethwait, J. and Mitani, H., 2004. A medaka gene map: the trace of ancestral vertebrate proto-chromosomes revealed by comparative gene mapping. *Genome research*, *14*(5), pp.820-828.

Richards, J.G., J.W. Semple, J.S. Bystriansky, and P.M. Schulte. 2003. Na /K -ATPase α-isoform switching in gills of rainbow trout (Oncorhynchus mykiss) during salinity transfer. Journal of Experimental Biology. 206:4475-4486.

Rosenthal, R., Günzel, D., Piontek, J., Krug, S.M., Ayala-Torres, C., Hempel, C., Theune, D. and Fromm, M., 2020. Claudin-15 forms a water channel through the tight junction with distinct function compared to claudin-2. *Acta Physiologica*, *228*(1), p.e13334.

Sakamoto, T., T. Kozaka, A. Takahashi, H. Kawauchi, and M. Ando. 2001. Medaka (Oryzias latipes) as a model for hypoosmoregulation of euryhaline fishes. Aquaculture. 193:347-354.

Shima, A. and Mitani, H., 2004. Medaka as a research organism: past, present and future. *Mechanisms of development*, *121*(7-8), pp.599-604.

Scott, G.R., J.B. Claiborne, S.L. Edwards, P.M. Schulte, and C.M. Wood. 2005. Gene expression after freshwater transfer in gills and opercular epithelia of killifish: insight into divergent mechanisms of ion transport. Journal of Experimental Biology. 208:2719-2729.

Takei, Y., and S.D. McCormick. 2013. Euryhaline Fishes: Hormonal control of fish euryhalinity. In Fish Physiology. Vol. 32. Elsevier. 69-123.

Tipsmark, C.K., D.A. Baltzegar, O. Ozden, B.J. Grubb, and R.J. Borski. 2008a. Salinity regulates claudin mRNA and protein expression in the teleost gill. American Journal of Physiology-Regulatory Integrative and Comparative Physiology. 294:R1004-R1014.

Tipsmark, C.K., J.P. Breves, D.B. Rabeneck, R.T. Trubitt, D.T. Lerner, and E.G. Grau. 2016. Regulation of gill claudin paralogs by salinity, cortisol and prolactin in Mozambique tilapia (Oreochromis mossambicus). Comparative Biochemistry and Physiology a-Molecular & Integrative Physiology. 199:78-86.

Tipsmark, C.K., J.P. Breves, A.P. Seale, D.T. Lerner, T. Hirano, and E.G. Grau. 2011. Switching of Na , K -ATPase isoforms by salinity and prolactin in the gill of a cichlid fish. Journal of Endocrinology. 209:237-244.

Tipsmark, C.K., C. Jorgensen, N. Brande-Lavridsen, M. Engelund, J.H. Olesen, and S.S. Madsen. 2009. Effects of cortisol, growth hormone and prolactin on gill claudin expression in Atlantic salmon. General and Comparative Endocrinology. 163:270-277.

Tipsmark, C.K., P. Kiilerich, T.O. Nilsen, L.O.E. Ebbesson, S.O. Stefansson, and S.S. Madsen. 2008b. Branchial expression patterns of claudin isoforms in Atlantic salmon during seawater acclimation and smoltification. American Journal of Physiology-Regulatory Integrative and Comparative Physiology. 294:R1563-R1574.

Tipsmark, C.K., and S.S. Madsen. 2009. Distinct hormonal regulation of Na ,K -atpase genes in the gill of Atlantic salmon (Salmo salar L.). Journal of Endocrinology. 203:301-310.
Tipsmark, C.K., S.S. Madsen, M. Seidelin, A.S. Christensen, C.P. Cutler, and G. Cramb. 2002. Dynamics of Na ,K ,2Cl cotransporter and Na ,K -ATPase expression in the branchial epithelium of brown trout (Salmo trutta) and Atlantic salmon (Salmo salar). Journal of Experimental Zoology. 293:106-118.

Tipsmark, C.K.; Sørensen, K.J.; Madsen, S.S. Aquaporin expression dynamics in osmoregulatory tissues of Atlantic salmon during smoltification and seawater acclimation. *J. Exp. Biol.* 2010, *213*, 368–379, doi:10.1242/jeb.034785.

Watanabe, S.; Kaneko, T.; Aida, K. Aquaporin-3 expressed in the basolateral membrane of gill chloride cells in Mozambique tilapia *Oreochromis mossambicus* adapted to freshwater and seawater. *J. Exp. Biol.* 2005, *208*, 2673–2682, doi:10.1242/jeb.01684

Wilson, J.M., P. Laurent, B.L. Tufts, D.J. Benos, M. Donowitz, A.W. Vogl, and D.J. Randall. 2000. NaCl uptake by the branchial epithelium in freshwater teleost fish: An immunological approach to ion-transport protein localization. J. Exp. Biol. 203:2279-2296.

Wittbrodt, J., Shima, A. and Schartl, M., 2002. Medaka—a model organism from the far East. *Nature Reviews Genetics*, *3*(1), pp.53-64.

Zachar, P.C. and Jonz, M.G., 2012. Neuroepithelial cells of the gill and their role in oxygen sensing. *Respiratory physiology & neurobiology*, *184*(3), pp.301-308.

Zimmer, A.M., Pan, Y.K., Chandrapalan, T., Kwong, R.W. and Perry, S.F., 2019. Loss-of-function approaches in comparative physiology: is there a future for knockdown experiments in the era of genome editing?. *Journal of Experimental Biology*, *222*(7).

Chapter 2 Differential Expression and Localization of Branchial AQP1 and AQP3 in Japanese Medaka (*Oryzias latipes*)

Laura V. Ellis[1], Rebecca J. Bollinger[1], Hannah M. Weber[1], Steffen S. Madsen[2], Christian K. Tipsmark[1]

[1] Department of Biological Sciences, University of Arkansas, Fayetteville, AR 72701, USA

[2] Department of Biology, University of Southern Denmark, Odense M, Denmark

2.1 Abstract

Aquaporins (AQPs) facilitate transmembrane water and solute transport, and in addition to contributing to transepithelial water transport, they safeguard cell volume homeostasis. This study examined the expression and localization of AQP1 and AQP3 in the gills of Japanese medaka (*Oryzias latipes)* in response to osmotic challenges and osmoregulatory hormones, cortisol, and prolactin (PRL). *AQP3* mRNA was inversely regulated in response to salinity with high levels in ion-poor water (IPW), intermediate levels in freshwater (FW), and low levels in seawater (SW). AQP3 protein levels decreased upon SW acclimation. By comparison, AQP1 expression was unaffected by salinity. In ex vivo gill incubation experiments, *AQP3* mRNA was stimulated by PRL in a time- and dose-dependent manner but was unaffected by cortisol. In contrast, *AQP1* was unaffected by both PRL and cortisol. Confocal microscopy revealed that AQP3 was abundant in the periphery of gill filament epithelial cells and co-localized at low intensity with Na^+,K^+-ATPase in ionocytes. AQP1 was present at a very low intensity in most filament epithelial cells and red blood cells. No epithelial cells in the gill lamellae showed immunoreactivity to AQP3 or AQP1. We suggest that both AQPs contribute to cellular volume regulation in the gill epithelium and that AQP3 is particularly important under hypo-osmotic conditions, while expression of AQP1 is constitutive.

2.2 Introduction

Euryhaline fish, such as the Japanese medaka (*Oryzias latipes*), are capable of acclimating to both freshwater (FW) and seawater (SW) environments. In FW, they are challenged by osmotic water inflow and passive ion loss and must combat this by actively absorbing ions from the environment and getting rid of excess water (Edwards and Marshall, 2013; Evans et al., 2005). Regulation of the body's ion balance is primarily taken care of by the gill, and water balance is

maintained by renal production of copious amounts of hypo-tonic urine (Evans et al., 2005). In SW, integumental ion and water fluxes are basically reversed, meaning that the passive influx of ions and loss of water must be compensated for by the active secretion of monovalent ions in the gill and solute-linked water absorption in the gastrointestinal tract. Thus, the function of the gill has extreme plasticity in euryhaline fish. Ionocytes in the gill are the cells responsible for the active transport of ions in both directions depending on the salinity. In addition to a high density of basolateral Na^+,K^+-ATPase (Nka), ionocytes are equipped with specific apical and basolateral ion transport proteins that work together in ion absorption and excretion. One FW-type ionocyte specifically expresses a gill-specific paralog of apical sodium chloride cotransporter protein (Ncc2: Hsu et al., 2014), and SW ionocytes express basolateral sodium-potassium-2-chloride cotransporter (Nkcc2: Marshall et al., 2002) and an apical cystic fibrosis transmembrane conductance regulator protein (Cftr: Marshall and Grosell, 2006). In addition to modifications in the expression pattern of transmembrane ion transport proteins, junctional complexes between these cells are modified from having a tight nature in FW to prevent sodium ion loss to being leakier in SW to allow for the removal of excess sodium ions (Wilson and Laurent, 2002).

The gill is a complex three-dimensional structure consisting of primary filaments and secondary lamellae, which create an expansion of the surface area in direct contact with the surrounding water (Evans et al., 2005). By having a very thin structure, the gill epithelium is optimized for gas transport but also becomes a gate for passive exchange of water and ions between the fish and its environment (the "osmo-respiratory compromise" (Nilsson 1986). Ideally, branchial transepithelial water permeability should be kept to a minimum; however, the high gas permeability puts a particular strain on epithelial cells covering the surface of the gill in terms of maintaining osmotic and cell volume homeostasis. Regulation of the osmotic permeability of the

branchial epithelium therefore becomes an interesting topic, which has been scarcely investigated thus far. Transepithelial water permeability (osmotic as well as diffusional) of gills has been analyzed in a few studies and has been found to be highest in FW and lowest in SW (e.g., eel (Motais et al., 1969; Isaia 1984).

Cell membranes are generally quite permeable to water (Hoffmann et al., 2009). Their permeability may be increased by the presence of aquaporins (AQPs), major intrinsic proteins that form transmembrane channels facilitating the transport of water and certain small solutes (Agre et al., 1993; Ecelbarger et al., 1995; Ishibashi et al., 2009; Tingaud-Sequeira et al., 2008). Functionally, aquaporins facilitate transepithelial movement of water, as well as cell volume regulation (Tingaud-Sequeira et al., 2008; Sugiyama et al., 2001; Boury-Jamot et al., 2006; Cutler and Cramb, 2007; Lee et al., 2017). Mammals have 13 AQP paralogs, the orthodox AQPs (AQP0, -1, -2, -4, -5, -6, and -8), the aquaglyceroporins (Aqp3, -7, -9, and -10), and the super-AQPs (AQP11 and -12) (Ecelbarger et al., 1995; Sugiyama et al., 2001; Boury-Jamot et al., 2006). Due to multiple genomic duplication events, certain teleost fishes such as Atlantic salmon (*Salmo salar*), have up to 42 AQP paralogs with multiple forms of the same AQP (Finn et al., 2014). In contrast, Japanese medaka express 11 paralogs. AQP1 and AQP3 are the main paralogs expressed in the gills of different fish species and are speculated to play roles in the regulation of branchial water homeostasis (Madsen et al., 2015). With the gill being in direct contact with a surrounding medium that typically has a very different osmotic composition compared with the internal milieu, it would be detrimental if AQPs created transcellular pathways for water movement in the superficial epithelial cell layer. Thus, it would rather be expected that they are localized deeper in the epithelium and/or in an asymmetrical pattern and that their role is concerned with cell volume

regulation. However, due to the lack of knowledge in this subject, studies are necessary to investigate their localization and expression dynamics in response to salinity.

When establishing aquaporin expression dynamics, it is interesting to also investigate the role of the endocrine system in the regulation of aquaporins. Several studies have addressed the endocrine regulation of branchial ion transport mechanisms (McCormick 2001), whereas we know relatively little about the expressional regulation of AQPs in any tissue of teleosts. Prolactin (PRL) is widely accepted as a FW adapting hormone in teleosts that stimulates ion uptake and the associated molecular elements in FW-type ionocytes and, at the same time, reduces the abundance of secretory SW-type ionocytes (Breves et al. 2014; Flik et al., 1994; Takei and McCormick 2013). Elevated plasma PRL may reduce circulating insulin-like growth factor-1 (IGF-1), which in turn leads to decreased branchial salt secretion and differentially regulates Nka alpha-subunit isoforms (McCormick 2001; Takei et al., 2013; Manzon 2002; Tipsmark and Madsen, 2009). In Mozambique tilapia (*Oreochromis mossambiccus*), PRL increased branchial *AQP3* expression, while cortisol had the ability to block the stimulation of *AQP3* (Breves et al. 2016). Dose-dependent stimulation of *NCC2* by PRL has been shown in zebrafish (*Danio rerio*) and medaka, and expression of this gene may be used as a marker for select FW-type ionocytes (Breves et al., 2013; Bossus et al., 2017). Cortisol is a mediator of both FW- and SW-adapting effects in the gill. It may interact with growth hormone (Gh) and IGF-1, thereby promoting salt secretory mechanisms and SW-acclimation (Takei and McCormick 2013; Tipsmark et al.,2007; Breves et al., 2010). On the other hand, cortisol can also interact with PRL and either exacerbate or antagonize the ion-regulatory effects of PRL (Tipsmark and Madsen, 2009; Breves et al., 2013). Previous work in various fish species does not provide a clear consensus concerning salinity effects on AQP1 and AQP3 nor concerning their cellular localization within the gill (Madsen et al. 2015).

Therefore, we here used the euryhaline medaka model to advance our understanding of these AQP paralogs' significance to gill function.

Japanese medaka has previously been used as a model organism for studying ionic and osmotic regulation in a euryhaline teleost (Hsu et al., 2014; Bossus et al., 2017; Sakamoto et al., 2001; Madsen et al., 2014; Bossus et al., 2015; Bollinger et al., 2016), and aquaporin tissue distribution was characterized in a previous study with a focus on the dynamics in the intestine [33]. The current study aims to answer three main questions: (i) in which cell types do we find the two aquaporin paralogs, AQP1 and AQP3, expressed in the gill of medaka?; (ii) how are branchial AQP1 and AQP3 mRNA and protein expression and localization affected by environmental salinity?; and (iii) are PRL and cortisol involved in endocrine control of AQP expression? Time-course salinity transfer experiments from FW to ion-poor water and from FW to SW were performed to investigate the expression dynamics at the mRNA and protein level. This was combined with confocal immunofluorescence analyses of branchial localization of the two paralogs, and ex vivo experiments were used to investigate the role of cortisol and PRL in regulating AQP1 and AQP3 expression in the gill.

2.3 Materials and Methods

2.3.1 Fish and Maintenance

Adult Japanese medaka (*O. latipes*, Temmink and Schlegel; total length: 25–35 mm, weight range: 250–350 mg) were obtained from Aquatic Research Organisms, Inc. (Hampton, NH, USA; N = 118). Fish were acclimated and kept in recirculated de-chlorinated biofiltered fresh water (FW; in mmol L^{-1}: 0.34 Na^+, 0.64 Ca^{2+}, 0.09 Mg^{2+}, 0.03 K^+). Medaka were maintained in a 14 h light/10 h dark photoperiod at a temperature of 20 °C. They were fed daily with Tetramin tropical flakes

(Tetra, United Pet Group, Blacksburg, VA, USA), and food was withheld 24 h prior to any sampling. Upon sampling, the fish were sacrificed by cervical dislocation. Subsequent pithing of the brain was performed, and the gill apparatus was removed. All handling and experimental procedures were approved by the Animal Care and Use Committee of the University of Arkansas (IACUC 14042 and 17091).

2.3.2 Salinity Transfer Experiments: FW–SW, FW–Ion-Poor Water (IPW).

To investigate the response of medaka to hyper-osmotic environments, 10 female and 10 male FW-acclimated medaka were transferred to both sham FW conditions and SW (28 ppt; Instant Ocean, Spectrum Brands, Blacksburg, VA, USA; N = 40) and sampled after 6, 24, and 168 h (n = 6 per group). The gills were removed and washed with phosphate-buffered saline (PBS, Roche Diagnostics, Indianapolis, IN, USA), and then, 4 gill arches were placed directly into 250 µL of TRI Reagent® (Sigma Aldrich, St. Louis, MO, USA) for mRNA analyses, while the other four were placed directly into 1.5 mL sonication tubes in 1X lithium dodecyl sulfate (LDS) NuPAGE Sample Buffer (Thermo Fisher Scientific, Waltham, MA, USA) with 50 mmol L^{-1} dithiothreitol (DTT, GE Healthcare Bio-Sciences, Pittsburgh, PA, USA).

To test the response of medaka to a dilute hypo-osmotic environment, 10 female and 10 male FW-acclimated medaka were transferred to sham FW conditions and IPW (90% deionized water and 10% tap water; N = 40). After 6, 24, and 168 h, gills (n=6 per group) were sampled and treated as described above.

2.3.3 Ex vivo Hormone Incubation Experiments

For all ex vivo incubation experiments, gill explants from FW-acclimated medaka (N = 38) were dissected, and the 4 paired gill arches with cartilage intact were separated from one another,

washed with PBS, and placed for 1 h of pre-incubation in Dulbecco's modified Eagle's medium (DMEM; Cellgro by Corning, manufactured by Mediatech, Inc., Manassas, VA, USA) with the addition of 50 U mL^{-1} of penicillin and 50 µg mL^{-1} of streptomycin (Thermo Fisher Scientific, Waltham, MA, USA), as previously described by Bossus et al*.,* 2017. Four separate experiments were conducted: Cortisol dose–response (0, 0.1, 1, and 10 µg of cortisol mL^{-1}) with 18 h incubation time (n = 5–6 per group); PRL dose–response (0, 0.01, 0.1, and 1µg of ovine PRL mL^{-1}) with 18 h incubation time (n = 7–8 per group); PRL time-course experiment using a dose of 1µg mL^{-1} and 2, 6, and 18 h of incubation (n = 7–8 per group); and a combination experiment with a control, cortisol 10 µg mL^{-1}, PRL 1µg mL^{-1}, and cortisol 10 µg mL^{-1} + PRL 1µg mL^{-1} (n = 7–8 per group). Cortisol (hydrocortisone hemisuccinate sodium salt; Sigma-Aldrich, St. Louis, MO, USA) was dissolved in molecular biology water-ultra pure (Sigma Aldrich, St. Louis, MO, USA). Purified ovine PRL (AFP10692C) was obtained from the National Hormone and Peptide Program (Torrance, CA, USA) and dissolved in molecular biology water-ultra pure (Sigma Aldrich, St. Louis, MO, USA). Hormone experiments were conducted by randomizing gill arches from pre-incubation and assigning 2 gill arches to each treatment (each fish provided gill tissue to all treatments). The experiments were terminated by transferring gill explants directly into 250 µL of TRI Reagent® (Sigma Aldrich, St. Louis, MO, USA) for RNA isolation.

2.3.4 RNA Isolation, cDNA Synthesis, and Real-Time qPCR

RNA isolation was conducted according to the manufacturer's protocol (TRI Reagent®; Sigma Aldrich, St. Louis, MO, USA). All samples were homogenized using a Power Max 200 rotating knife homogenizer (Advanced Homogenizing System; Manufactured by PRO Scientific for Henry Troemner LLC, Thorofare, NJ, USA). In individual experiments, 300 or 500 ng of total RNA was used for cDNA synthesis using the Applied Biosystems High Capacity cDNA Reverse

Transcription kit (Thermo Fisher). qPCR primers were previously validated and published in Bossus et al., 2015 and Madsen et al., 2014. Elongation Factor 1 alpha (*EF1a*), beta actin (*bact*), and ribosomal protein L7 (*RPL7*) were analyzed as normalization genes in all experiments. Real-time qPCR was run on a Bio-Rad CFX96 platform (BioRad, Hercules, CA, USA) using SYBR® Green JumpStart™ (Sigma Aldrich, St. Louis, MO, USA). qPCR cycling was conducted using the following protocol: initial denaturation/activation phase (94 °C) for 3 min, 40 cycles of a 15 s denaturation step and an annealing/elongation step for 60 s (60 °C), followed by a melting curve analysis at an interval of 5 s per degree from 55 to 94 °C. The absence of primer–dimer association was verified with no template controls (NTC). As an alternative to DNAse treatment, the absence of significant genomic DNA amplification was confirmed using total RNA samples instead of cDNA in a no reverse transcriptase control (NRT). Primer amplification efficiency was analyzed using a standard curve method with dilutions of the primers from 2 to 16 times. Amplification efficiency was used to calculate the relative copy numbers of the individual targets. Relative copy numbers were calculated by $E_a^{\Delta Ct}$, where C_t is the threshold cycle number and E_a is the amplification efficiency (Pfaffl 2001) Data were normalized to the geometric mean of the three normalization genes and were presented relative to the control group.

2.3.5 Western Blot Analysis

Medaka gills from the salinity transfer experiments were placed directly into 1.5 mL sonication tubes in 1x LDS buffer with 50 mM DTT and then placed in an ultrasonic bath (Ultrasonic Liquid Processor 3000, Farmingdale, NY, USA). Gill samples were sonicated and manually homogenized in accordance with the procedure described by Bollinger et al., 2018. Following sonication, samples were transferred to microcentrifuge tubes and heated at 70 °C for 10 min. Denatured protein samples were run on a 4%–12% Bis-Tris Gel with 2-(*N*-morpholino)

ethanesulfonic acid sodium dodecyl sulfate (MES SDS) running buffer with antioxidants. Gels were electrophoresed and then blotted onto 0.2 µm nitrocellulose membranes with transfer buffer containing 10% methanol. Membranes were blocked with LI-COR Blocking Buffer (LI-COR Biosciences, Lincoln, NE, USA) for 1 h at room temperature. Membranes were incubated with a cocktail of affinity-purified homologous rabbit anti medaka AQP1 antibody validated previously (Madsen et al., 2014) or rabbit anti medaka AQP3 antibody (see below), in combination with mouse anti human β-actin (Abcam; cat. no. ab8224) in blocking buffer and incubated overnight at 4 °C on an orbital rotator. Antibodies were used at the following concentrations: AQP1 (0.1 µg mL^{-1}), AQP3 (0.1 µg mL^{-1}), β-actin (0.2 µg mL^{-1}). Membranes were washed four times for 5 min with 1X tris-buffered saline with Tween 20 (TBST: 20 mM Tris, 140 mM NaCl and 0.1% Tween-20). Western blotting solutions and materials were NuPAGE™ from Thermo Fisher, unless stated otherwise. Incubation with secondary antibodies in blocking buffer was performed in dark conditions at room temperature for 1 h (IRDye® 800CW Goat anti-Rabbit IgG and IRDye® 680LT Goat anti-Mouse IgG, LI-COR Biosciences, Lincoln, NE, USA). After washing, membranes were dried and imaged using an Odyssey infrared scanner (LI-COR Bioscience, Lincoln, NE, USA). The AQP3 antibody was generated in rabbit against an epitope in the cytoplasmic C-terminal domain of the medaka AQP3 sequence CFHVEGEVRDKREKM, chosen based on antigenicity and its low similarity with other proteins (GenScript, Piscataway, NJ, USA). The AQP3 sequence has some identity with other predicted proteins in Japanese medaka (https://blast.ncbi.nlm.nih.gov/Blast.cgi; identity is defined as 6–7 of 14 amino acids). These are high-molecular-weight proteins (87, 188, and 212 kDa) that do not occur on western blots. The specificity of the medaka AQP3 was validated by control neutralization with the antigenic peptide in 400x molar excess overnight at 4 °C before probing the membrane. Aquaporin expression (band

intensity) was quantified using Image Studio version 2.0 software (LI-COR Biosciences, Lincoln, NE, USA) and normalized against β-actin loading control. The 7-day treatment group was chosen for protein determination to allow for the translation of the messenger and the buildup of the functional protein.

2.3.6 Immunohistochemistry

Gills from medaka transferred from FW to FW, IPW, or SW for 7 days were fixed overnight in 4% phosphate-buffered paraformaldehyde (PFA) and then rinsed and stored in 70% EtOH at 4 °C. They were dehydrated in graded series of EtOH and xylene and embedded in paraffin. Then, 5-µm thick sagittal sections (see Figure 2.9A) were cut on a microtome, and sections were placed on Superfrost Plus slides (Gerhard Menzel GmbH, Braunschweig, Germany) before being heated for 2 h at 60 °C. The tissue sections were hydrated through washes in xylene; 99%, 96%, and 70% EtOH; and finally, Na-citrate (10 mM Na-citrate, pH 6.0). Antigen retrieval was performed by boiling the sections in the citrate solution for 5 min in a microwave oven and leaving them in the warm citrate solution for 30 min before being washed 2 times for 5 min each in PBS. This was followed by blocking for 1 h (3% bovine serum albumin/2% goat serum in PBS). The sections were then incubated overnight at 4 °C with a cocktail of primary rabbit antibodies against medaka AQP1 (1 µg mL^{-1}) or AQP3 (0.8 µg mL^{-1}) in combination with a mouse antibody against the alpha subunit of the Nka (a5; the Developmental Studies Hybridoma Bank developed under the auspices of the National Institute of Child Health Development and maintained by the University of Iowa, Department of Biological Sciences, Iowa City, IA, USA) in blocking buffer. The homologous Japanese medaka aquaporin antibodies (AQP1 and AQP3) were the same as those used in the western blot analysis described above. Sections were washed repeatedly in PBS before being incubated with a cocktail of secondary antibodies (goat anti-rabbit IgG Oregon Green®

488/goat anti-mouse IgG Alexa Fluor® 568, 1:1000, Invitrogen, Carlsbad, CA, USA) for 1 h at 37 °C. Sections were finally washed 4 times for 5 min in PBS, and cover slips were mounted using ProLong Gold antifade reagent (Invitrogen). In some cases, nuclei were stained with 4',6-diamidino-2-phenylindole (DAPI, 0.1 μg mL^{-1} in PBS) for 10 min after washing with PBS and before mounting. Slides were visualized on a Zeiss LSM510 confocal microscope (Carl Zeiss Microscopy GmbH, Jena, Germany), and representative images were collected using the Zeiss Image Browser 4.2.0 software (Carl Zeiss Microscopy GmbH, Jena, Germany) and processed using Image J (Schindelin, et al., 2012).

2.3.7 Statistical Analysis

All data analysis was conducted using GraphPad Prism 6.0 software (San Diego, CA, USA). Dose-dependent ex vivo experiments were analyzed using one-way ANOVA followed by Tukey's multiple comparisons test. Data from the salinity transfer experiments, PRL and cortisol time-course experiment, and hormone combination experiment were analyzed via two-way ANOVA followed by Sidak multiple comparisons test of time-matched groups, when there was significant interaction between the two factors (salinity and time or PRL and cortisol). Western blot data were analyzed using two-tailed Student's t-test. When required, data were log or square-root transformed to meet the ANOVA assumption of homogeneity of variances as tested with Bartlett's test. Significant differences were accepted when $P < 0.05$.

2.4 Results

2.4.1 Aquaporin mRNA Response to Osmotic Challenges

Transfer from FW to SW induced a significant and lasting overall decrease in *AQP3* mRNA in the gill compared with the FW–FW sham treatment (Figure 2.1B). By comparison, *AQP1* was not significantly affected by salinity (Figure 2.1A), and *NCC2b* responded by an overall decline in response to SW (Figure 2.1C). Exposure to IPW induced an initial increase in *AQP3* mRNA at 6 h followed by a return to basal FW levels (Figure 2.2B). *AQP1* and *NCC2b* mRNA levels were not significantly affected by transfer to IPW (Figure 2.2 A,C).

2.4.2 Western Blotting and Aquaporin Protein Levels

An antibody was raised against medaka AQP3. In western blot analysis, the antibody recognized one major immunoreactive band with an apparent molecular weight of 18 kDa, which is lower than the predicted 33 kDa for medaka AQP3 (Figure 2.3). The 18 kDa band disappeared when the antibody was neutralized with excess antigenic peptide. A comparison of gill samples from 7-day acclimated FW and SW medaka showed no significant differences in AQP1 abundance, whereas AQP3 protein levels were lower in SW compared with those in FW (Figure 2.4A). Transfer to IPW for 7 days did not induce any significant change in the protein expression of either AQP1 or AQP3 compared with those in FW (Figure 2.4B).

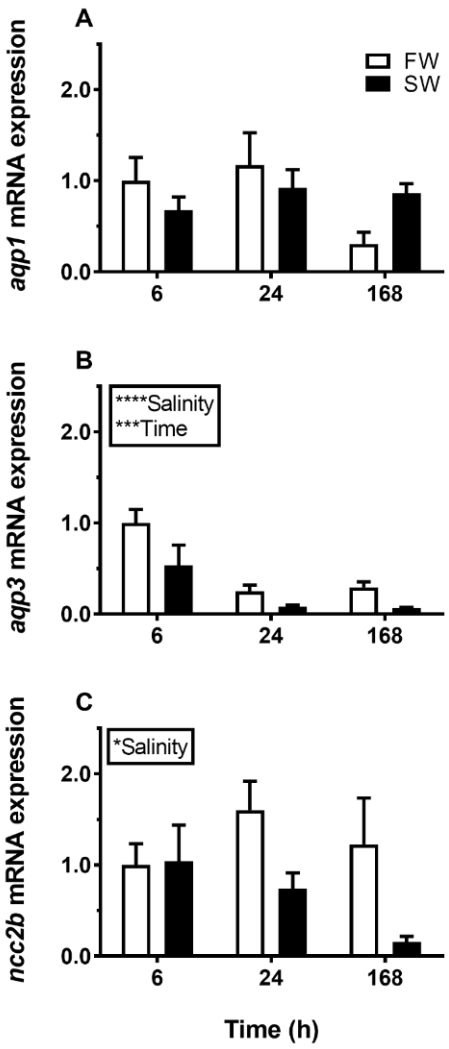

Figure 2.1 Effect of transfer from freshwater (FW) to (SW) on branchial *aquaporin 1* (*AQP1)* (**A**), *AQP3* (**B**), and *NCC2b* (**C**) expression in medaka at 6, 24, and 168 h timepoints. FW–FW sham transfer (open bars), FW–SW transfer (solid bars). The level of each target was normalized to the geometric mean of the normalization genes *EF1a*, *bact*, and *RPL7* and presented relative to the control group at 6 h. Data are presented as mean ± standard error of the mean (n = 7–8). Statistically significant factor effects (two-way ANOVA, P <0.05) are denoted by asterisks next to salinity or time (**P* <0.05, ****P* <0.001, *****P* <0.0001). No significant interaction between factors was found, and post-hoc tests were therefore redundant.

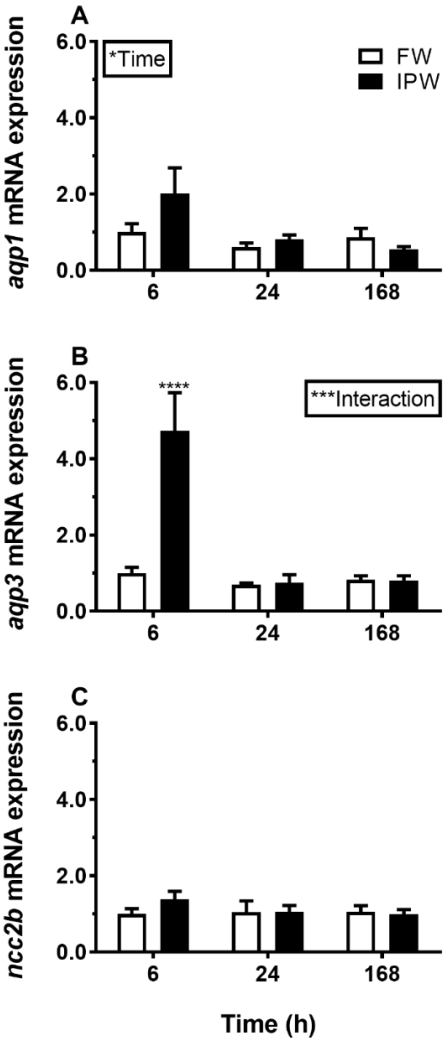

Figure 2.2 Effect of transfer from FW to 90% ion-poor water (IPW) on branchial *AQP1* (**A**), *AQP3* (**B**), and *NCC2b* (**C**) expression medaka at 6, 24, and 168 h timepoints. FW–FW sham transfer (open bars); FW–IPW transfer (solid bars). The level of each target was normalized to the geometric mean of the normalization genes *EF1a*, *bact*, and *RPL7* and presented relative to the control group at 6 h. Data are presented as mean ± standard error of the mean (n = 7–8). Statistically significant factor effects (two-way ANOVA, $P < 0.05$) are denoted by asterisks (*$P < 0.05$). When the interaction between the time and salinity factor was significant (***$P < 0.001$), asterisks were placed above the IPW group indicating difference from the time-matched control (Sidak multiple comparisons test, ****$P < 0.0001$).

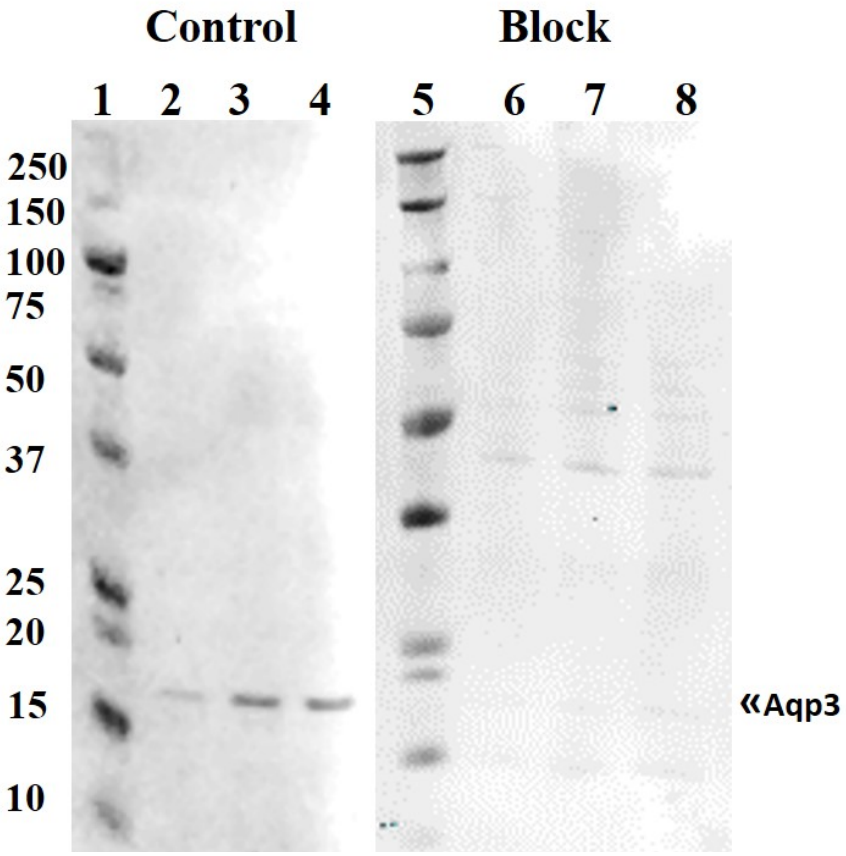

Figure 2.3 Western blot of FW medaka gill protein probed with an antibody against medaka AQP3. Lanes 2–4 were probed with the AQP3 antibody; lanes 5–8 were probed with the antibody after neutralization with 400x molar excess of the antigenic peptide. Lanes 1 and 5 contained a molecular mass marker (Protein Plus, BIO-RAD, Hercules, CA); lanes 2–4 and 6–8 contained 5, 10, and 15 µg of total loaded protein, respectively. A single immunoreactive band at ~18 kDa was detected, which was not present after antibody neutralization.

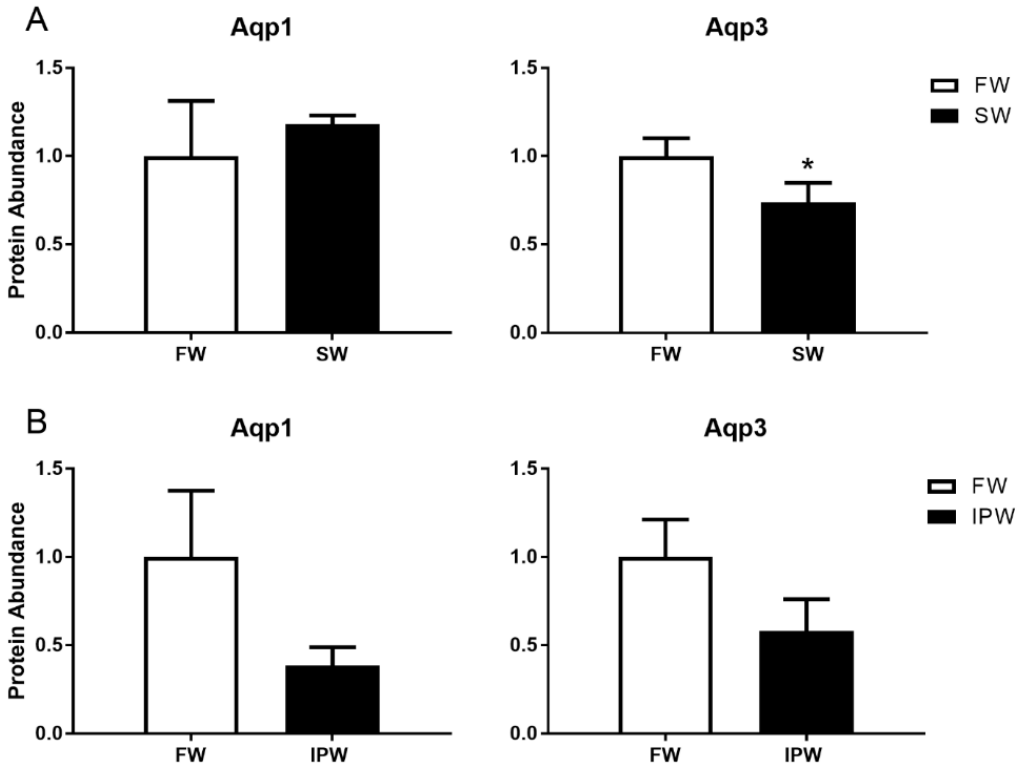

Figure 2.4 Western blot analysis of AQP1 (left) and AQP3 (right) protein levels in medaka gills 7 days after transfer from FW (open bars) to (**A**) SW (solid bars) or (**B**) IPW (solid bars). Immunoreactive AQP bands were analyzed and normalized to the level of β-actin in each sample. Values are presented relative to the FW control group. Statistically significant effects (two-tailed Student's t-tests, $P < 0.05$) are denoted by asterisks. Data are presented as mean ± standard error of the mean (n = 5–6).

2.4.3 Branchial Aquaporin Localization

Nka immunoreactivity (NKIR), which was used as a marker of branchial ionocytes appeared at high intensity in ionocytes along the gill filaments and was rarely observed in the lamellar epithelium (Figures 2.5 and 2.6). NKIR cells were larger in the SW- than in the FW-acclimated medaka. AQP1 immunoreactivity in the gill was generally weak in IPW, FW, and SW (Figure 2.5) and was localized primarily in the periphery of cells in the interlamellar area of the filament. There was no apparent overlap between AQP1 immunoreactivity and NKIR, and the intensity was unaffected by environmental salinity. AQP1 was predominately localized in epithelial cells adjacent to NKIR cells on the filament. In addition, AQP1 immunoreactivity was observed in the membrane of red blood cells in the lamellae (Figure 2.7). AQP3 immunostaining was generally much stronger than AQP1 immunoreactivity and found in interlamellar space in the filament, that includes NKIR cells (Figures 2.6, 2.8). AQP3 staining appeared strongest in the deeper cell layers of the filament and was circumferential with nuclei unstained and centered in the middle (Figure 2.6). In Figure 8, nuclei were stained with DAPI, and there was clearly no overlap with the localization of AQP3. AQP3 staining appeared similar in intensity irrespective of salinity (Figure 2.6). In gill sections incubated without a primary antibody, there was a very weak autofluorescence in ionocytes, and red blood cells at both the green and red laser lines (Figure 2.9B).

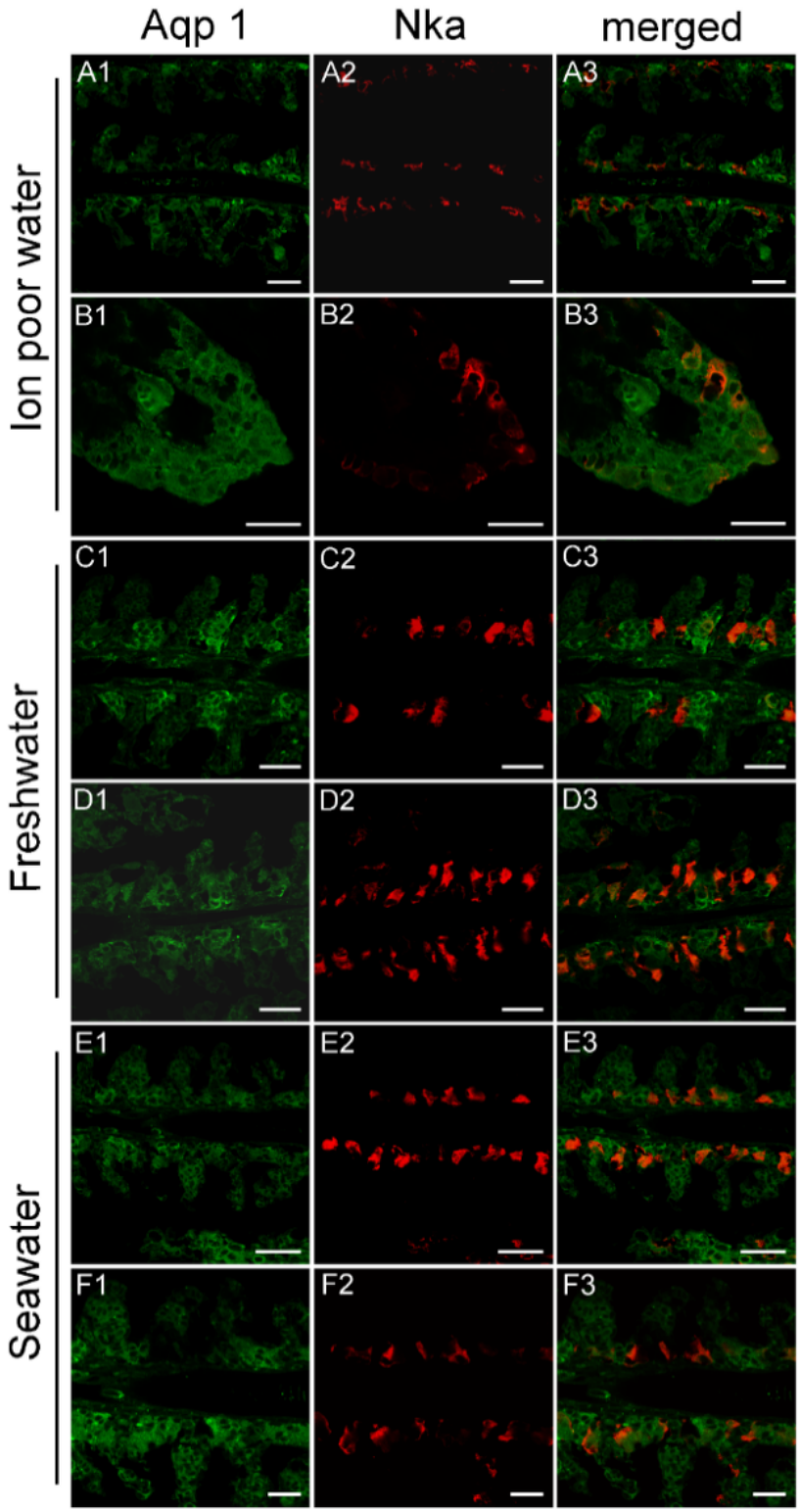

Figure 2.5 Representative confocal images of sagittal sections of medaka gills showing immunoreactivity against medaka AQP1 (green), the Na^+,K^+-ATPase alpha subunit (red), and merged. Rows A and B are from IPW fish, C and D are from FW fish, and E and F are from SW fish. Scale bar = 20 μm. For orientation see Figure 2.9A.

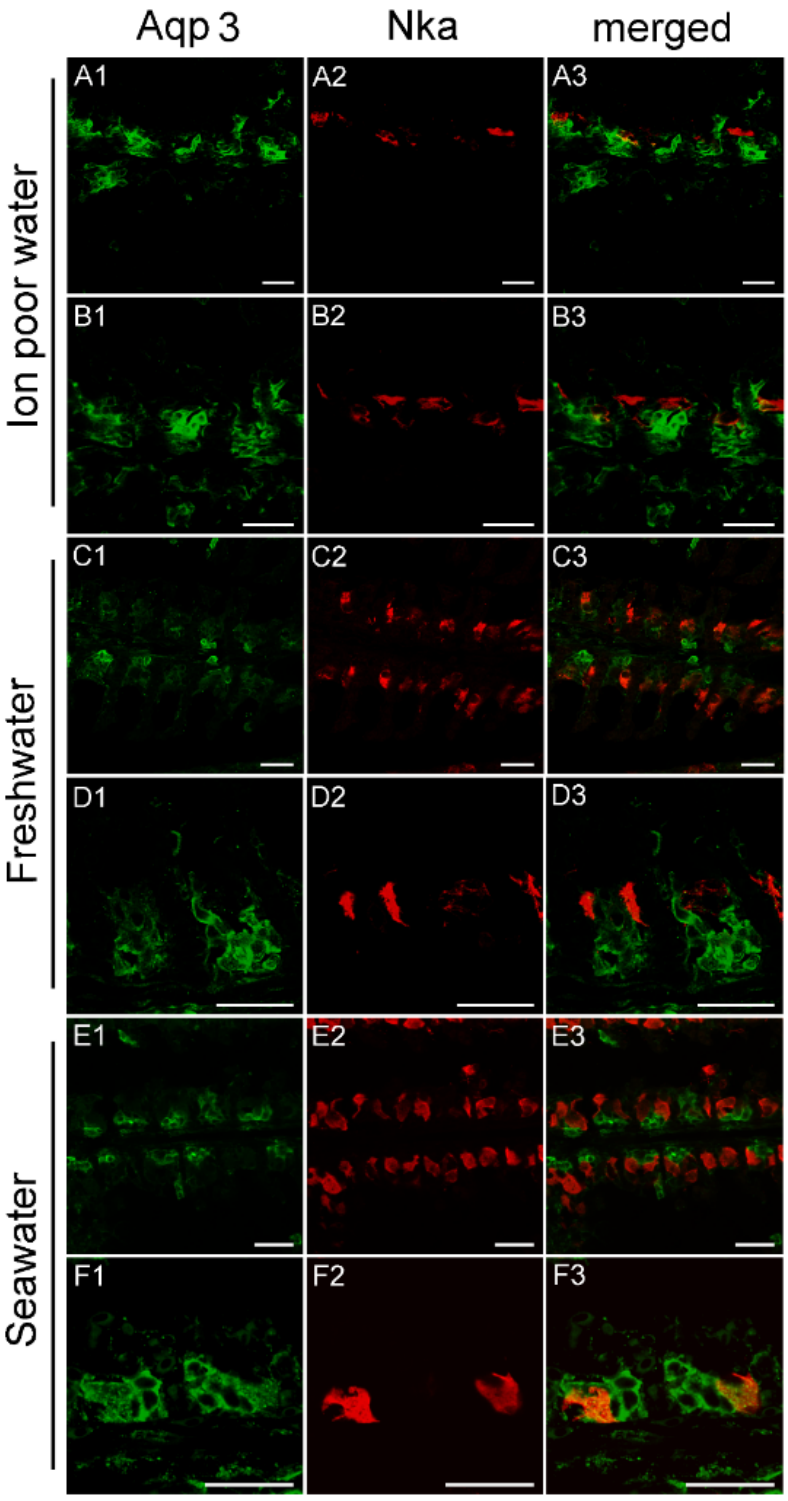

Figure 2.6 Representative confocal images of sagittal sections of medaka gills showing immunoreactivity against medaka AQP3 (green), the Na^+,K^+-ATPase alpha subunit (red), and merged. Rows A and B are from IPW fish, C and D are from FW fish, and E and F are from SW fish. Scale bar = 20 µm. For orientation see Figure 2.9A.

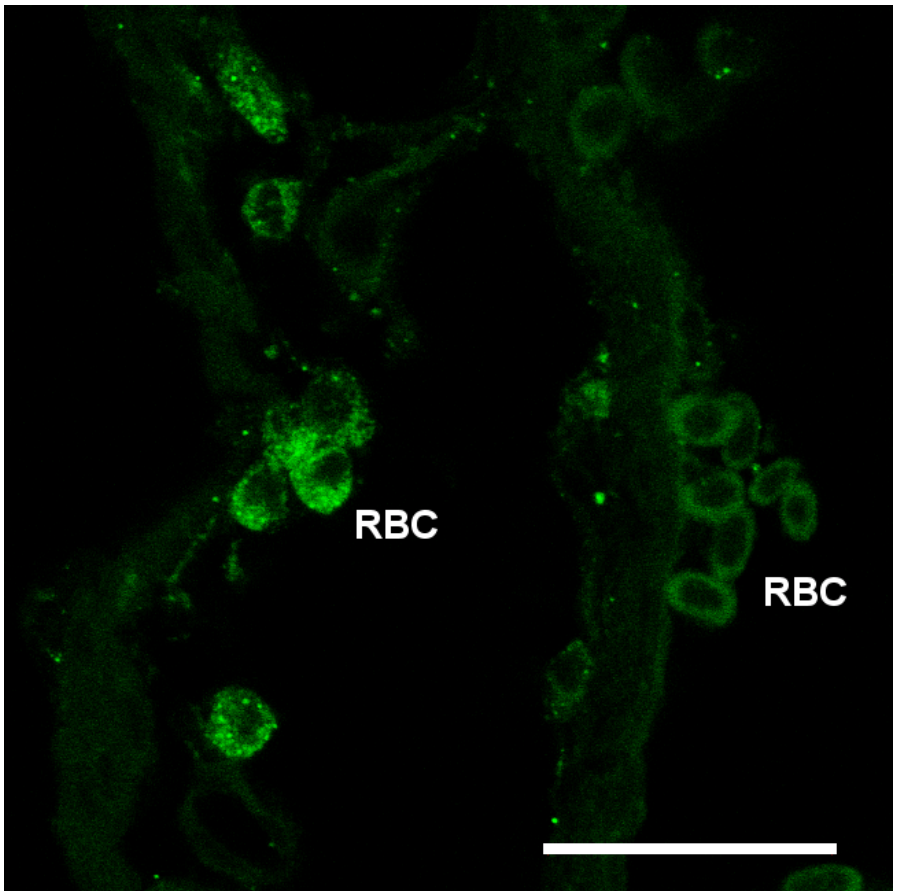

Figure 2.7 Confocal image of red blood cells (RBC) showing immunoreactivity against medaka AQP1 (green). Scale bar = 20 μm.

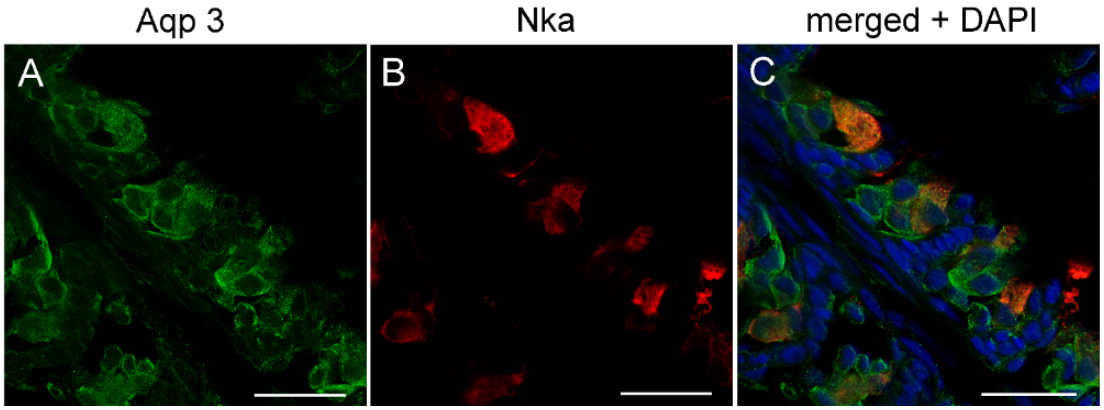

Figure 2.8 Confocal image of sagittal sections of FW medaka gills showing immunoreactivity against medaka (**A**) AQP3 (green), (**B**) Na^+,K^+-ATPase (red), and (**C**)merged channels overlaid with nuclear staining (blue 4',6-diamidino-2-phenylindole (DAPI)). Scale bar = 20 μm.

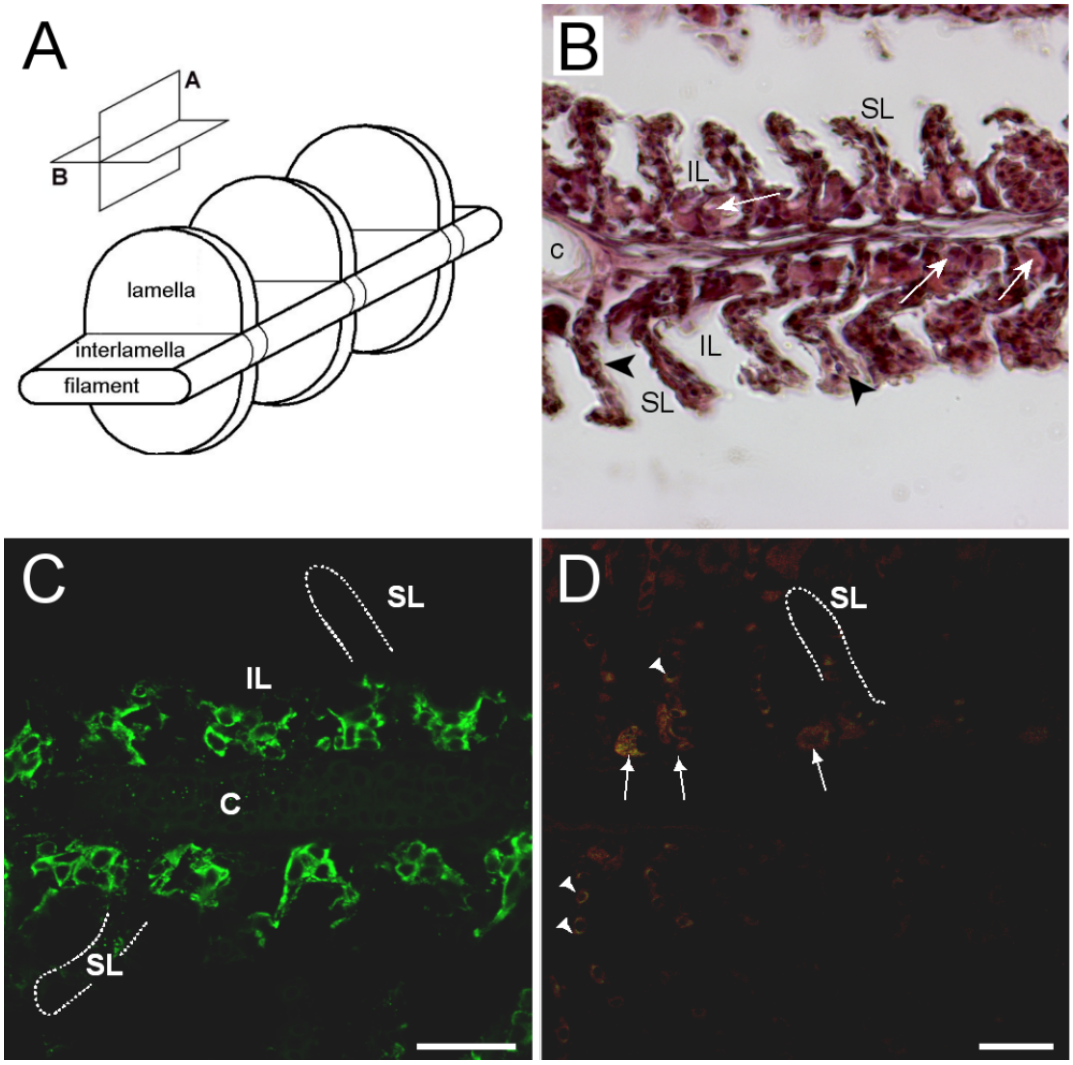

Figure 2.9 (**A**) three-dimensional (3D) diagram of gill filament morphology with orientation planes; (**B**) bright field image of sagittal gill section (plane A) of hematoxylin–eosin-stained gill filament; (**C**) representative confocal image of sagittal section from FW medaka gills showing immunoreactivity against medaka AQP3 (green)); and (**D**) negative control sagittal gill section incubated without primary antibodies. Abbreviations: SL = secondary lamella; IL = interlamellar space; and c = cartilage. Arrows point to ionocytes, and arrowheads point to red blood cells showing weak autofluorescence in (**D**). The outlines drawn in (**C**) and (**D**) show the contour of secondary lamellae for orientation. Scale bars = 20 μm.

2.4.4 Hormonal Effects on AQP Expression Ex Vivo

Incubation of gill explants for 18 h with cortisol had no significant effect on *AQP1, AQP3,* or *NCC2b* mRNA levels at any of the doses tested when compared with the control (Figure 2.10).

Incubation with ovine PRL induced dose-dependent increases in *AQP3* and *NCC2b* mRNA levels and no overall effect on *AQP1* mRNA levels (Figure 2.11). The effect of PRL was further investigated in a time-course experiment with 2, 6, and 18 h of incubation. Stimulation of *AQP3* was significant after 6 h of incubation, while control *AQP3* expression decreased with time (Figure 2.12B). There was no effect of PRL or time on *AQP1* levels (Figure 12A), whereas there was an overall stimulatory effect of PRL on *NCC2b* (Figure 2.12C). To test for interactive effects of cortisol and PRL, a combined incubation with the two hormones was conducted. This experiment confirmed the overall stimulatory effect of PRL on *AQP3* and *NCC2b* expression, while cortisol had no significant effect alone nor any interactive effect with PRL (Figure 2.13 B,C). *AQP1* expression was statistically unaffected by any of the hormone treatments (Figure 2.13A).

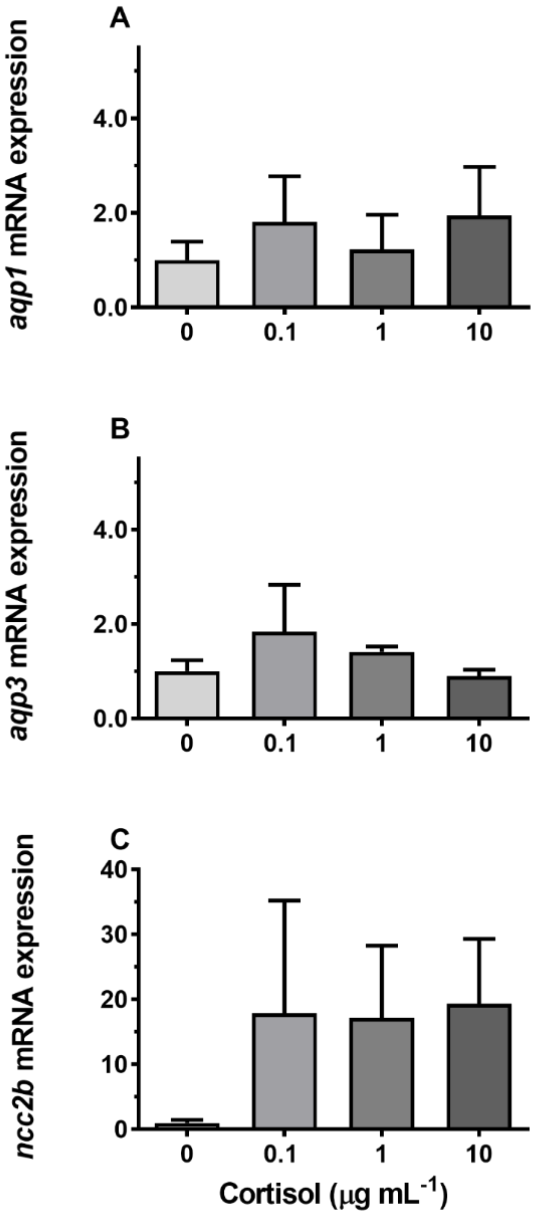

Figure 2.10 Ex vivo dose–response of cortisol (0, 0.1, 1, and 10 μg mL^{-1}) on *AQP1*, *AQP3*, and *NCC2b* expression in FW medaka gills. Gill explants were incubated for 18 h at room temperature. Expression of each target was normalized to the geometric mean of the three normalization genes: *EF1a*, *bact*, and *RPL7* and presented relative to the control. Data are presented as mean ± standard error of the mean (n = 4–6). No significant effects were observed (one-way ANOVA, $P < 0.05$).

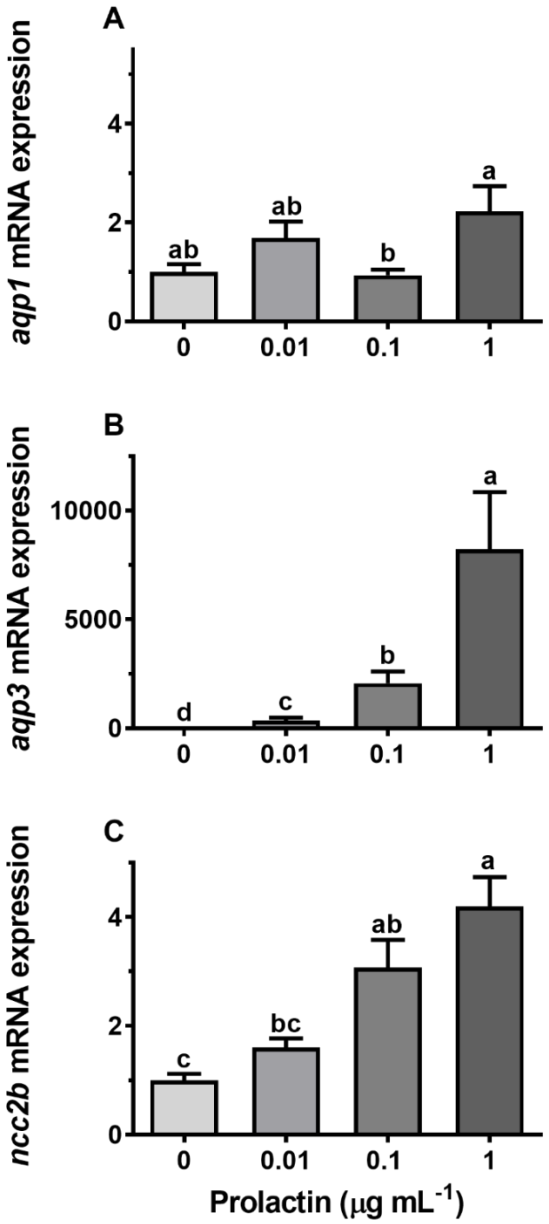

Figure 2.11 Ex vivo dose–response of prolactin (PRL, 0.01, 0.1, and 1 μg mL^{-1}) on *AQP1*, *AQP3*, and *NCC2b* expression in FW medaka gills. Gill explants were incubated for 18 h at room temperature. Expression of each target was normalized to the geometric mean of the three normalization genes: *EF1a*, *bact*, and *RPL7* and presented relative to the control. Data are presented as mean ± standard error of the mean (n = 7–8). Bars sharing a letter are not statistically different (one-way ANOVA, $P < 0.05$).

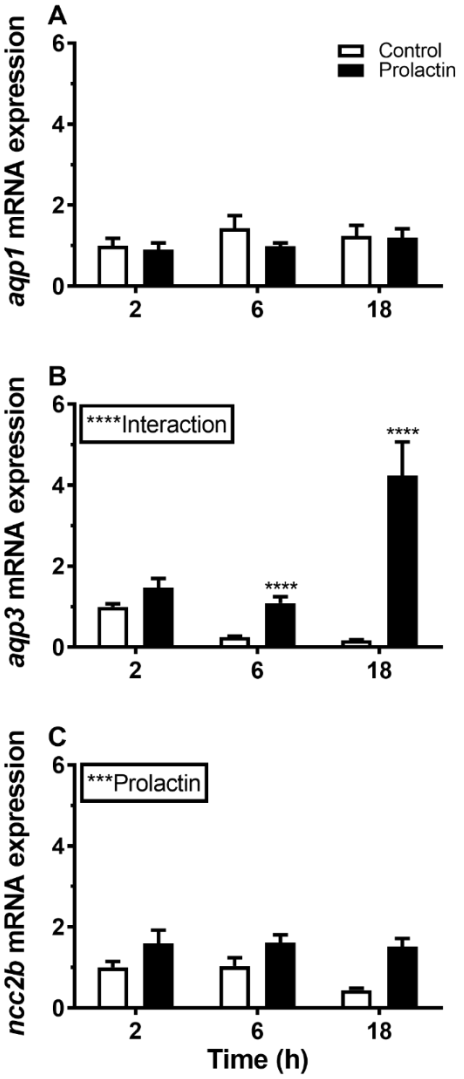

Figure 2.12 Ex vivo time-course effect of ovine PRL (1 μg mL^{-1}) on *AQP1*, *AQP3*, and *NCC2b* expression in FW medaka gills. Gill explants were incubated for 2, 6, and 18 h at room temperature. Control incubation (open bars); PRL incubation (solid bars). Expression of each target was normalized to the geometric mean of the three normalization genes: *EF1a*, *bact*, and *RPL7* and presented relative to the control. Data are presented as mean ± standard error of the mean (n = 7–8). Statistically significant factor effects (two-way ANOVA) are denoted by asterisks next to PRL (***P <0.001). When the interaction between the time and prolactin factor was significant, ****P <0.0001), asterisks were placed above the PRL group to indicate difference from the time-matched control (Sidak multiple comparisons test, ****P <0.0001).

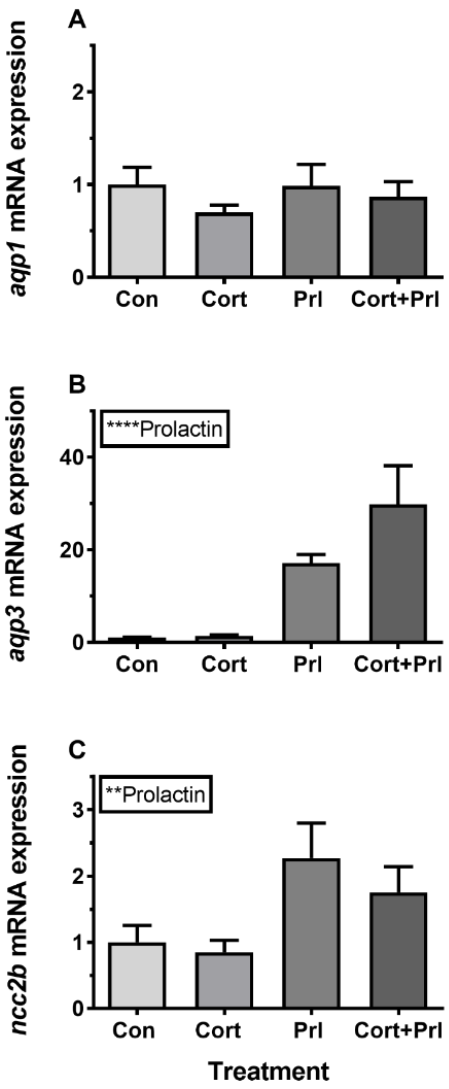

Figure 2.13 Ex vivo effect of cortisol (10 μg mL^{-1}), ovine PRL (1 μg mL^{-1}), and their combination on *AQP1*, *AQP3*, and *NCC2b* expression in FW medaka gills. Gill explants were incubated for 18 h at room temperature. Expression of each target was normalized to the geometric mean of the three normalization genes: *EF1a*, *bact*, and *RPL7.* Data are presented as mean ± standard error of the mean (n = 7–8). Statistically significant overall effects of prolactin (two-way ANOVA, P <0.05) are denoted by asterisks: **P <0.01, ****P <0.0001. No significant interaction between cortisol and prolactin factor was found, and post-hoc tests were therefore redundant.

2.5 Discussion

Japanese medaka is a euryhaline fish, which tolerates experimental transfers between different salinities, such as FW and SW and in the present study, IPW. Previous studies have shown that

ion-osmotic homeostasis is reestablished within a few days after transfer (Sakamoto et al., 2001; Madsen et al., 2014). It therefore serves as a good model species to study the plasticity of osmoregulatory organs. The present study investigated events related to water balance in the gill and focused on the response of two aquaporin paralogs expressed in whole gill: AQP1 and AQP3. We demonstrated a differential response of *AQP1* and *AQP3* when exposed to changing salinity and further investigated how the response may be mediated by osmoregulatory hormones. AQP3 mRNA and protein is stimulated in hypo-osmotic environments, a response which is possibly mediated by PRL, whereas AQP1 is constitutively expressed at low levels and unaffected by both salinity and the hormones PRL and cortisol.

2.5.1 Salinity Response of Branchial Aquaporins

The two investigated aquaporins, *AQP1* and *AQP3* were both expressed in whole gill tissue, which is in accordance with Madsen et al., 2014. Judging from the Ct-values of individual samples in our qPCR analyses (*AQP3*: 22–24, *AQP1*: 28–30), *AQP3* is overall expressed at a much higher transcript level than *AQP1*. Furthermore, *AQP3* levels were consistently down-regulated when fish were acclimated from FW to SW and with an initial increase (6 h) after transfer from FW to IPW. The decreased transcript level in SW was corroborated by a decrease in AQP3 protein, while the level remained constant 7 days after transfer to IPW. Overall, this suggests that AQP3 serves an important homeostatic function in the gill in response to osmotic changes, in particular during acclimation to hypo-osmotic conditions. By contrast, AQP1 mRNA and protein were unaffected by the present osmotic manipulations, suggesting that this paralog may serve a generic function independent of the osmotic environment. Thus, a differential regulation of the two aquaporins occurs in the gill in response to changes in the osmotic environment. The *NCC2b* cotransporter gene was measured as a marker of FW-type NCC ionocytes. NCC2 is essential for NaCl

homeostasis in hypo-osmotic environments by facilitating apical uptake of Na^+ and Cl^- (Hiroi et al., 2008; Inokuchi et al., 2008; Wang et al., 2009; Kwong et al., 2009; Kwong et al., 2016), and as expected we found that SW transfer was accompanied by a lasting decrease in *NCC2b* expression. Transfer to IPW, however, did not further stimulate *NCC2b* expression, suggesting that this transporter function is not a bottleneck in ion absorption under the present ion-poor conditions.

Previous papers have investigated the branchial expression of *AQP3* mRNA in different teleost species, and there is a developing consensus that expression of this aquaporin is lower in SW than in FW (European eel: (Cutler and Cramb 2002; Lignot et al. 2002); Japanese eel: (Tse et al., 2006); European seabass: (Giffard-Mena et al., 2007; Giffard-Mena et al., 2008); tilapia☹Breves et al., 2016); river pufferfish: (Jeong et al. 2014); silver seabream: (Deane and Woo, 2006); Atlantic salmon: (Tipsmark et al., 2010); marine medaka:(Kim et al., 2014); and killifish: (Jung et al., 2012). A report on sockeye salmon, however, showed up-regulation of branchial *AQP3* in SW-acclimated parr, while it was down-regulated in smolts (Choi et al. 2013). Branchial *AQP1* expression has also been investigated in relation to salinity in a few teleosts, but variable effects of salinity have been reported. In black porgy (An et al., 2008) and in marine medaka (Kim et al., 2014), a higher gill *AQP1* level was found in FW than in SW, whereas no salinity effect was found in seabass (Giffard-Mena et al. 2008), river pufferfish (Jeong et al. 2014), and climbing perch (Ip et al., 2013), the latter being in accordance with the present study in Japanese medaka. In Atlantic salmon, two related *AQP1* paralogs are expressed in gill tissue, *AQP1aa* and *AQP1ab*, which are inversely regulated by salinity (Tipsmark et al., 2010B), thus adding more diversity to the regulation of this aquaporin.

2.5.2 Immunolocalization and Physiological Function of Branchial Aquaporins

The cellular localization of the two aquaporin paralogs was investigated by immunofluorescence confocal microscopy. Our data showed a widespread immunoreactivity of AQP3 in cells in the interlamellar region of the filament, apparently in the periphery (membrane) of epithelial cells, as well as co-localizing with NKIR in ionocytes. This staining intensity was relatively weak and more scattered in ionocytes than other cell types, probably due to its localization in the basolateral tubular network. As reviewed by Madsen et al., 2015, previous investigations have emphasized that AQP3 is localized in filament chloride cells co-localizing with Nka in European eel (Lignot et al., 2002), Japanese eel (Tse et al., 2006), tilapia (Watanabe et al., 2005), rainbow wrasse (Brunelli et al. 2010), and killifish (Jung et al. 2012). Furthermore, electron microscopy studies by Lignot et al., 2002 and Watanabe et al., 2005 demonstrated that this aquaporin was localized in the basolateral membrane network and not in the apical area facing the surrounding water. However, upon closer inspection of these studies, AQP3 is also present in additional cells in the interlamellar region of the filament, named accessory cells in the study of Brunelli et al., 2010. Tse et al., 2006 found that *AQP3* is expressed in both chloride cells and pavement cells isolated from eel, and transcript levels decreased upon SW acclimation in both cell types. A study in killifish (Jung et al., 2012) reported AQP3 immunoreactivity to be present in pillar cells on the lamellae, which no other studies have confirmed, including the present study. Interestingly, a recent study in tilapia (Breves et al., 2016) reported AQP3 immunoreactivity in various epithelial cells of the gill, including ionocytes, mucous cells and pavement cells. The web-like mosaic of peripheral staining in interlamellar cells' staining pattern in their study closely resembles what we presently observed in Japanese medaka. These cells may be of different types, such as accessory cells and/or immature ionocytes. Thus, despite possible species differences, it

seems that AQP3 expression is not strictly confined to ionocytes but appears more widespread and may be important in other filament cell types.

Characteristically, AQP3 immunoreactivity appeared below the epithelial surface in cells deeper in the filament. The intensity of AQP3 immunoreactivity appeared quantitatively similar irrespective of salinity, thus not confirming the semi-quantitative western blot data showing slightly decreased whole gill AQP3 protein expression in SW fish. Based on the present localization pattern, it seems reasonable to conclude that AQP3 is functionally involved in epithelial cell volume control. Apical immunoreactivity in the epithelial surface facing the water was generally not observed. This makes sense, because steep osmotic gradients across the apical membrane of surface epithelia exist in both FW and SW, and low apical water permeability is important to keep transepithelial water fluxes to a minimum. Meanwhile, basolateral AQPs could support rapid cell volume adjustments coupled to the serosal compartment. It should also be kept in mind that AQP3 is classified as an aquaglyceroporin, meaning that it may facilitate transport of other small molecules, such as glycerol, which may have an important role in metabolism and the hydration status of these cells. In mammals, it is well established that AQP3 is expressed in the skin, where it is essential for epidermal glycerol transport and consequently hydration status (Hara-Chikuma and Verkman, 2006).

The present data overall show very weak AQP1 immunoreactivity in the gill, matching the lower mRNA level of this paralog. The staining pattern resembles that of AQP3, except that AQP1 does not seem to be present in NKIR ionocytes. Furthermore, AQP1 immunoreactivity is unaffected by salinity, suggesting that the paralogs have a generic function. As expected, AQP1 is also expressed in red blood cells, which agrees with the consensus in mammals (Madsen et al., 2015; King, et al., 2004). When analyzing whole tissue mRNA levels, the expression in (nucleated)

red blood cells may have masked subtle changes in mRNA expression within the epithelial cells in response to salinity. However, it is not possible to avoid this problem when analyzing whole tissue expression. The present protein data (western and immunofluorescence) support the stability of AQP1 expression. Localization of branchial AQP1 has only been investigated in a few studies. Using a homologous antibody, Cerdá and Finn 2010 detected AQP1 along the surface of the gill lamellae in zebrafish, whereas Brunelli et al., 2010 found strong reactivity in chloride cells in the rainbow wrasse using a heterologous rat AQP1 antibody. Preliminary data from Atlantic salmon also show AQP1 immunoreactivity in chloride cells using a homologous antibody (unpublished observations: Madsen, S.S.). Kwong et al., 2013 localized AQP1 basolaterally in ionocytes of the yolk sac of zebrafish larvae, where it was assigned a role in volume regulation. Thus, there seems to be species differences in localization of AQP1, and unfortunately, choice and quality of antibody may add to this divergence. AQP1 is also suspected of playing a role in CO_2 (and NH_3) transport (Chen et al., 2010; Horng et al., 2015); the former may be of functional importance in red blood cells and the latter may contribute to ammonia excretion across the gill surface (Ip et al., 2013).

2.5.3 Endocrine Regulation of Branchial Aquaporins

Surprisingly little attention has been given to the endocrine regulation of aquaporin expression in any vertebrate tissue or cell type. Whereas many molecular details about the classic vasopressin effect on AQP2 in the mammalian nephrons (Jung and Kwon, 2016) are known, other hormones and other AQPs remain largely unexplored. In fishes, the first study that addressed the endocrine regulation of any AQP was in European eel (Cutler et al., 2007B), where cortisol down-regulates *AQP3* mRNA in gills, thus mimicking the effect of SW-acclimation in this species. Due to the relatively small magnitude of the effect, the authors concluded that other factors might be involved in order to mediate the effect of hyper-osmotic exposure. Many years later, Breves et al. 2016

followed up on this initial attempt to get insight into the endocrinology of branchial AQP3 regulation and demonstrated in a series of in vivo and ex vivo experiments that pituitary PRL is a potent stimulatory factor of branchial AQP3 expression at both the mRNA and protein level. They also found that cortisol antagonizes the action of PRL, which supports the data of Cutler et al., 2007B in eel. At the same time, PRL may be the factor to fill in the gap in Cutler et al.'s study, because circulating PRL levels are known to be high in FW and low in SW, defining PRL as a FW hormone in teleosts (Manzon 2002; Cutler et al., 2007). Our data in medaka support the conclusion that PRL stimulates branchial *AQP3* expression in a dose- and time-dependent manner. As a control for the FW-acclimating action of PRL, we confirmed that the transcript level of the *NCC2* gene was also stimulated by the hormone, which is in agreement with Breves et al.'s (Breves et al., 2013; Breves et al., 2010B) observation in tilapia and zebrafish. *AQP3* has been linked to the osmosensing ability of Mozambique tilapia pituitary PRL secreting cells and their release of PRL in hypo-osmotic environments, further connecting this hormone with hypo-osmotic acclimation (Watanabe et al., 2009). In comparison with *AQP3*, *AQP1* expression was unaffected by PRL, which is congruent with the lack of effect of the osmotic environment. To our knowledge, no other studies have investigated hormonal effects on gill AQP1 in any teleost. Cortisol, the main corticosteroid in teleost fish, did not have a significant effect on *AQP3* expression either alone or in combination with PRL. The effect of PRL was also not modulated by the presence of cortisol in ex vivo hormone experiments, which is contrary to findings in European eel (Cutler et al., 2007B) and in tilapia (Breves et al., 2010).

2.6 Conclusions

This study has increased our understanding of the localization and of AQP1 and AQP3 within a euryhaline fish gill. There is a partial overlap in the cellular localization of these two paralogs in

the gill epithelium, suggesting that they both play roles in cellular volume homeostasis. They are however, differentially regulated in response to environmental salinity and hormonal manipulation. AQP1 is stably expressed irrespective of salinity and hormone manipulation, whereas AQP3 mRNA and protein respond dynamically and inversely to environmental salinity and are stimulated by PRL. Transfer from FW to ion-poor conditions does not further affect AQP3 expression, suggesting that cell volume homeostasis is not further challenged by this manipulation.

2.7 References

Agre, P.E.; Preston, G.M.; Smith, B.L.; Jung, J.S.; Raina, S.U.; Moon, C.H.; Guggino, W.B.; Nielsen, S.B. Aquaporin CHIP: The archetypal molecular water channel. *Am. J. Phys.-Renal* 1993, *265*, 463–476, doi:10.1152/ajprenal.1993.265.4.F463.

An, K.W.; Kim, N.N.; Choi, C.Y. Cloning and expression of aquaporin 1 and arginine vasotocin receptor mRNA from the black porgy, *Acanthopagrus schlegeli*: Effect of freshwater acclimation. *Fish Phys. Biochem.* 2008, *34*, 185–194, doi:10.1007/s10695-007-9175-0.

Bollinger, R.J.; Madsen, S.S.; Bossus, M.C.; Tipsmark, C.K. Does Japanese medaka (*Oryzias latipes*) exhibit a gill Na^+/K^+-ATPase isoform switch during salinity change? *J. Comp. Phys. B* 2016, *186*, 485–501, doi:10.1007/s00360-016-0972-6.

Bollinger, R.J.; Ellis, L.V.; Bossus, M.C.; Tipsmark, C.K. Prolactin controls Na^+, Cl^- cotransporter via Stat5 pathway in the teleost gill. *Mol. Cell. Endocrinol.* 2018, *477*, 163–171, doi:10.1016/j.mce.2018.06.014.

Boury-Jamot, M.; Sougrat, R.; Tailhardat, M.; Le Varlet, B.; Bonte, F.; Dumas, M.; Verbavatz, J.M. Expression and function of aquaporins in human skin: Is aquaporin-3 just a glycerol transporter? *BBA-Biomembranes* 2006, *1758*, 1034–1042, doi:10.1016/j.bbamem.2006.06.013.

Bossus, M.C.; Madsen, S.S.; Tipsmark, C.K. Functional dynamics of claudin expression in Japanese medaka (*Oryzias latipes*): Response to environmental salinity. *Comp. Biochem. Phys. A* 2015, *187*, 74–85, doi:10.1016/j.cbpa.2015.04.017.

Bossus, M.C.; Bollinger, R.J.; Reed, P.J.; Tipsmark, C.K. Prolactin and cortisol regulate branchial claudin expression in Japanese medaka. *Gen. Comp. Endocrinol.* 2017, *240*, 77–83, doi:10.1016/j.ygcen.2016.09.010.

Breves, J.P.; Watanabe, S.; Kaneko, T.; Hirano, T.; Grau, E.G. Prolactin restores branchial mitochondrion-rich cells expressing Na^+/Cl^- cotransporter in hypophysectomized Mozambique tilapia. *Am. J. Phys.-Reg. I* 2010, *299*, 702–710, doi:10.1152/ajpregu.00213.2010.

Breves, J.P.; Hirano, T.; Grau, E.G. Ionoregulatory and endocrine responses to disturbed salt and water balance in Mozambique tilapia exposed to confinement and handling stress. *Comp. Biochem. Phys. A* 2010 B, *155*, 294–300, doi:10.1016/j.cbpa.2009.10.033.

Breves, J.P.; Serizier, S.B.; Goffin, V.; McCormick, S.D.; Karlstrom, R.O. Prolactin regulates transcription of the ion uptake Na^+/Cl^- cotransporter (ncc) gene in zebrafish gill. *Mol. Cell. Endocrinol.* 2013, *369*, 98–106, doi:10.1016/j.mce.2013.01.021.

Breves, J.P.; McCormick, S.D.; Karlstrom, R.O. Prolactin and teleost ionocytes: New insights into cellular and molecular targets of prolactin in vertebrate epithelia. *Gen. Comp. Endocrinol.* 2014, *203*, 21–28, doi:10.1016/j.ygcen.2013.12.014.

Breves, J.; Inokuchi, M.; Yamaguchi, Y.; Seale, A.P.; Hunt, B.; Watanabe, S.; Lerner, D.; Kaneko, T., Grau, G. Hormonal regulation of aquaporin 3: Opposing actions of prolactin and cortisol in tilapia gill. *J. Endocrinol.* 2016, doi:10.1530/JOE-16-0162.

Brunelli, E.; Mauceri, A.; Salvatore, F.; Giannetto, A.; Maisano, M.; Tripepi, S. Localization of aquaporin 1 and 3 in the gills of the rainbow wrasse. *Coris julis*. *Acta Histochem.* 2010, *112*, 251–258, doi:10.1016/j.acthis.2008.11.030.

Cerdà, J.; Finn, R.N. Piscine aquaporins: An overview of recent advances. *J. Exp. Zool. A* 2010, *313*, 623–650, doi:10.1002/jez.634.

Chen, L.-M.; Zhao, J.; Musa-Aziz, R.; Pelletier, M.F.; Drummond, I.A.; Boron, W.F. Cloning and characterization of a zebrafish homologue of human AQP1: A bifunctional water and gas channel. *Am. J. Phys.-Reg. I* 2010, *299*, 1163–1174, doi:10.1152/ajpregu.00319.2010.

Choi, Y.J.; Shin, H.S.; Kim, N.N.; Cho, S.H.; Yamamoto, Y.; Ueda, H.; Lee, J.; Choi, C.Y. Expression of aquaporin-3 and-8 mRNAs in the parr and smolt stages of sockeye salmon, *Oncorhynchus nerka*: Effects of cortisol treatment and seawater acclimation. *Comp. Biochem. Phys. A* 2013, *165*, 228–236, doi:10.1016/j.cbpa.2013.03.013.

Cutler, C.P.; Cramb, G. Branchial expression of an aquaporin 3 (AQP-3) homologue is downregulated in the European eel *Anguilla anguilla* following seawater acclimation. *J. Exp. Biol.* 2002, *205*, 2643–2651, doi:0022-0949.

Cutler, C.P.; Martinez, A.S.; Cramb, G. The role of aquaporin 3 in teleost fish. *Comp. Biochem. Phys. A* 2007, *148*, 82–91, doi:10.1016/j.cbpa.2006.09.022.

Cutler, C.P.; Phillips, C.; Hazon, N.; Cramb, G. Cortisol regulates eel (*Anguilla anguilla*) aquaporin 3 (AQP3) mRNA expression levels in gill. *Gen. Comp. Endocrinol.* 2007 B, *152*, 310–313, doi:10.1016/j.ygcen.2007.01.031.

Deane, E.E.; Woo, N.Y. Tissue distribution, effects of salinity acclimation, and ontogeny of aquaporin 3 in the marine teleost, silver sea bream (*Sparus sarba*). *Mar. Biotechnol.* 2006, *8*, 663–671, doi:10.1007/s10126-006-6001-0.

Ecelbarger, C.A.; Terris, J.A.; Frindt, G.U.; Echevarria, M.I.; Marples, D.; Nielsen, S.; Knepper, M.A. Aquaporin-3 water channel localization and regulation in rat kidney. *Am. J. Phys.-Renal* 1995, *269*, 663–672, doi:10.1152/ajprenal.1995.269.5.F663.

Edwards, S.L.; Marshall, W.S. Principles and patterns of osmoregulation and euryhalinity in fishes. In *Fish Physiology*; McCormick, S., Farrel, A., Brauner, C., Eds.; Elsevier: Cambrdige, MA, USA, 2013; Volume 32, pp. 1–44, ISBN 9780123969514.

Evans, D.H.; Piermarini, P.M.; Choe, K.P. The multifunctional fish gill: Dominant site of gas exchange, osmoregulation, acid-base regulation, and excretion of nitrogenous waste. *Phys. Rev.* 2005, *85*, 97–177, doi:10.1152/physrev.00050.2003.

Finn, R.N.; Chauvigné, F.; Hlidberg, J.B.; Cutler, C.P.; Cerdà, J. The lineage-specific evolution of aquaporin gene clusters facilitated tetrapod terrestrial adaptation. *PLoS ONE* 2014, 9, e113686, doi:10.1371/journal.pone.0113686.

Flik, G.; Rentier-Delrue, F.; Wendelaar Bonga, S. Calcitropic effects of recombinant prolactins in *Oreochromis mossambicus*. *Am. J. Phys.-Reg. I* 1994, *266*, 1302–1308, doi:10.1152/ajpregu.1994.266.4.R1302.

Giffard-Mena, I.; Boulo, V.; Aujoulat, F.; Fowden, H.; Castille, R.; Charmantier, G.; Cramb, G. Aquaporin molecular characterization in the sea-bass (*Dicentrarchus labrax*): The effect of salinity on AQP1 and AQP3 expression. *Comp. Biochem. Phys. A* 2007, *148*, 430–444, doi:10.1016/j.cbpa.2007.06.002.

Giffard-Mena, I.; Lorin-Nebel, C.; Charmantier, G.; Castille, R.; Boulo, V. Adaptation of the sea-bass (*Dicentrarchus labrax*) to fresh water: Role of aquaporins and Na^+/K^+-ATPases. *Comp. Biochem. Phys. A* 2008, *150*, 332–338, doi:10.1016/j.cbpa.2008.04.004.

Hiroi, J.; Yasumasu, S.; McCormick, S.D.; Hwang, P.P.; Kaneko, T. Evidence for an apical Na-Cl cotransporter involved in ion uptake in a teleost fish. *J. Exp. Biol.* 2008, *211*, 2584–2599, doi:10.1242/jeb.018663.

Hara-Chikuma, M.; Verkman, A. Physiological roles of glycerol-transporting aquaporins: The aquaglyceroporins. *Cell. Mol. Life Sci.* 2006, *63*, 1386–1392, doi:10.1007/s00018-006-6028-4.

Hoffmann, E.K.; Lambert, I.H.; Pedersen, S.F. Physiology of cell volume regulation in vertebrates. *Phys. Rev.* 2009, *89*, 193–277, doi:10.1152/physrev.00037.2007.

Horng, J.-L.; Chao, P.-L.; Chen, P.-Y.; Shih, T.-H.; Lin, L.-Y. Aquaporin 1 is involved in acid secretion by ionocytes of zebrafish embryos through facilitating CO2 transport. *PLoS ONE* 2015, *10*, e0136440, doi:10.1371/journal.pone.0136440.

Hsu, H.H.; Lin, L.Y.; Tseng, Y.C.; Horng, J.L.; Hwang, P.P. A new model for fish ion regulation: Identification of ionocytes in freshwater-and seawater-acclimated medaka (*Oryzias latipes*). *Cell Tissue Res.* 2014, *357*, 225–243, doi:10.1007/s00441-014-1883-z.

Inokuchi, M.; Hiroi, J.; Watanabe, S.; Lee, K.M.; Kaneko, T. Gene expression and morphological localization of NHE3, NCC and NKCC1a in branchial mitochondria-rich cells of Mozambique tilapia (*Oreochromis mossambicus*) acclimated to a wide range of salinities. *Comp. Biochem. Phys. A* 2008, *151*, 151–158, doi:10.1016/j.cbpa.2008.06.012.

Ip, Y.K.; Soh, M.M.L.; Chen, X.L.; Ong, J.L.Y.; Chng, Y.R.; Ching, B.Y.; Wong, W.P.; Lam, S.H.; Chew, S.F. Molecular characterization of branchial aquaporin 1aa and effects of seawater acclimation, emersion or ammonia exposure on its mRNA expression in the gills, gut, kidney and skin of the freshwater climbing perch, *Anabas testudineus*. *PLoS ONE* 2013, *8*, doi:10.1371/journal.pone.0061163.

Isaia, J. Water and nonelectrolyte permeation. In *Fish physiology*; Hoar, W.S., Randall, D.J., Eds.; Academic Press: London, UK, 1984; Volume 10, pp. 1–38, ISBN 1546-5098.

Ishibashi, K.; Hara, S.; Kondo, S. Aquaporin water channels in mammals. *Clin. Exp. Nephrol.* 2009, *13*, 107–117, doi:10.1007/s10157-008-0118-6.

Jeong, S.-Y.; Kim, J.-H.; Lee, W.-O.; Dahms, H.-U.; Han, K.-N. Salinity changes in the anadromous river pufferfish, Takifugu obscurus, mediate gene regulation. *Fish Phys. Biochem.* 2014, *40*, 205–219, doi:10.1007/s10695-013-9837-z.

Jung, D.; Sato, J.D.; Shaw, J.R.; Stanton, B.A. Expression of aquaporin 3 in gills of the Atlantic killifish (*Fundulus heteroclitus*): Effects of seawater acclimation. *Comp. Biochem. Phys. A* 2012, *161*, 320–326, doi:10.1016/j.cbpa.2011.11.014.

Jung, H.J.; Kwon, T.-H. Molecular mechanisms regulating aquaporin-2 in kidney collecting duct. *Am. J. Phys.-Renal* 2016, *311*, 1318–1328, doi:10.1152/ajprenal.00485.2016.

Kim, Y.K.; Lee, S.Y.; Kim, B.S.; Kim, D.S.; Nam, Y.K. Isolation and mRNA expression analysis of aquaporin isoforms in marine medaka *Oryzias dancena*, a euryhaline teleost. *Comp. Biochem. Phys. A* 2014, *171*, 1–8, doi:10.1016/j.cbpa.2014.01.012.

King, L.S.; Kozono, D.; Agre, P. From structure to disease: The evolving tale of aquaporin biology. *Nat. Rev. Mol. Cell. Biol.* 2004, *5*, 687, doi:10.1038/nrm1469.

Kwong, A.K.Y.; Ng, A.H.Y.; Leung, L.Y.; Man, A.K.Y.; Woo, N.Y.S. Effect of extracellular osmolality and ionic levels on pituitary prolactin release in euryhaline silver sea bream (*Sparus sarba*). *Gen. Comp. Endocrinol.* 2009, *160*, 67–75, doi:10.1016/j.ygcen.2008.10.024.

Kwong, R.W.M.; Kumai, Y.; Perry, S.F. The role of aquaporin and tight junction proteins in the regulation of water movement in larval zebrafish (*Danio rerio*). *PLoS ONE* 2013, *8*, doi:10.1371/journal.pone.0070764.

Kwong, R.W.M.; Kumai, Y.; Perry, S.F. Neuroendocrine control of ionic balance in zebrafish. *Gen. Comp. Endocrinol.* 2016, *234*, 40–46, doi:10.1016/j.ygcen.2016.05.016.

Lee, S.Y.; Nam, Y.K.; Kim, Y.K. Characterization and expression profiles of aquaporins (AQPs) 1a and 3a in mud loach *Misgurnus mizolepis* after experimental challenges. *Fish. Aquat. Sci.* 2017, *20*, 23, doi:10.1186/s41240-017-0068-6.

Lignot, J.-H.; Cutler, C.P.; Hazon, N.; Cramb, G. Immunolocalisation of aquaporin 3 in the gill and the gastrointestinal tract of the European eel *Anguilla anguilla* (L.). *J. Exp. Biol.* 2002, *205*, 2653–2663, doi:0022-0949.

Madsen, S.S.; Bujak, J.; Tipsmark, C.K. Aquaporin expression in the Japanese medaka (*Oryzias latipes*) in freshwater and seawater: Challenging the paradigm of intestinal water transport? *J. Exp. Biol.* 2014, *217*, 3108–3121, doi:10.1242/jeb.105098.

Madsen, S.S.; Engelund, M.B.; Cutler, C.P. Water transport and functional dynamics of aquaporins in osmoregulatory organs of fishes. *Biol. Bull.* 2015, *229*, 70–92, doi:10.1086/BBLv229n1p70.

Manzon, L.A. The role of prolactin in fish osmoregulation: A review. *Gen. Comp. Endocrinol.* 2002, *125*, 291–310, doi:10.1006/gcen.2001.7746.

Marshall, W.S.; Lynch, E.A.; Cozzi, R.R.F. Redistribution of immunofluorescence of CFTR anion channel and NKCC cotransporter in chloride cells during adaptation of the killifish *Fundulus heteroclitus* to sea water. *J. Exp. Biol.* 2002, *205*, 1265–1273, ISSN 0022-0949.

Marshall, W.S.; Grosell, M. Ion transport, osmoregulation, and acid -base regulation. In *The Physiology of Fishes;* Evans, D.H., Clairborne, J.B., Eds.; Taylor and Francis Group: Boca Raton, FL, USA, 2006; pp. 177–210, ISBN 978-0849380426.

McCormick, S.D. Endocrine control of osmoregulation in teleost fish. *Am. Zool.* 2001, *41*, 781–794, doi:10.1093/icb/41.4.781.

Motais, R.; Isaia, J.; Rankin, J.; Maetz, J. Adaptive changes of the water permeability of the teleostean gill epithelium in relation to external salinity. *J. Exp. Biol.* 1969, *51*, 529–546, doi:0022-0949.

Nilsson, S. Control of gill blood flow. In *Fish Physiology: Recent Advances*; Nilsson, S., Ed.; Springer: New York, NY, USA, 1986; pp. 86–101, ISBN 978-94-011-6560-0.

Pfaffl, M.W. A new mathematical model for relative quantification in real-time RT-PCR. *Nucleic Acids Res.* 2001, *29*, doi:10.1093/nar/29.9.e45.

Sakamoto, T.; Kozaka, T.; Takahashi, A.; Kawauchi, H.; Ando, M. Medaka (*Oryzias latipes*) as a model for hypoosmoregulation of euryhaline fishes. *Aquaculture* 2001, *193*, 347–354, doi:10.1016/S0044-8486(00)00471-3.

Schindelin, J.; Arganda-Carreras, I.; Frise, E.; Kaynig, V.; Longair, M.; Pietzsch, T.; Preibisch, S.; Rueden, C.; Saalfeld, S.; Schmid, B.; et al. Fiji: An open-source platform for biological-image analysis. *Nat. Methods* 2012, *9*, 676–682, doi:10.1038/nmeth.2019.

Sugiyama, Y.; Ota, Y.; Hara, M.; Inoue, S. Osmotic stress up-regulates aquaporin-3 gene expression in cultured human keratinocytes. *BBA-Gene Struct. Expr.* 2001, *1522*, 82–88, doi:10.1016/S0167-4781(01)00320-7.

Takei, Y.; McCormick, S.D. Euryhaline fishes: Hormonal control of fish euryhalinity. In *Fish Physiology;* McCormick, S., Farrel, A., Brauner, C., Eds.; Elsevier: Cambrdige, MA, USA, 2013; Volume 32, pp. 69–123, ISBN 9780123969514.

Tingaud-Sequeira, A.; Chauvigné, F.; Fabra, M.; Lozano, J.; Raldúa, D.; Cerdà, J.A. Structural and functional divergence of two fish aquaporin-1 water channels following teleost-specific gene duplication. *BMC Evol. Biol.* 2008, *8*, 259, doi:10.1186/1471-2148-8-259.

Tipsmark, C.K.; Luckenbach, J.A.; Madsen, S.S.; Borski, R.J. IGF-I and branchial IGF receptor expression and localization during salinity acclimation in striped bass. *Am. J. Phys.-Reg. I* 2007, *292*, 535–543, doi:10.1152/ajpregu.00915.2005.

Tipsmark, C.K.; Madsen, S.S. Distinct hormonal regulation of Na^+,K^+-Atpase genes in the gill of Atlantic salmon (*Salmo salar* L.). *J. Endocrinol.* 2009, *203*, 301–310, doi:10.1677/joe-09-0281.

Tipsmark, C.K.; Sørensen, K.J.; Madsen, S.S. Aquaporin expression dynamics in osmoregulatory tissues of Atlantic salmon during smoltification and seawater acclimation. *J. Exp. Biol.* 2010, *213*, 368–379, doi:10.1242/jeb.034785.

Tipsmark, C.K.; Sørensen, K.J.; Hulgard, K.; Madsen, S.S. Claudin-15 and-25b expression in the intestinal tract of Atlantic salmon in response to seawater acclimation, smoltification and hormone treatment. *Comp. Biochem. Phys. A* 2010 B, *155*, 361–370, doi:10.1016/j.cbpa.2009.

Tse, W.K.F.; Au, D.W.T.; Wong, C.K.C. Characterization of ion channel and transporter mRNA expressions in isolated gill chloride and pavement cells of seawater acclimating eels. *Biochem. Biophys. Res. Commun.* 2006, *346*, 1181–1190, doi:10.1016/j.bbrc.2006.06.028.

Wang, Y.F.; Tseng, Y.C.; Yan, J.J.; Hiroi, J.; Hwang, P.P. Role of SLC12A10.2, a Na-Cl cotransporter-like protein, in a Cl uptake mechanism in zebrafish (*Danio rerio*). *Am. J. Phys.-Reg. I* 2009, *296*, 1650–1660, doi:10.1152/ajpregu.00119.2009.

Watanabe, S.; Kaneko, T.; Aida, K. Aquaporin-3 expressed in the basolateral membrane of gill chloride cells in Mozambique tilapia *Oreochromis mossambicus* adapted to freshwater and seawater. *J. Exp. Biol.* 2005, *208*, 2673–2682, doi:10.1242/jeb.01684

Watanabe, S.; Hirano, T.; Grau,E.G.; Kaneko, T. Osmosensitivity of prolactin cells is enhanced by the water channel aquaporin-3 in a euryhaline Mozambique tilapia (*Oreochromis mossambicus*). *Am. J. Phys.-Reg. I* 2009, *296*, 446–453, doi:10.1152/ajpregu.90435.2008.

Wilson, J.M.; Laurent, P. Fish gill morphology: Inside out. *J. Exp. Zool.* 2002, *293*, 192–213, doi:10.1002/jez.10124.

Chapter 3 Regulation and Localization of Claudin-30c in Gill and Larval Integument of Japanese Medaka, *Oryzias latipes*

Laura V. Ellis[1], Christian K. Tipsmark[1]

[1] Department of Biological Sciences, University of Arkansas, Fayetteville, AR 72701, USA

3.1 Abstract

The dynamic shift in osmoregulation between FW and SW environments, including the changes in gill cell composition, allows euryhaline fish, such as the Japanese medaka to persist and thrive while exposed to changes in environmental salinities. The tight junction within the fish gill epithelium controls paracellular ion and water movement (Evans et al., 2005). Within the hypoosmotic FW environment, the tight junctions counter the paracellular loss of ions and influx of water, while active uptake from the environment through the use of ion transporters aids in the regulation of internal osmotic concentrations. Conversely in SW, the passive gain of ions and loss of water is a constant threat to homeostasis. In addition, active ion secretion is dependent on active transcellular Cl^- secretion by MRCs coupled to a paracellular "leaky" pathway for Na^+ . Of the claudin isoforms present in the tight junctions, Claudin 30c (Cldn30c) is a barrier forming claudin abundant in the euryhaline fish gill. Research focused on the regulation of Claudin30c mRNA expression and protein abundance in response to salinity challenges in the medaka gill and hatchling medaka. Initial ion poor water exposure caused a significant increase in *cldn30c* mRNA expression, while long term acclimation in SW caused a decrease in Cldn30c protein abundance. Immunolocalization studies showed Cldn30c to be in the periphery of polygonal cells on the integument of two day old hatchlings.

3.2 Introduction

Euryhaline fish, such as the Japanese medaka (*Oryzais latipes),* are capable of maintaining their internal osmotic concentrations (350mOsm) while experiencing a wide range of environmental fluctuations in salinity (Evans et al., 2005; Bossus et al., 2015). The phenotypic plasticity of the gill, kidney, and intestine are the major contributing organs responsible for the

ability to acclimate from freshwater (FW) (1mOsm) to full strength seawater (SW) (1050 mOsm) (Evans et al., 2005; Bossus et al., 2015). The gills of medaka goes through dynamic changes during salinity fluctuations. In FW, mitochondrion-rich cells (MRCs) are associated with pavement cells (PVCs) and have deep junctions between them that act as a barrier to water and ion movement (Marshal and Grosell, 2006). Conversely in SW, the junctions formed between MRCs and accessory cells (ACs) are shallow and are considered "leaky" with respect to ion movement (Sardet et al., 1979).

Tight junctions are composed of multiple proteins, claudins (Cldns), occludins, tricellulin, and junctional adhesion molecules (Kwong and Perry, 2013; Rosenthal et al., 2020). Tight junction proteins are similar in composition with four transmembrane domains, two extracellular loops, and are linked to the cytoskeleton by a cytosolic carboxyl- terminal, which interacts with adaptor molecules like zonula occludens (Gonzalez-Mariscal et al., 2008; Bossus et al., 2015; Rosenthal et al., 2020). Claudins are a super-family of tight junction proteins which regulate the permeability and ion selectivity of the tight junctions (Van Italie et al., 2001; Rosenthal et al., 2020). While there have been 27 mammalian claudins described, teleost fish have between 54-56 due to genetic duplication (Baltzegar et al., 2013; Gunzel and Yu, 2013). Claudin isoforms have been demonstrated to be regulated by salinity and expressed in a tissue specific manner (Tipsmark et al., 2008).

Claudin 30c (Cldn30c) is highly expressed in the gills of medaka and has been demonstrated to be involved in control of gill epithelia (Tipsmark et al., 2008; Engelund et al., 2012, Bossus et al., 2015). Tissue distribution shows that Cldn30c is present in the kidney,

intestine, muscle, and liver of medaka but predominantly found in the gill (Bossus et al., 2015). Previous work within our lab, showed that *cldn30c* mRNA expression in long term freshwater (FW) and seawater acclimated medaka is similar, therefore leading us to believe that Cldn30c has generic barrier function within the tight junction complex (Bossus et al., 2015). Therefore, Cldn30C may be involved in the maintenance of the deep tight junctions within the gill cell matrix, and the overall gill integrity (Bossus et al., 2015). Investigations into Cldn30c have been predominately focused on response to salinity, with one study showing functional significance in a heterologous mammalian expression system (Engelund et al., 2012). However, new techniques have become available to investigate the effects of loss of function on the ability of fish to respond to ionic and osmotic stressors.

Japanese medaka, in addition to their euryhaline capability, are a useful model species for investigating general vertebrate physiology (Yan and Hwang, 2019). Medaka are easy to rear in the lab, have a fully sequenced genome, and have clear embryos which are ideal for injections (Tanaka 1995; Iwamatsu 2004; Hubbard et al., 2007). The embryos develop within 10 days in a 28 °C incubator and after hatching the fish reach sexual maturity within 2 months (Iwamatsu 2004). Medaka are ideal models for loss of function studies as they have a smaller genome than their stenohaline distant relative the zebrafish (*Danio rerio*) (800Mb vs 1700Mb), can withstand fluctuations in salinity as well as temperature, and breeding is induced readily through increased feeding of mating pairs.

Loss of function, such as the knockdown of protein translation through the use of morpholinos, have become a common tool used in physiological studies from frogs to fish

(Heasman et al., 2000; Nasevicius and Ekker, 2000). Morpholino antisense oligionucleotides are commonly used to block the translation of mRNA through binding to the beginning of the coding region or block splicing through binding to the introns/exons (Zimmer et al.. 2019). Morpholinos are built against a specific sequence within the mRNA and the complementary base pairs act as a barrier to halt the translation from mRNA to fully functional proteins. Since the invention of vivo-morpholinos in 2008, the knockdown effects seen previously in only early development can now be seen throughout adults and even in cell culture (Morcos et al., 2008; Moulton and Shan, 2009; Ferguson et al., 2014). Vivo-morpholinos contain an octa-guanidine dendrimer conjugate which, when bound to the morpholino, can penetrate cell membranes (Morcos et al., 2018). Medaka have been used in previous studies to investigate development, gastrulation, orientation of the spinal cord, and the formation of bone, however no study to date has used the technique in medaka to investigate osmoregulation or ion regulation (Kinoshita et al., 2001; Shima and Mitani, 2004; Herpin et al., 2008; Yang et al., 2018; Zimmer et al., 2019).

Our study aims to understand the role of Cldn30c within the tight junction complex of the gill of Japanese Medaka through localization and expression studies with the ultimate goal to use loss of function methods, like morpholinos, to establish functional significance. Based on previous work, we had four objectives: 1 challenge medaka with salinity changes to investigate the time course regulatory patterns of Cldn30c during acclimation from FW to SW and FW to ion poor water IPW; 2 localize Cldn30c within the integumental epithelium of hatchling medaka; 3 validate Cldn30c antibody and examine protein abundance levels in adults acclimated to FW and SW and hatchling medaka; and 4 knockdown Cldn30c using morpholinos and examine effects on paracellular permeability.

This study's final aim was to knockdown Cldn30c using morpholinos and we were able to complete one round of embryo injections before the COVID 19 pandemic forced University and research labs to close. Continued research is necessary to utilize morpholino knockdowns in osmoregulatory studies.

3.3 Methods

3.3.1 Fish and Maintenance

Adult Japanese medaka (*O. latipes*, Temmink & Schlegel; size range: 25-35 mm, weight range: 250-350 mg) were obtained from Aquatic Research Organisms, Inc. (Hampton, NH, USA). Fish were acclimatized and kept in recirculating de-chlorinated filtered water (in mmol L^{-1}: 0.34 Na^+, 0.64 Ca^{2+}, 0.09 Mg^{2+}, 0.03 K^+). Fish were maintained in a 14 h light: 10 h dark photoperiod at a temperature of 20°C. Medaka were fed daily with Tetramin tropical flakes (Tetra, United Pet Group, Blacksburg, VA, USA) and food withheld 24 h prior to sampling. Medaka were sacrificed by cervical dislocation and subsequent pithing of the brain after which the gill apparatus, or other tissues, were removed and washed with PBS (Phosphate Buffer Saline, Roche Diagnostics, Indianapolis, IN, USA).

Breeding was conducted by creating breeding pairs with two females and one male in Aquaneering system tanks (Aquaneering, San Diego CA. Breeding conditions were induced by feeding freshly hatched brine shrimp three times daily, water was constantly circulated and maintained from 26-28°C. Female medaka lay eggs at sunrise each day, eggs were collected each morning from the females or off the bottom of the tank. The eggs are fertilized post lay by the male through the environment. Embryos were maintained in a 28°C incubator and media was changed daily. Embryos hatched after 8-10 days in incubation and were kept until 2 days post

hatch. Hatchling medaka are sacrificed by MS222 (2ug/ml). All handling and experimental procedures were approved by the Animal Care and Use Committee of the University of Arkansas (IACUC 14042 and 17091).

3.3.2 RNA Isolation, cDNA synthesis and quantitative PCR

cDNA synthesis RNA isolation was conducted according to the published manufactures protocol TRI Reagent® (Sigma Aldrich, St. Louis, MO, USA). All samples were homogenized using a Power Max 200 rotating knife homogenizer (Advanced Homogenizing System; Manufactured by PRO Scientific for Henry Troemner LLC, Thorofare, NJ, USA). Gill RNA, 500ng from salinity trials, was used for cDNA synthesis in the Applied Biosystems high capacity cDNA reverse transcription kit (Thermo Fisher). Primers used were previously validated and published (Bossus et al. 2016, Madsen et al. 2014). Elongation Factor 1 alpha, *ef1a*, beta-actin, *bact*, ribosomal protein PO, *rpl7*, were used as normalization genes for all experiments. Quantitative real-time qPCR was run on a Bio-Rad CFX96 (BioRad, Hercules, CA, USA) using SYBR® Green Jump Start™ (Sigma Aldrich). Quantitative real-time qPCR cycling was conducted using the published protocol, (Bossus et al. 2016, Bollinger et al. 2018). Data were normalized to the geometric mean of the three normalization genes and were presented relative to control group.

3.3.3 Western Blot Analysis

Gills were placed directly into 1.5 mL sonication tubes in 1xLDS (Lithium Dodecyl Sulfate) and 50mM DTT (Dithiotheritol) and then placed in an ultrasonic bath (Ultrasonic Liquid Processor 3000, Farmingdale, NY, USA). Gill samples were sonicated and manually

homogenized using the published protocol in Bollinger et al. 2018. Hatchling medaka after 2 days post hatch, were euthanized in 2ug/ml MS222 and then transferred into 1x LDS and 50mM DTT. Varying concentrations of hatchlings were used, 2 and 4 hatchlings were placed into 250µl, and 8, 10, and 20 were placed into 1ml LDS and DTT. Following sonication, samples were transferred to microcentrifuge tubes and heated at 70°C for 10 min. Denatured protein samples were run on a 4-12% Bis-Tris Gel with MES SDS Running Buffer with antioxidant. Gels were electrophoresed and then blotted onto 0.2 µm nitrocellulose membranes with transfer buffer containing10% methanol. Membranes were blocked with Li-Cor Blocking Buffer (LI-COR Biosciences, Lincoln, NE, USA) for one hour at room temperature. Membranes were incubated with a cocktail of affinity-purified homologous rabbit anti medaka Cldn30c antibody (see below), in combination with mouse anti human beta-actin (Abcam; cat. no. ab8224) in blocking buffer and incubated overnight at 4 °C on an orbital rotator. Antibodies were used at the following concentrations: Cldn30c (0.1 µg mL^{-1}), NKA α5 (0.5 µg mL^{-1}), beta-actin (0.2 µg mL^{-1}). Primary antibodies in blocking buffer were placed onto the blot and left overnight at 4°C on an orbital rotator. Membranes were washed four times with 1X TBST (five min each). Western blotting solutions and materials were NuPAGE TM from Thermo Fisher, unless stated. Incubation with secondary antibodies in blocking buffer were performed in dark conditions at room temperature for one h (IR Dye® 800CW Goat anti-Rabbit IgG and IR Dye® 680LT Goat anti-Mouse IgG, LI-COR). After washing, membranes were dried and imaged using an Odyssey infrared scanner (LI-COR). The Cldn30C antibody was generated in rabbit against an epitope in the cytoplasmic C-terminal domain of the medaka Cldn30c sequence C-AARSDISSPPGKLS (GenScript, Piscataway, NJ, USA). The specificity of the medaka Cldn30c was validated by control neutralization with the antigenic peptide in 400x molar excess overnight at 4 °C before

probing the membrane. Claudin30C expression (band intensity) was quantified using Image Studio version 2.0 software (LI-COR Biosciences, Lincoln, NE, USA) and normalized against beta-actin loading control.

3.3.4 Immunohistochemistry

Hatchling medaka after 2 days post hatch, were euthanized in 2ug/ml MS222 and placed into 4% PFA (Mallinckrodt Chemicals, Phillipsburg, NJ, USA) in 1X PBS overnight at 4C. Medaka were transferred to 70% EtOH for storage at -20°C. Sampled medaka were rinsed three times with 1X PBS (Phosphate Buffered Saline) for intervals of 30, 15, and 15 minutes. Samples were blocked using blocking buffer:1X PBS, 5% normal goat serum (Sigma Aldrich) and 0.3%Triton™ X-100 (EMD Millipore) for 1 hour at room temperature on an orbital rotator. Primary antibodies: Cldn30c (1:1000) and a5 (Na+/K+-ATPase alpha subunit; 0.7 µgmL-1) were placed onto the gills and incubated overnight at 4°C on an orbital rotator. Medaka were rinsed with 1X PBS for 30, 15, and 15 minute intervals. Secondary conjugate antibodies (Alexa Fluor® 488and Alexa Fluor® 568; both 0.2µgmL-1; Molecular Probes, Burlington, ON, Canada) were incubated for 1 hour in dark conditions on an orbital rotator at room temperature. Samples were washed with 1X PBS for 30, 15, and 15 minute intervals and then transferred to slides. Slides had Prolong® Gold Antifade Reagent media added to them and covered with glass coverslips (Molecular Probes) and were stored flat in the dark at 4°C until visualization. Slides were visualized on a Nikon Ti2 microscope (Melville, NY, USA). Images were collected using the Nikon NIS elements software and processed using Fiji/Image J (Schindelin et al.2012).

3.3.5 Microinjections

Medaka embryos were harvested from the tanks or off the females, just after being deposited at sunrise. In accordance with Kinoshita et al, 1996, medaka embryos were injected before first cleavage. Embryos were injected at stage 1 with 4nl of control 1X PBS buffer to test for injection stress using a FemtoJet 4 (Eppendorf, Hauppauge, NY). Stage development was confirmed using a dissection scope, in accordance with Iwamatsu 2004 guidelines for medaka development.

3.4 Experiments

3.4.1 Series 1. SW acclimation

To test the response of medaka to a hyper-osmotic environment, 10 adult female and 10 adult male FW-acclimated medaka were transferred to sham FW conditions and SW (28 ppt N = 40). After 6, 24, and 168 h, gills (n=6 per group) were sampled and treated as described above.

3.4.2 Series 2. IPW acclimation

To test the response of medaka to a dilute hypo-osmotic environment, 10 female and 10 male FW-acclimated medaka were transferred to sham FW conditions and IPW (90% deionized water and 10% tap water; N = 40). After 6, 24, and 168 h, gills (n=6 per group) were sampled and treated as described above.

3.4.3 Series 3. Hatchling and Gill Protein Expression

To understand the abundance of Cldn30c found with in hatchling medaka, animals were sampled post hatch 2 days and compared to gill protein levels in adult medaka. Gill samples for

long term 7 days acclimation to FW and SW conditions were excised and treated as described above for protein quantification. Validation of the Cldn30c medaka antibody was conducted to ensure specificity of the antibody for both quantification and localization using microscopy.

3.4.4 Series 4. Microinjections

To investigate the use of knockdown morpholinos, medaka eggs at the one cell stage were microinjected in the cytosol using micro-pipettes. After harvesting the eggs and during the procedure they were kept in water from their tanks and placed on ice to slow development. After injection they were maintained in a 28°C incubator

3.4.5 Statistics

Series 1 and 2 salinity transfer experiments data were analyzed via two-way ANOVA followed by Bonferroni adjusted Fishers LSD if the interaction between factors where significant. Series 3 western blotting data were analyzed using a t-test. The statistical significance level of $P < 0.05$ was used throughout the analysis. All data analysis was conducted using GraphPad Prism 7.0 software (San Diego, CA, USA).

3.5 Results

3.5.1mRNA Expression in Time Course Salinity Transfer Experiments

Medaka gills from FW to SW and FW to IPW transfer experiments were used to determine *cldn30c* expression in response to salinity challenges. Gills were sampled at 6, 24 and 168 hours. Expression of *cldn30C* was statistically unchanged when exposed to hyperosmotic SW conditions at all time points (figure 3.1A). mRNA expression of *cldn30c* was significantly

upregulated in response to IPW at 6 hours exposure compared to FW control, while expression was reduced back to control levels at 24 and 168 hours (figure 3.1B).

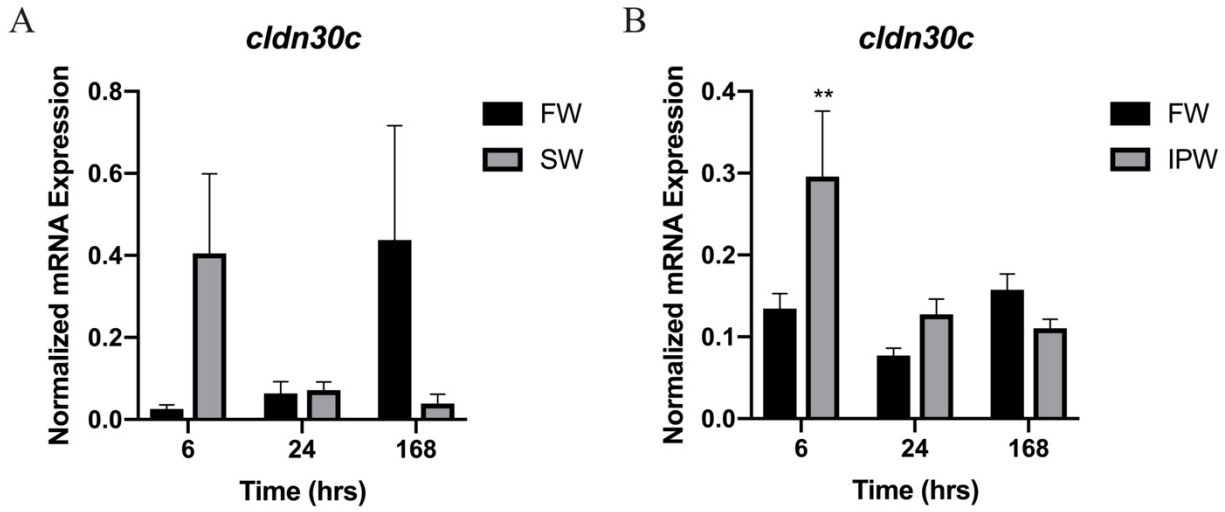

Figure 3.1 Effect of transfer from freshwater, FW to seawater, SW, (A) and 90% ion poor water, IPW, (B) on branchial medaka *cldn30c* expression at 6, 24, and 168 hrs time points. The level of each target was normalized to the geometric mean of the normalization genes *ef1a*, *bactin*, and *rpl7*. Data are presented as mean ± standard error of the mean (n = 7-8). Statistically significant effect (two-way ANOVA, followed by Bonferroni adjusted Fishers LSD) are denoted by asterisks (**P <0.01).

3.5.2 Protein Expression in FW and SW Acclimated Fish

Medaka Cldn30c protein expression was quantified using western blot analysis. Cldn30c antibody was validated using a peptide blocking protocol of 400 times molar excess of the peptide (figure 3.2). A single immunoreactive band was found at ~18kDa, while it was notably absent in the peptide blocking experiment (figure 3.2). Weeklong acclimation to hyperosmotic conditions (SW) induced a significant decrease in gill protein abundance compared to FW samples (figure 3.3B). Gill NKA was significantly increased in SW (figure 3.3C). The loading control, beta-actin, showed no significant changes in protein expression between FW and SW (figure 3.3D).

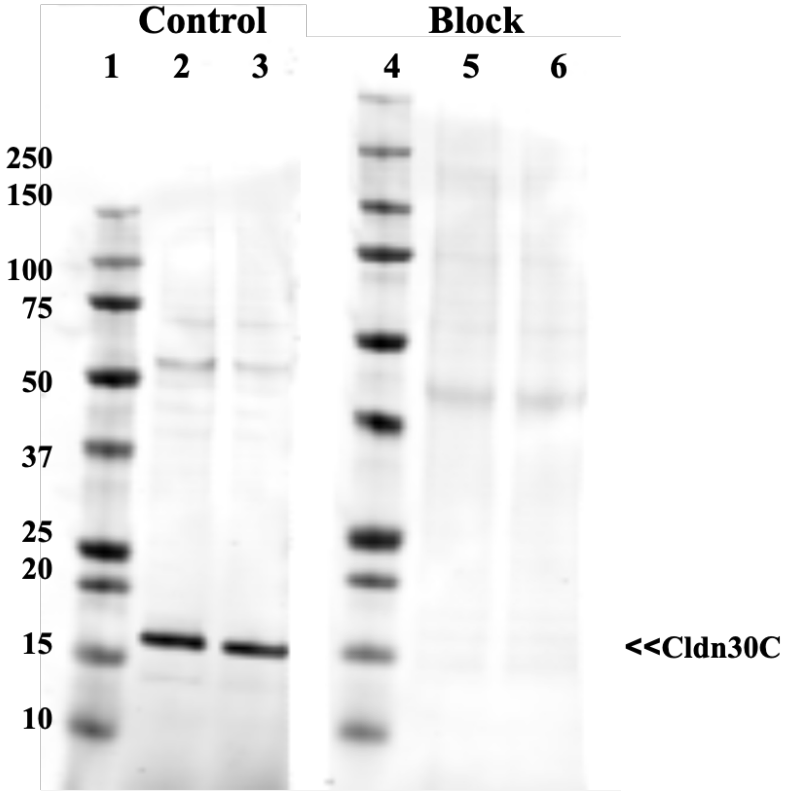

Figure 3.2 Western Blot of freshwater medaka gill samples probed with Cldn30c antibody. Lanes 1-3 were probed with the Cldn30c antibody; lanes 4-6 were probed with Cldn30c antibody after neutralization with 400x molar excess of the antigenic peptide. Lanes 1 and 4 contained a molecular mass marker ((Protein Plus, BIO-RAD, Hercules, CA); lanes 2-3 and 5-6 contained 10 and 15 µg of total loaded protein, respectively. A single immunoreactive band at ~18 kDa was detected, which was not present post antibody neutralization.

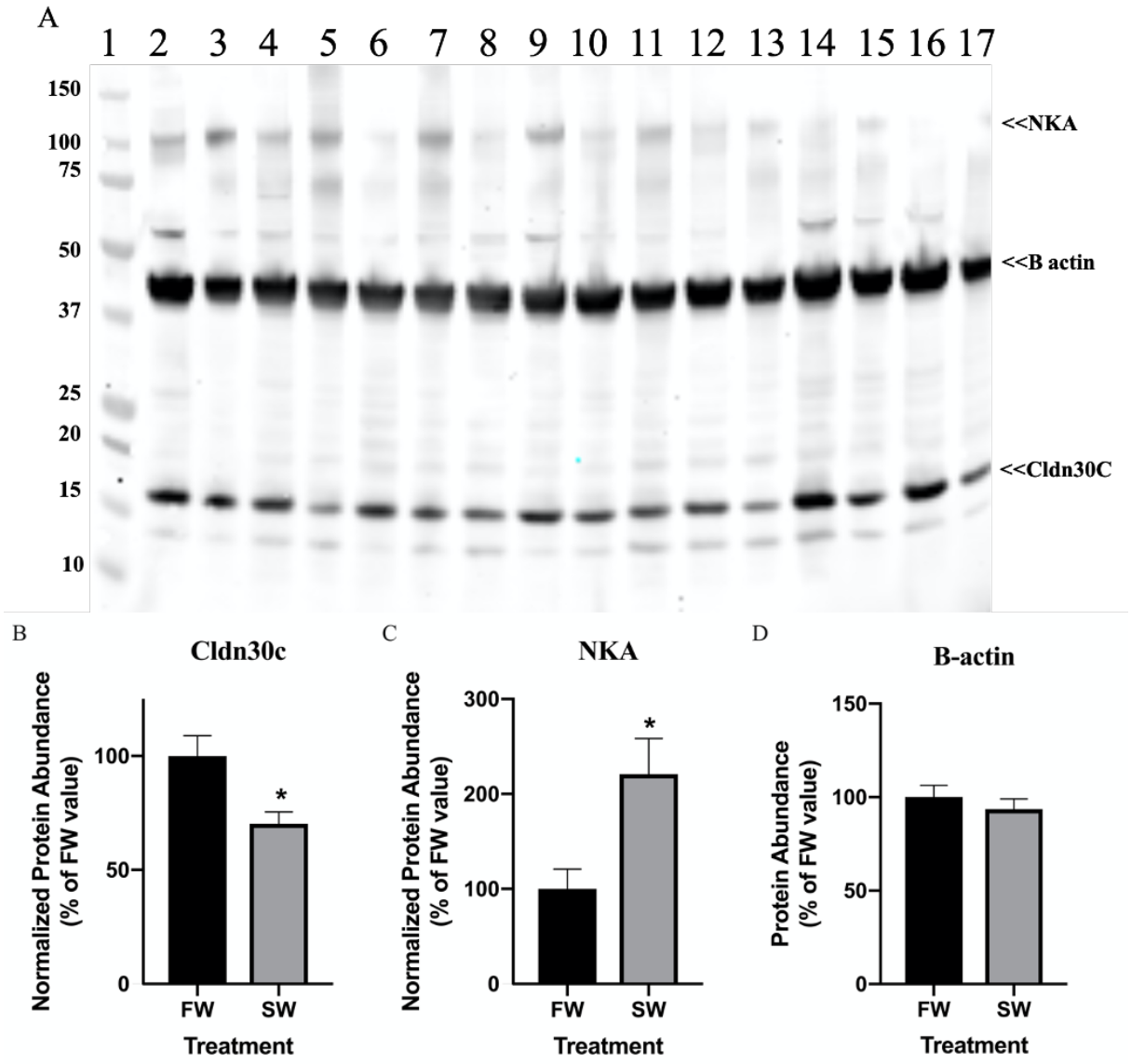

Figure 3.3 Western blot of freshwater and seawater adapted medaka gill protein probed with Na^+,K^+-ATPase alpha subunit ,NKA, B-actin, and medaka Cldn30C (A). Lane 1 contained a molecular mass marker (Protein Plus, BIO-RAD, Hercules, CA); lanes with even numbers 2-16 are freshwater samples, odd lanes 3-17 are seawater samples and all contain 15 µg of total loaded protein. Signal abundance normalized against Bactin for Cldn30c (B) and NKA (C). the loading control beta-actin is shown in D. Statistical significance (unpaired two-tailed t-test) denoted by asterisks (*P <0.05).

Two-day old hatchlings were used to compare protein composition and confirm detection in larval samples. Varying amounts of hatchlings were placed into LDS and DTT to compare protein abundance in the samples. Cldn30c was demonstrated in the preparations with 4

hatchlings into 250 µL (16 hatchlings per mL, lane 3) and 8 hatchlings per mL (lane 4) but paradoxically higher intensity in the more diluted sample (figure 3.4). The Cldn30c band was absent in the 2 and 10 hatchlings sample. Gills from FW adapted medaka were used as a positive control and demonstrated Cldn30C protein expression (figure 3.4).

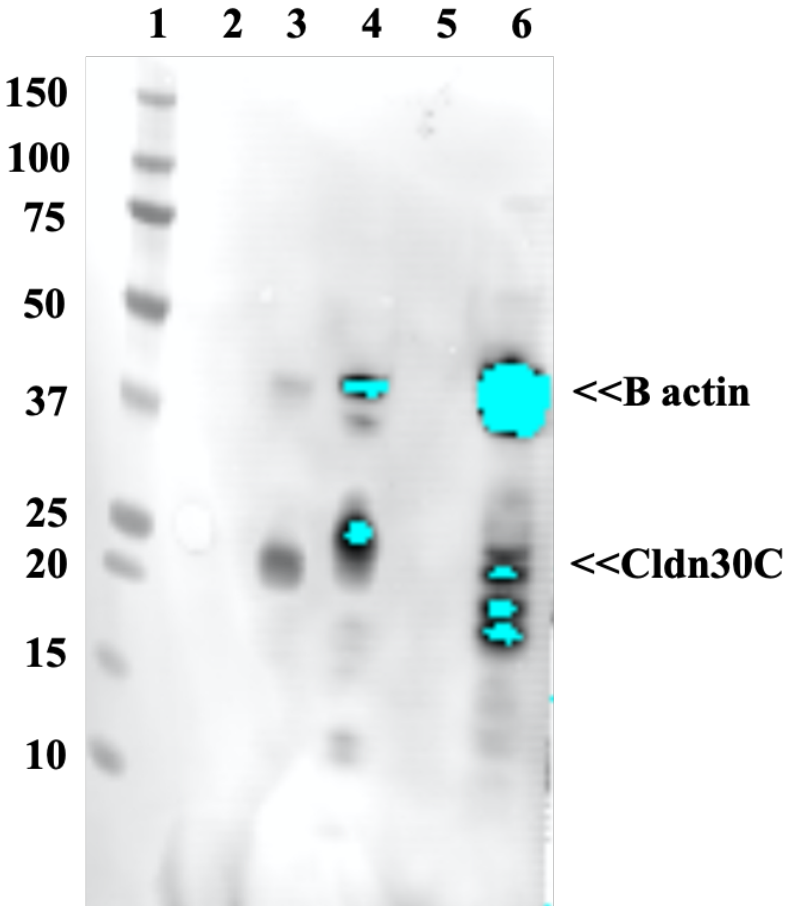

Figure 3.4 Western blot on two-day old hatchling medaka and gill from freshwater acclimated adult medaka as positive control. The nitrocellulose membranes were probed with antibody against medaka Cldn30c and Bactin. Lane 1 contained a molecular mass marker, lane 2 -5 has 2 and 4 hatchlings into 250µl, 8, and 10 hatchling into 1ml 1x sample buffer and lane 6 one half gill arch from adult into 200µL sample buffer. 15µL was loaded into each well. Cldn30c immunoreactive band was detected at ~22kDa and Bactin at ~42kDa.

3.5.3 Microscopy

Immunohistochemistry on whole mounted 2 day old hatchlings demonstrated diffuse Cldn30c staining in the tail region of the fish at low magnification, while localization of NKA

showed punctate staining in the skin above the developing gills and the tail (figure 3.5). A closer view on the stomach and tail region shows clear cellular staining of NKA (figure 3.5B). The diffuse staining of the Cldn30c is under higher magnification appears to surround the periphery of cells (figure 3.5B).

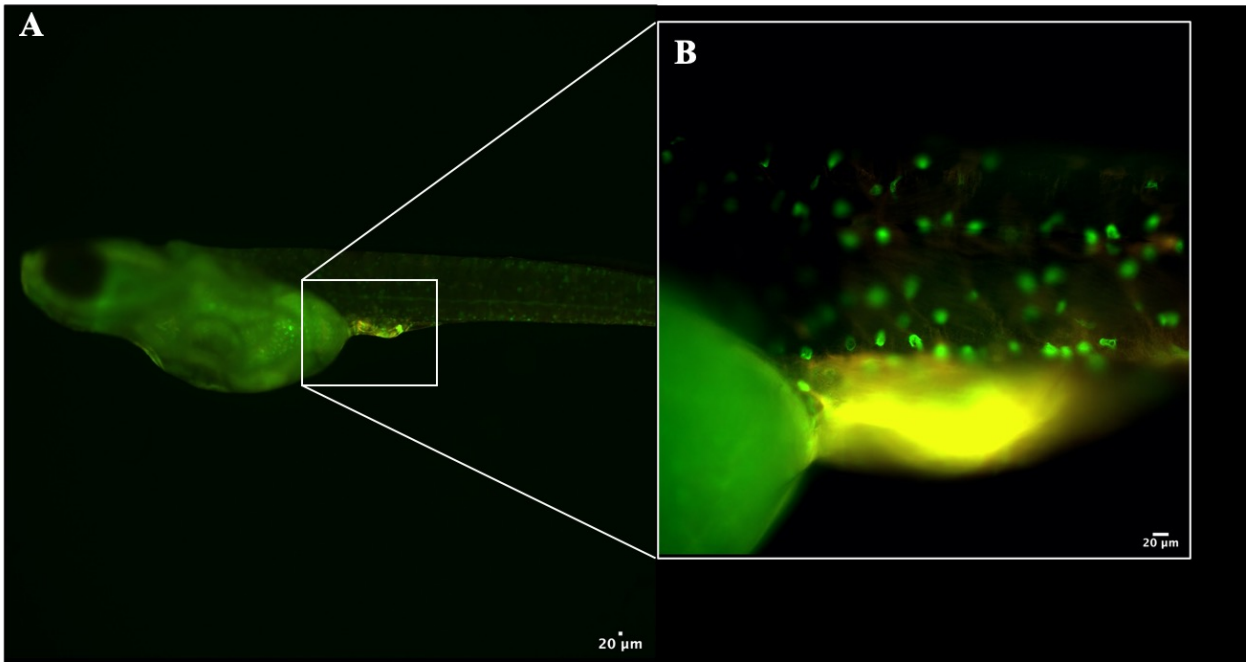

Figure 3.5 Representative microscope images of 2 day old whole mounted hatchling showing the Na^+,K^+-ATPase alpha subunit, NKA (green) and Cldn30c (red). The whole medaka with punctate staining of NKA in ionocytes and more diffuse Cldn30c staining at this low magnification (A). Zoomed in on the stomach and tail region highlights the diffuse staining on the tail (B). Scale bar = 20 µm.

Whole mount two-day old hatchlings, under 100x magnification, demonstrated clear Cldn30c in the periphery of cells (figure 3.6A). In the zoom it is clearly seen that Cldn30c was localized to the edges of pavement cells, signifying the tight junctions between cells (figure 3.6B).

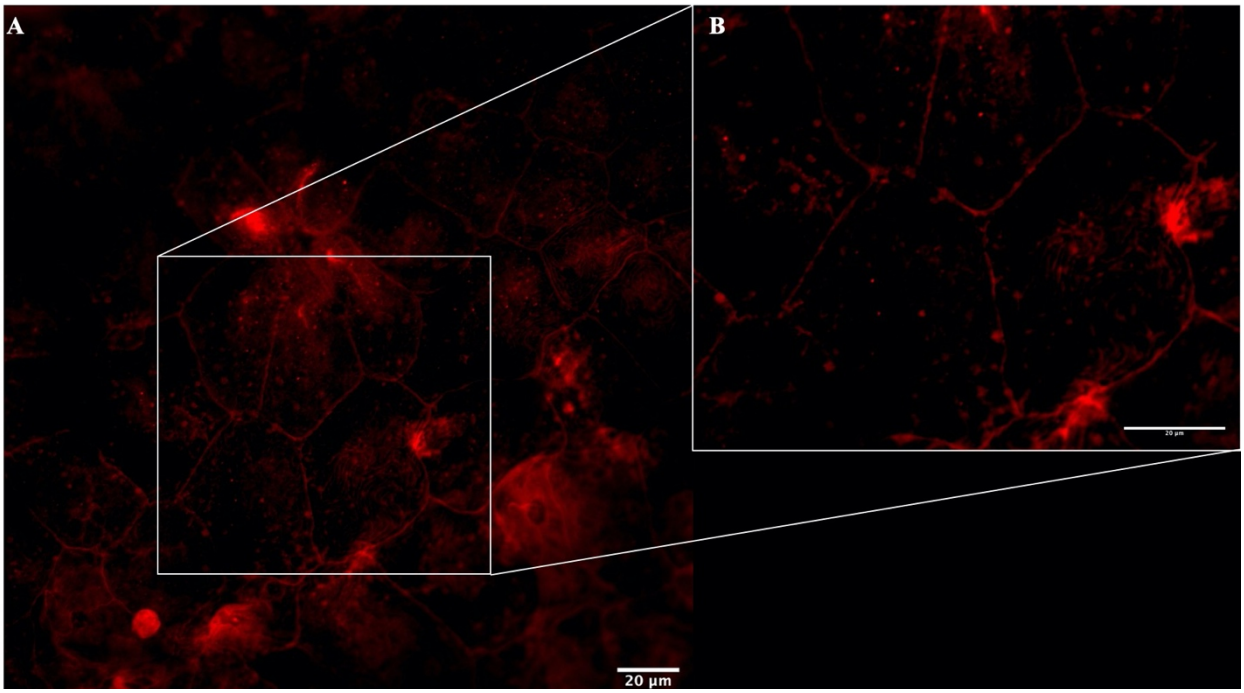

Figure 3.6 Representative microscope images of Cldn30c on the skin over the gills of 2 day old hatchling medaka. Under 100X magnification, Cldn30c (red) is surrounding the cells (A), while a zoomed in view shows tight junction staining (B). Scale bar = 20 µm.

3.5.4 Microinjections

A single round of injections was attempted, though possibly due the stress of injections or prolonged exposure to the cold from being on ice, led to mortality of all injected embryos (Kinoshita et al., 1996). These injections were the only round completed before COVID 19 shut down all research at the University of Arkansas.

3.6 Discussion

This study investigated the regulation of the tight junction protein Claudin30c in the gill of Japanese medaka and in developing hatchlings. We found that Cldn30c mRNA and protein are not constitutively expressed under all salinity challenges, similarly to previous work in medaka (Bossus et al., 2015). Novel significant increases in *cldn30c* expression after initial acclimation to ion poor water conditions were observed. Additionally, gill Cldn30c protein

abundance was significantly decreased in long term SW acclimated fish comparative to the FW control. Salinity sensitive expression of Cldn30c in the gill, suggests a role in regulation of the phenotypic plasticity required for acclimation to varying environments.

The extreme hypoosmotic environment of IPW caused mRNA expression of *cldn30c* at 6 hours to be significantly upregulated (figure 3.1). Initial increase in mRNA expression was not continued at the long-term acclimation of 1 and 7 days, which remained constant compared to the FW control (figure 3.1). Conversely, salinity challenge in SW demonstrated no significant changes in *cldn30c* expression at any time points (figure 3.1). The data confirms previous work done in the Tipsmark lab which transferred medaka from FW to SW, and SW to FW (Bossus et al., 2015). In the previous study, *cldn30c* expression was constitutive regardless of movement from FW into SW or from SW into FW over 1 and 3 day exposure (Bossus et al. 2015). This evidence leads us to believe it is the extreme low ion concentration of the IPW causing the increased need for a barrier protein mRNA.

Paracellular pathway regulation through the use of endocrine factors, cortisol and prolactin have been documented previously in medaka (Bossus et al. 2017). Cortisol regulated *cldn30c*, specifically causing an upregulation of mRNA expression after exposure to higher levels of cortisol (Bossus et al. 2017). Effects on *cldn30c* due to cortisol have been demonstrated in other fish, such as Atlantic salmon (Tipsmark et al. 2009). Prolactin, though commonly accepted as a FW adapting hormone, had no significant effect on expression of *cldn30c* (Bossus et al. 2017, Yan and Hwang 2019). The response to cortisol and lack of response to prolactin

suggests regulation of *cldn30c* may play a role in short term acclimation to newly introduced environments.

Validation of the Cldn30c antibody, in figure 3.2, allowed us to quantify protein changes which is more in depth than only the regulation of mRNA. The Cldn30c antibody demonstrated a singular immunoreactive band at ~18kDa, which was notably absent in the presence of the 400X molar excess of the peptide (figure 3.2) The regulation on protein expression of Cldn30c due to salinity showed a decrease in expression under long term exposure to SW conditions (figure 3.3B). At 7 days exposure to SW, Cldn30c protein expression was significantly decreased compared to FW, which was not the pattern observed in work investigating the mRNA regulation (figure 3.3B Bossus et al., 2015). Significant decrease in Cldn30c protein expression highlights the importance of protein quantification following transcript analysis in order to access biological relevant changes.

Regulation of SW conditions also caused NKA abundance to be significantly increased comparative to FW (figure 3.3C). Medaka regulation of gill NKA, specifically the alpha isoforms, has previously been investigated in response to salinity (Kang et al., 2008; Bollinger et al., 2015). Medaka do not exhibit an isoform switch of the alpha subunit during salinity change, like some other euryhaline species, but the overall gill NKA activity is higher in SW than FW (Bollinger et al., 2015), which is in accordance with the present findings of elevated NKA abundance. The normalization protein used as a loading control, beta-actin, was statically unchanged compared to FW, which supports the use of this protein as loading control (figure 3.3 D. Loading controls are used to ensure the wells have a similar amount of protein and so that the protein abundance measured is not impacted by possible variances in protein concentration

between samples. A significant decrease in Cldn30c protein abundance could be the result of the tight junctions switching to the SW type leaky junctions, where sodium moves out of the fish gill via the paracellular pathway (Evans et al. 2005). Ours is the first study to show the regulation of medaka Cldn30c is decreased in SW conditions. Though *cldn30c* mRNA can go on to signal the translation of protein, the correlation between the two are not a direct ratio, meaning an increase in mRNA does not always signal an increase in the protein (Ellis et al., 2019). There is clear divergence between mRNA and protein regulation, which can be attributed to changes in translational efficiency or protein turnover (McCarthy et al., 1994; Tuller et al., 2010).

Optimization of the protein abundance in hatchling medaka was done by varying the number of hatchlings per sample, ideally reaching sufficient abundance for easy detection, without needing to inject large quantities each round. Cldn30c bands were detected in the 4 hatchlings in 250µl sample, and the 8 hatchlings in 1ml sample (figure 3.4). Sample preparation error, either insufficient homogenization of the protein or suboptimal buffer to sample ratio could be responsible for the lack of detection in the other two lanes and the lack of a dose response relationship (figure 3.4). Future work will need to optimize the preparation process to determine if the protein concentration within the samples are similar and if the proteins are properly prepared for electrophoresis.

Medaka develop gills during ontogenesis and before gill development the integument represents the largest surface area and serve the same roles as the gill in the adult fish. It can therefore be used as a two-dimensional, more simple proxy, for understanding gill function and tight junctions. When looking at the hatchling medaka at low magnification, Cldn30c staining is

diffuse along much of the body, though some peripheral cellular staining can be seen when zooming in (figure 3.5 A & B). Punctate staining of NKA was observed in MRCs along the tail and in the skin near the developing gills (figure 3.5). To further determine if Cldn30c expression was in the tight junction of cells, higher magnification microscopy was used (figure 3.6). Whole mount IHC showed clear peripheral staining of the cells in the integument (figure 3.6). Under high resolution magnification, the staining of edges of polygonal pavement cells is observed, demonstrating the Cldn30c specific localization to the intercellular junctions (figure 3.6). The tight junction between cells are thus clearly seen and notable is also the lack of florescence in the center of the cell.

An increase in barrier-forming protein expression has been documented previously when some fish species are acclimated to a dilute environment (Tipsmark et al. 2008; Chasiotis et al. 2012; Duffy et al. 2011). These barrier forming proteins include claudin isoforms like Cldn30c. The extra whole genome duplication and additional tandem duplications seen in the teleost lineage left this fish group with multiple paralogs of the same claudins. Out of the claudins previously studied, *Cldn30c* has the highest expression in the gill (Bossus et al., 2015). Additionally, Cldn30C is an ortholog to the formerly named Cldn b of importance in zebrafish integument (Kwong and Perry, 2013). Zebrafish have been used as models for physiology studies previously, including the knockdown of protein expression using morpholinos, just as in our study (Kwong and Perry 2013). Cldn b is also a tight junction protein that regulates the epithelial permeability and sodium ion regulation in developing zebrafish (Kwong and Perry, 2013). Zebrafish Cldn b knockdowns demonstrated the role of Cldn b in sodium regulation in

this stenohaline species, as a significant increase in sodium efflux occurred in response to decreased protein expression.

The use of knockdown and or knockout techniques have become prevalent in physiological vertebrate models in the past decade. The use of morpholinos to decrease the expression of targeted proteins to ascertain or investigate their roles within development and regulation (Zimmer et al., 2019). Morpholinos can be used in loss of function studies to investigate the physiology of the targeted model species. Most fish-specific morpholino studies involve zebrafish, which are not an ideal model for investigation of all forms of osmoregulation, as they are not capable of hypoosmoregulation (Zimmer et al., 2019). Medaka are capable of survival in a variety of salinities and can be used to investigate hypoosmoregulation and hyperosmotegulation (Bossus et al., 2017). Medaka an ideal candidate for osmoregulatory studies where decrease in protein abundance, due to morpholino knockdown, may affect the ability to regulate tight junctions under salinity pressures.

This study is the first to approach morpholino use in loss of function studies to investigate osmoregulation in an euryhaline species. Though the data presented here is preliminary, it forms a platform on which future work will focus on the regulatory function of Cldn30c within the tight junction. We aim to use morpholinos as a tool to better understand the regulation of the tight junction in response to salinity changes.

Additionally, medaka embryos were able to withstand an immediate salinity change upon being deposited by the female (Ellis, unpublished observations). Embryos were separated from

the same clutch and half placed into FW and half into SW (ppt=28) for the entirety of the 10 days to develop. Embryos underwent no notable change in size and had no delay in development. Hatchings persisted in their respective salinities and no notable differences were observed.

3.7 Conclusions

Claudin 30c is a regulatory barrier forming protein found in the medaka gill, that plays an essential role in the regulation of the paracellular pathways between cells. Our findings showed that *cldn30c* is regulated upon entering an extreme hypoosmotic environment, IPW. This increase in expression could lead to the "tightening" of the junctions between cells. Through the generation of Cldn30c specific antibodies, we demonstrated the difference in protein expression between medaka exposed to differing salinities as well as the localization of Cldn30c within the fish epithelium. We found higher level of gill Cldn30c protein expression in FW versus SW acclimated medaka with no change in mRNA levels. The differences seen between mRNA and protein expression demonstrates the importance of protein studies as follow-up to transcripts examinations. IHC shows clear staining of Cldn30c around the periphery of cells within hatchling medaka, further demonstrating the localization of Cldn30c to the tight junctions surrounding the cell. Hatchlings where sampled for dose response comparison of Cldn30c protein abundance. Optimization of the protocol remains, however the ability to detect protein in hatchlings was achieved. The initial experiments encourage the use of injected embryos and hatchling medaka in physiological loss of function studies. With additional studies we may be able to use medaka as a model organism for knockdown studies investigating the specific

mechanisms by which Cldn30c and other gill claudins can regulate the paracellular movement of sodium.

3.8 References

Baltzegar, D.A., Reading, B.J., Brune, E.S. and Borski, R.J., 2013. Phylogenetic revision of the claudin gene family. *Marine genomics*, *11*, pp.17-26.

Bollinger, R.J., Ellis, L.V., Bossus, M.C. and Tipsmark, C.K., 2018. Prolactin controls Na+, Cl− cotransporter via Stat5 pathway in the teleost gill. *Molecular and cellular endocrinology*, *477*, pp.163-171.

Bossus, M.C., R.J. Bollinger, P.J. Reed, and C.K. Tipsmark. 2017. Prolactin and cortisol regulate branchial claudin expression in Japanese medaka. General and Comparative Endocrinology. 240:77-83. 21

Bossus, M.C., S.S. Madsen, and C.K. Tipsmark. 2015. Functional dynamics of claudin expression in Japanese medaka (Oryzias latipes): Response to environmental salinity. Comparative Biochemistry and Physiology. Part A, Physiology. 187:74-85.

Chasiotis, H., D. Kolosov, P. Bui, and S.P. Kelly. 2012. Tight junctions, tight junction proteins and paracellular permeability across the gill epithelium of fishes: A review. Respiratory Physiology & Neurobiology. 184:269-281.

Duffy, N.M., P. Bui, M. Bagherie-Lachidan, and S.P. Kelly. 2011. Epithelial remodeling and claudin mRNA abundance in the gill and kidney of puffer fish (Tetraodon biocellatus)

Ellis, L.V., Bollinger, R.J., Weber, H.M., Madsen, S.S. and Tipsmark, C.K., 2019. Differential Expression and Localization of Branchial AQP1 and AQP3 in Japanese Medaka (Oryzias latipes). *Cells*, *8*(5), p.422.

Engelund, M.B., Yu, A.S.L., Li, J., Madsen, S.S., Færgeman, N.J. and Tipsmark, C.K., 2012. Functional characterization and localization of a gill-specific claudin isoform in Atlantic salmon. *American Journal of Physiology-Regulatory, Integrative and Comparative Physiology*, *302*(2), pp.R300-R311.

Evans, D.H., P.M. Piermarini, and K.P. Choe. 2005. The multifunctional fish gill: Dominant site of gas exchange, osmoregulation, acid-base regulation, and excretion of nitrogenous waste. Physiological Reviews. 85:97-177. 24

Ferguson, D.P., Dangott, L.J. and Lightfoot, J.T., 2014. Lessons learned from vivo-morpholinos: How to avoid vivo-morpholino toxicity. *Biotechniques*, *56*(5), pp.251-256.

Gonzalez-Mariscal, L., R. Tapia, and D. Chamorro. 2008. Crosstalk of tight junction components with signaling pathways. Biochimica Et Biophysica Acta-Biomembranes. 1778:729-756.

Günzel, D. and Yu, A.S., 2013. Claudins and the modulation of tight junction permeability. *Physiological reviews*, *93*(2), pp.525-569.

Heasman, J., Kofron, M. and Wylie, C., 2000. βCatenin signaling activity dissected in the early Xenopus embryo: a novel antisense approach. *Developmental biology*, *222*(1), pp.124-134.

Herpin, A., Fischer, P., Liedtke, D., Kluever, N., Neuner, C., Raz, E. and Schartl, M., 2008. Sequential SDF1a and b-induced mobility guides Medaka PGC migration. *Developmental biology*, *320*(2), pp.319-327.

Hubbard, T.J., Aken, B.L., Beal, K., Ballester, B., Cáccamo, M., Chen, Y., Clarke, L., Coates, G., Cunningham, F., Cutts, T. and Down, T., 2007. Ensembl 2007. *Nucleic acids research*, *35*(suppl_1), pp.D610-D617.

Iwamatsu, T., 2004. Stages of normal development in the medaka Oryzias latipes. *Mechanisms of development*, *121*(7-8), pp.605-618.

Kinoshita, M., Toyohara, H., Sakaguchi, M., Inoue, K., Yamashita, S., Satake, M., Wakamatsu, Y. and Ozato, K., 1996. A stable line of transgenic medaka (Oryzias latipes) carrying the CAT gene. *Aquaculture*, *143*(3-4), pp.267-276.

Kinoshita, M., Morita, T., Toyohara, H., Hirata, T., Sakaguchi, M., Ono, M., Inoue, K., Wakamatsu, Y. and Ozato, K., 2001. Transgenic medaka overexpressing a melanin-concentrating hormone exhibit lightened body color but no remarkable abnormality. *Marine Biotechnology*, *3*(6), pp.536-543.

Kwong, R.W. and Perry, S.F., 2013. The tight junction protein claudin-b regulates epithelial permeability and sodium handling in larval zebrafish, Danio rerio. *American Journal of Physiology-Regulatory, Integrative and Comparative Physiology*, *304*(7), pp.R504-R513.

Madsen, S.S., J. Bujak, and C. Tipsmark. 2014. Aquaporin expression in the Japanese medaka (Oryzias latipes) in freshwater and seawater: challenging the paradigm of intestinal water transport? J. Exp. Biol. 217:3108-3121.

Marshall, W.S., and M. Grosell. 2006. Ion transport, osmoregulation and acid-base balance. In The Physiology of Fishes. D.H. Evans and J.B. Clairborne, editors. Taylor and Francis Group, Boca Raton, Fl. 177-210.

McCarthy, I.D., Houlihan, D.F. and Carter, C.G., 1994. Individual variation in protein turnover and growth efficiency in rainbow trout, Oncorhynchus mykiss (Walbaum). *Proceedings of the Royal Society of London. Series B: Biological Sciences*, *257*(1349), pp.141-147.

Morcos, P.A., Li, Y. and Jiang, S., 2008. Vivo-Morpholinos: a non-peptide transporter delivers Morpholinos into a wide array of mouse tissues. *Biotechniques*, *45*(6), pp.613-623.

Moulton, J.D. and Jiang, S., 2009. Gene knockdowns in adult animals: PPMOs and vivo-morpholinos. *Molecules*, *14*(3), pp.1304-1323.

Nasevicius, A. and Ekker, S.C., 2000. Effective targeted gene 'knockdown'in zebrafish. *Nature genetics*, *26*(2), pp.216-220.

Rosenthal, R., Günzel, D., Piontek, J., Krug, S.M., Ayala-Torres, C., Hempel, C., Theune, D. and Fromm, M., 2020. Claudin-15 forms a water channel through the tight junction with distinct function compared to claudin-2. *Acta Physiologica*, *228*(1), p.e13334.

Sardet, C., Pisam, M. and Maetz, J., 1979. The surface epithelium of teleostean fish gills. Cellular and junctional adaptations of the chloride cell in relation to salt adaptation. *The Journal of cell biology*, *80*(1), pp.96-117.

Schindelin, J., I. Arganda-Carreras, E. Frise, V. Kaynig, M. Longair, T. Pietzsch, S. Preibisch, C. Rueden, S. Saalfeld, B. Schmid, J.Y. Tinevez, D.J. White, V. Hartenstein, K. Eliceiri, P. Tomancak, and A. Cardona. 2012. Fiji: an open-source platform for biological-image analysis. Nature Methods. 9:676-682.

Shima, A. and Mitani, H., 2004. Medaka as a research organism: past, present and future. *Mechanisms of development*, *121*(7-8), pp.599-604.

Tanaka, M., Fukada, S., Matsuyama, M. and Nagahama, Y., 1995. Structure and promoter analysis of the cytochrome P-450 aromatase gene of the teleost fish, medaka (Oryzias latipes). *The Journal of Biochemistry*, *117*(4), pp.719-725.

Tipsmark, C.K., P. Kiilerich, T.O. Nilsen, L.O.E. Ebbesson, S.O. Stefansson, and S.S. Madsen. 2008b. Branchial expression patterns of claudin isoforms in Atlantic salmon during seawater acclimation and smoltification. American Journal of Physiology-Regulatory Integrative and Comparative Physiology. 294:R1563-R1574.

Tipsmark, C.K., and S.S. Madsen. 2009. Distinct hormonal regulation of Na ,K -atpase genes in the gill of Atlantic salmon (Salmo salar L.). J. Endocrinol. 203:301-310.

Tuller, T., Carmi, A., Vestsigian, K., Navon, S., Dorfan, Y., Zaborske, J., Pan, T., Dahan, O., Furman, I. and Pilpel, Y., 2010. An evolutionarily conserved mechanism for controlling the efficiency of protein translation. *Cell*, *141*(2), pp.344-354.

Van Italie CM, Anderson JM. Claudins and epithelial paracellular transport. Annu. Rev. Physiol. 2006; 68:403-429.

Yan, J.J. and Hwang, P.P., 2019. Novel discoveries in acid-base regulation and osmoregulation: a review of selected hormonal actions in zebrafish and medaka. *General and comparative endocrinology*, *277*, pp.20-29.

Yang, W.K., Chiang, L.F., Tan, S.W. and Chen, P.J., 2018. Environmentally relevant concentrations of di (2-ethylhexyl) phthalate exposure alter larval growth and locomotion in medaka fish via multiple pathways. *Science of The Total Environment*, *640*, pp.512-522.

Zimmer, A.M., Pan, Y.K., Chandrapalan, T., Kwong, R.W. and Perry, S.F., 2019. Loss-of-function approaches in comparative physiology: is there a future for knockdown experiments in the era of genome editing?. *Journal of Experimental Biology*, *222*(7).

Chapter 4 Conclusion

Euryhaline fish, such as the Japanese medaka, face unique challenges associated with the ability to survive in salinity gradients. The plasticity of the gill, specifically the ability to regulate ion and water movement, allows these animals to move between freshwater and seawater (Edwards and Marshall, 2006; Gilmour and Perry, 2018). Gill function changes are due to alterations in protein abundance, localization within the cell, changes in gill cell composition, changes in the tight junctions between cells, or interlamellar cell mass (Sakamoto et al., 2001; Tipsmark et al., 2009; Marshall and Bellamy, 2010; Kwong and Perry, 2013; Gilmour and Perry, 2018; Yan and Hwang, 2019). The patterns of regulation by hormones and environmental stressors like salinity changes, can be key to understanding the role of each protein plays in the overall regulation of homeostasis.

4.1 Teleost fish models

Physiological studies typically use a model organism in place of a human test subject, which can provide insight into function and regulation, and mechanisms of diseases, without the possibility of harming humans. Studies typically utilize another mammal instead and rodents in particular are model organism of choice due to their physiological similarities to humans. Teleost fish however, are becoming more common in biological studies of vertebrate gene function and regulation.

Fish are genetically similar to humans, even though they look nothing alike, with 70% of human genes found in the zebrafish genome (Howe et al. 2013). Teleost underwent a full genome duplication event, so they have multiple copies of genes, while other vertebrates only have one. This provides a unique situation that allow researchers to study multiple paralogs of the same gene within different tissues or regulatory patterns.

Model species in most vertebrate studies are typically limited to rats, rabbits, and zebrafish. Teleost fish while having similar genes to humans, are ideal candidates for modeling vertebrate osmotic regulation and epithelial function. Teleost fish additionally, have a similar endocrine system to mammalian models, which allows researchers to investigate endocrine regulation. While zebrafish are the typical fish model, they evolutionarily separated from medaka about 110 million year ago (Whittbrodt et al., 2002). Medaka have been used for over 100 years in physiological, genetic, and developmental studies, and are a complementary model to zebrafish research (Whittbrodt et al., 2002). Medaka are a good model species because they have fully sequenced genomes, can use similar or the same genetic tools as zebrafish, and are easy to rear (Koster et al., 1997; Sakamoto et al., 2001; Shima and Mitani 2004; Naruse et al., 2004; Kirchmaier et al., 2015; Roy et al., 2017). Compared to the stenohaline zebrafish, they have a smaller genome. As they are euryhaline, medaka are capable of transferring to a variety of salinities at all life stages. These factors coupled together, make medaka an unique model for biological studies.

Medaka have previously been used to model a variety of human diseases. These include kidney disease, fatty liver disease, stress of space travel, and cancer (Mochizuki et al., 2005; Mishra et al., 2014; Murata et al., 2015; Fujisawa et al., 2019). Several human diseases are linked to genes found in the medaka, including ion transporters, aquaporins, and claudins. A mutation of the sodium chloride cotransporter localized in the distal convoluted tubule of the nephron causes Gitleman's syndrome (Valdez-Flores et al., 2016). While, Aquaporins 1 and 3 play a key role in human renal disease (Devuyst et al., 1996; Bedford et al., 2003). Upregulation and expression of aquaporin 1, localized in the proximal tubule, is found in mammalian kidney

lesions. Notably decreased expression of aquaporin 3 is associated with interstitial renal fibrosis and nephron loss (Bedford et al., 2003).

A number of claudins have been identified as factors in human diseases, including cancers, deafness, and inflammatory bowel diseases (Wilcox et al., 2001; Soini 2004; Weber et al., 2008). Cancers, specifically epithelial cancers, are associated with the change in claudins 1, 3, 4, and 7 expression (Morin 2005). Claudin 1 has been shown to decrease in breast and colon cancer, while claudin 7 is down regulated in neck cancer (Morin 2005). Claudin 3 and 4 are both linked to prostate cancer, and claudin 3 is specifically upregulated in prostate adenocarcinoma cells (Long et al., 2001). Deafness is associated with the DFNB29 mutation in Claudin 14 affecting the cochlear duct (Wilcox et al., 2001), while an increase in claudin 14 expression in Down syndrome patients, leads to late onset deafness in adults (Wilcox et al., 2001). Claudin 1 and 2 expression is elevated in inflammatory bowel disease (Weber et al., 2008). Claudin1 and 2 are linked through the cell -cell adhesion signaling pathway associated with ß-catenin signaling. The claudin promoter is believed to lead to an increase in ß-catenin transcriptional activity and causes the formation of polyps (Weber et al., 2008).

Teleost fish are a suitable model organism for biological research, specifically investigations into key genes with disease modeling. The advantage of the use of a euryhaline medaka over a more traditional zebrafish, is the added ability to understand epithelial function due to the high phenotypical plasticity in osmoregulatory organs.

4.2 Summary of Results

The experiments conducted within this thesis were aimed to examine facets of fish osmotic and ionic regulation through analysis of gene expression, protein expression, and

localization and effects of salinity and hormones. This is a summary of the findings of the work presented in this dissertation.

4.2.1 Japanese medaka utilize Aqp3 to regulate cell volume in response to salinity challenges

Aquaporins are transmembrane channels that facilitate the movement of water and solutes across the cellular membrane (Agre et al., 1993, Ecelbarger et al., 1995; Ishibasji et al., 2009; Tingaud-Sequeira et al., 2008; Cerdà et al., 2013). Of the 42 aquaporin (AQP) paralogs present in the teleost fish, AQP1 and AQP3 are the two found in highest abundance within the medaka gill. In chapter 2, we investigated the regulatory patterns and roles of each AQP in the Japanese medaka.

Aquaporins affect the permeability of the cell membrane to water and expression of AQPs can regulate more than just water movement, including solute transport, and cell volume regulation (Sugiyama et al., 2001; Boury-Jamot et al., 2006; Cutler, et al., 2007; Tingaud-Sequeira et al., 2008; Lee et al., 2017). Functionally AQP1 and AQP3 have differing roles within the epithelium, AQP1 is an orthodox AQP while AQP3 is an aquaglyceroporin, capable of transporting glycerol in addition to water (Ecelbarger et al., 1995; Sugiyama et al., 2001; Boury-Jamot et al., 2006). AQP 1 can theoretically only transport water (Ecelbarger et al., 1995; Sugiyama et al., 2001; Boury-Jamot et al., 2006). Volume fluctuations within the cell are a result of changing osmolality due to the change of external environments. In a freshwater (FW) environment, the dilute external environment causes the passive gain of water. Conversely in seawater (SW) there is a passive loss of water due to the more concentrated outer environment. In Ion Poor Water (IPW) Aqp3 was significantly upregulated, while Aqp1 remains constitutively

expressed. In SW conditions Aqp3 was reduced, while Aqp1 remained unchanged. *Ex vivo* hormone studies demonstrated stimulation of Aqp3 by prolactin, while Aqp1 was unaffected by this hormone. Cortisol alone had no statistically significant effect on the regulation of Aqp1 or Aqp3 nor was there a significant interaction between the two hormones on any of the paralogs. Localization of AQPs within the medaka gill showed Aqp1 does not colocalize with the cells expressing NKA and was not affected by salinity. Aqp1 immunoreactivity was found in the cells of the gill filament. Aqp3 immunoreactivity was also found primarily on the filament, however Aqp3 was also colocalized with cells expressing NKA, demonstrating that Aqp3 and Aqp1 are not expressed in all the same cell types.

These findings combined lead us to the conclusion that AQP3, not AQP,1 is the AQP responsible for safeguarding cell volume during rapid fluctuations due to hypoosmotic challenges. The change in expression pattern, altered by salinity and the hormone prolactin, demonstrate the importance of a regulatory AQP concerning cell volume shifts.

4.2.2 Claudin 30C in Japanese medaka gill

Teleost fish gill is the main organ involved in homeostasis especially concerning the movement of ions, water, and waste. Euryhaline fish, such as the Japanese medaka, rainbow trout, Atlantic killifish, and Mozambique tilapia, are in part able to persist and thrive in varying environments including both FW and SW due to the plasticity of the gill (Evans et al. 2005; Bossus et al. 2015). Tight junctions between cells within the teleost gill help maintain the regulatory pathways for the movement of ions and water. Claudin isoforms, including Cldn30C, are part of the tight junction complex within the gill.

Cldn30C is highly expressed in the gill and has previously been shown to be regulated by salinity (Tipsmark et al. 2008b; Bossus et al. 2015). Hypoosmotic exposure in the form of 90% deionized water, IPW, for 6 hours, lead to a significant increase in Cldn30C expression compared to FW. Significant increase at initial exposure of Cldn30C expression could be demonstrating the regulation of the tight junction barrier between cells. Longer term exposure, over 7 days, showed no significant change however, demonstrating the mRNA expression may be transient and only increased for initial exposure. Western blot studies confirmed higher abundance of protein in FW adapted medaka over SW at 7 days exposure. Microscopy studies demonstrated the Cldn30C immunofluorescence localized in polygonal shapes surrounded pavement cells, typical of tight junction staining. Additionally, the embryonic medaka were able to survive and develop in both salinities and hatched with no delay compared to FW. These studies, coupled with the beginning stages of an injection series, may supply the framework for the use of medaka as a loss of function model to understand tight junction function. Knock down studies when completed can link tight junction Cldn30C expression to paracellular permeability in FW and SW hatchlings.

4.3 Perspectives

This thesis focuses on describing and understanding basic epithelial function in medaka while developing this euryhaline teleost model. Japanese medaka, though similar to other studied euryhaline models, do not follow the same patterns of regulation concerning AQP1 and AQP3 within the gill. Our study provides insight into how regulatory patterns between species are not always conserved. Aqp1 was unaffected by salinity pressures or osmoregulatory hormones. Conversely, Aqp3 was regulated by both and had a different response to the combination of

cortisol and prolactin, comparative to the Mozambique tilapia (Breves et al., 2016). Cortisol had no negative impact on the stimulatory effect of prolactin on gill Aqp3 expression in medaka, which is different from findings in tilapia where cortisol counteracted the stimulatory effect of prolactin (Breves et al., 2016). The differences in findings between model euryhaline species reinforces the concepts that generalized patterns of osmotic and ionic regulation can't be applied to all teleost, let alone all vertebrates. Many animals experience a shift in salinity, throughout development, sexual maturation, tidally in their environment, and during seasonal migration, each animal must be investigated to understand how transport protein contributes to the overall ability to persists and survive in varying environments (Evans et al., 2005; Tipsmark et al., 2008; Tipsmark et al., 2009; Breves et al., 2016; Ellis et al., 2019). Multiple studies must be conducted to observe the patterns of the regulation of essential transmembrane proteins, especially when using teleost fish as a model for vertebrate protein regulation.

4.4 References

Agre, P.E.; Preston, G.M.; Smith, B.L.; Jung, J.S.; Raina, S.U.; Moon, C.H.; Guggino, W.B.; Nielsen, S.B. Aquaporin CHIP: The archetypal molecular water channel. *Am. J. Phys.-Renal* 1993, *265*, 463–476, doi:10.1152/ajprenal.1993.265.4.F463.

Bedford, J.J., Leader, J.P. and Walker, R.J., 2003. Aquaporin expression in normal human kidney and in renal disease. *Journal of the American Society of Nephrology*, *14*(10), pp.2581-2587.

Breves, J.; Inokuchi, M.; Yamaguchi, Y.; Seale, A.P.; Hunt, B.; Watanabe, S.; Lerner, D.; Kaneko, T., Grau, G. Hormonal regulation of aquaporin 3: Opposing actions of prolactin and cortisol in tilapia gill. *J. Endocrinol.* 2016, doi:10.1530/JOE-16-0162.

Boury-Jamot, M., Sougrat, R., Tailhardat, M., Le Varlet, B., Bonte, F., Dumas, M. and Verbavatz, J.M., 2006. Expression and function of aquaporins in human skin: Is aquaporin-3 just a glycerol transporter?. *Biochimica et Biophysica Acta (BBA)-Biomembranes*, *1758*(8), pp.1034-1042.

Cerdà, J., Zapater, C., Chauvigné, F. and Finn, R.N., 2013. Water homeostasis in the fish oocyte: new insights into the role and molecular regulation of a teleost-specific aquaporin. *Fish physiology and biochemistry*, *39*(1), pp.19-27.

Cutler, C.P., Martinez, A.S. and Cramb, G., 2007. The role of aquaporin 3 in teleost fish. *Comparative Biochemistry and Physiology Part A: Molecular & Integrative Physiology*, *148*(1), pp.82-91.

Devuyst, O., Burrow, C.R., Smith, B.L., Agre, P., Knepper, M.A. and Wilson, P.D., 1996. Expression of aquaporins-1 and-2 during nephrogenesis and in autosomal dominant polycystic kidney disease. *American Journal of Physiology-Renal Physiology*, *271*(1), pp.F169-F183.

Ecelbarger, C.A.; Terris, J.A.; Frindt, G.U.; Echevarria, M.I.; Marples, D.; Nielsen, S.; Knepper, M.A. Aquaporin-3 water channel localization and regulation in rat kidney. *Am. J. Phys.-Renal* 1995, *269*, 663–672, doi:10.1152/ajprenal.1995.269.5.F663.

Edwards, S.L., and W.S. Marshall. 2013. Euryhaline Fishes: Principles and Patterns of Osmoregulation and Euryhalinity in Fishes. Elsevier. 1-44 pp.

Ellis, L.V., Bollinger, R.J., Weber, H.M., Madsen, S.S. and Tipsmark, C.K., 2019. Differential Expression and Localization of Branchial AQP1 and AQP3 in Japanese Medaka (Oryzias latipes). *Cells*, *8*(5), p.422.

Evans, D.H., P.M. Piermarini, and K.P. Choe. 2005. The multifunctional fish gill: Dominant site of gas exchange, osmoregulation, acid-base regulation, and excretion of nitrogenous waste. Physiological Reviews. 85:97-177. 24

Fujisawa, K., Takami, T., Nagatomo, T., Fukui, Y., Hoshida, H., Saeki, I., Matsumoto, T., Hidaka, I., Yamamoto, N. and Sakaida, I., 2019. Usefulness of adult medaka fish as a model for the evaluation of alcoholic fatty liver. *Alcohol*, *77*, pp.147-154.

Gilmour, K.M. and Perry, S.F., 2018. Conflict and compromise: using reversible remodeling to manage competing physiological demands at the fish gill. *Physiology*, *33*(6), pp.412-422.

Howe, K., Clark, M.D., Torroja, C.F., Torrance, J., Berthelot, C., Muffato, M., Collins, J.E., Humphray, S., McLaren, K., Matthews, L. and McLaren, S., 2013. The zebrafish reference genome sequence and its relationship to the human genome. *Nature*, *496*(7446), pp.498-503.

Ishibashi, K., Hara, S. and Kondo, S., 2009. Aquaporin water channels in mammals. *Clinical and experimental nephrology*, *13*(2), pp.107-117.

Kirchmaier, S., Naruse, K., Wittbrodt, J. and Loosli, F., 2015. The genomic and genetic toolbox of the teleost medaka (Oryzias latipes). *Genetics*, *199*(4), pp.905-918.

Koster, R., Stick, R., Loosli, F. and Wittbrodt, J., 1997. Medaka spalt acts as a target gene of hedgehog signaling. *Development*, *124*(16), pp.3147-3156.

Kwong, R.W. and Perry, S.F., 2013. The tight junction protein claudin-b regulates epithelial permeability and sodium handling in larval zebrafish, Danio rerio. *American Journal of Physiology-Regulatory, Integrative and Comparative Physiology*, *304*(7), pp.R504-R513.

Lee, S.Y.; Nam, Y.K.; Kim, Y.K. Characterization and expression profiles of aquaporins (AQPs) 1a and 3a in mud loach *Misgurnus mizolepis* after experimental challenges. *Fish. Aquat. Sci.* 2017, *20*, 23, doi:10.1186/s41240-017-0068-6.

Long, H., Crean, C.D., Lee, W.H., Cummings, O.W. and Gabig, T.G., 2001. Expression of Clostridium perfringens enterotoxin receptors claudin-3 and claudin-4 in prostate cancer epithelium. *Cancer research*, *61*(21), pp.7878-7881.

Marshall, W.S. and Bellamy, D., 2010. The 50 year evolution of in vitro systems to reveal salt transport functions of teleost fish gills. *Comparative Biochemistry and Physiology Part A: Molecular & Integrative Physiology*, *155*(3), pp.275-280.

Mishra, R.R., Kneitz, S. and Schartl, M., 2014. Comparative analysis of melanoma deregulated miRNAs in the medaka and Xiphophorus pigment cell cancer models. *Comparative Biochemistry and Physiology Part C: Toxicology & Pharmacology*, *163*, pp.64-76.

Mochizuki, E., Fukuta, K., Tada, T., Harada, T., Watanabe, N., Matsuo, S., Hashimoto, H., Ozato, K. and Wakamatsu, Y., 2005. Fish mesonephric model of polycystic kidney disease in medaka (Oryzias latipes) pc mutant. *Kidney international*, *68*(1), pp.23-34.

Morin, P.J., 2005. Claudin proteins in human cancer: promising new targets for diagnosis and therapy. *Cancer research*, *65*(21), pp.9603-9606.

Murata, Y., Yasuda, T., Watanabe-Asaka, T., Oda, S., Mantoku, A., Takeyama, K., Chatani, M., Kudo, A., Uchida, S., Suzuki, H. and Tanigaki, F., 2015. Histological and transcriptomic analysis of adult Japanese Medaka sampled onboard the international space station. *PLoS One*, *10*(10), p.e0138799.

Naruse, K., Tanaka, M., Mita, K., Shima, A., Postlethwait, J. and Mitani, H., 2004. A medaka gene map: the trace of ancestral vertebrate proto-chromosomes revealed by comparative gene mapping. *Genome research*, *14*(5), pp.820-828.

Roy, S.R., Wang, J., Rana, M.R., Nakashima, M. and Tokumoto, T., 2017. Characterization of membrane progestin receptor α (mPRα) of the medaka and role in the induction of oocyte maturation. *Biomedical Research*, *38*(1), pp.79-87.

Sakamoto, T., T. Kozaka, A. Takahashi, H. Kawauchi, and M. Ando. 2001. Medaka (Oryzias latipes) as a model for hypoosmoregulation of euryhaline fishes. Aquaculture. 193:347-354.

Shima, A. and Mitani, H., 2004. Medaka as a research organism: past, present and future. *Mechanisms of development*, *121*(7-8), pp.599-604.

Soini, Y., 2004. Claudins 2, 3, 4, and 5 in Paget's disease and breast carcinoma. *Human pathology*, *35*(12), pp.1531-1536.

Sugiyama, Y., Ota, Y., Hara, M. and Inoue, S., 2001. Osmotic stress up-regulates aquaporin-3 gene expression in cultured human keratinocytes. *Biochimica et Biophysica Acta (BBA)-Gene Structure and Expression*, *1522*(2), pp.82-88.

Tingaud-Sequeira, A., Chauvigné, F., Fabra, M., Lozano, J., Raldúa, D. and Cerdà, J., 2008. Structural and functional divergence of two fish aquaporin-1 water channels following teleost-specific gene duplication. *BMC evolutionary biology*, *8*(1), p.259.

Tipsmark, C.K.; Kiilerich, P.; Nilsen, T.O.; Ebbesson, L.O.E.; Stefansson, S.O.; Madsen, S.S. Branchial expression patterns of claudin isoforms in Atlantic salmon during seawater acclimation and smoltification. *Am. J. Physiol.* 2008, *294*, R1563-R1574. DOI: 10.1152/ajpregu.00915.2007

Tipsmark, C.K., C. Jorgensen, N. Brande-Lavridsen, M. Engelund, J.H. Olesen, and S.S. Madsen. 2009. Effects of cortisol, growth hormone and prolactin on gill claudin expression in Atlantic salmon. General and Comparative Endocrinology. 163:270-277.

Valdez-Flores, M.A., Vargas-Poussou, R., Verkaart, S., Tutakhel, O.A., Valdez-Ortiz, A., Blanchard, A., Treard, C., Hoenderop, J.G., Bindels, R.J. and Jeleń, S., 2016. Functionomics of NCC mutations in Gitelman syndrome using a novel mammalian cell-based activity assay. *American Journal of Physiology-Renal Physiology*.

Weber, C.R., S.C. Nalle, M. Tretiakova, D.T. Rubin, and J.R. Turner. 2008. Claudin-1 and claudin-2 expression is elevated in inflammatory bowel disease and may contribute to early neoplastic transformation. Laboratory Investigation. 88:1110-1120.

Wilcox, E.R., Q.L. Burton, S. Naz, S. Riazuddin, T.N. Smith, B. Ploplis, I. Belyantseva, T. Ben-Yosef, N.A. Liburd, R.J. Morell, B. Kachar, D.K. Wu, A.J. Griffith, and T.B. Friedman. 2001. Mutations in the gene encoding tight junction claudin-14 cause autosomal recessive deafness DFNB29. Cell. 104:165-172.

Wittbrodt, J., Shima, A. and Schartl, M., 2002. Medaka—a model organism from the far East. *Nature Reviews Genetics*, *3*(1), pp.53-64.

Yan, J.J. and Hwang, P.P., 2019. Novel discoveries in acid-base regulation and osmoregulation: a review of selected hormonal actions in zebrafish and medaka. *General and comparative endocrinology*, *277*, pp.20-29.

Chapter 5 Supplemental Claudin 15 and water handling in the intestine of Japanese medaka, *Oryzias latipes*

Christian K. Tipsmark[1*], Andreas M. Nielsen[2], Maryline C. Bossus[1,3], Laura V. Ellis[1], Christina Baun[4], Thomas L. Andersen[4], Jes Dreier[5], Jonathan R. Brewer[5] and Steffen S. Madsen[1,2]

[1] Department of Biological Sciences, University of Arkansas, SCEN 601, Fayetteville, Arkansas 72701, USA
[2] Department of Biology, University of Southern Denmark, Campusvej 55, 5230 Odense M, Denmark
[3] Department of Math and Sciences, Lyon College, 2300 Highland Rd, Batesville Arkansas 72501, USA
[4] Department of Nuclear Medicine, Odense University Hospital, Sdr. Boulevard 29, 5000 Odense C, Denmark
[5] Department of Biochemistry and Molecular Biology, University of Southern Denmark, Campusvej 55, 5230 Odense M, Denmark
***** Correspondence: tipsmark@uark.edu; Tel.: +1-479-575-8436

5.1 Abstract

When euryhaline fish move between fresh water (FW) and seawater (SW) the intestine undergoes functional changes to handle imbibed SW. In Japanese medaka, the potential transcellular aquaporin-mediated conduits for water are paradoxically downregulated during SW-acclimation suggesting paracellular transport to be of principal importance in hyper-osmotic conditions. In mammals, intestinal claudin-15 (CLDN15) forms paracellular channels for small cations and water, which may participate in water transport. Since two *cldn15* paralogs, *cldn15a* and *cldn15b*, have previously been identified in medaka, we examined salinity effects on their mRNA expression and immunolocalization in the intestine. In addition, we analyzed drinking rate and intestinal water handling by adding non-absorbable radio-tracers, 51-Cr-EDTA or 99-Tc-DTPA, to the water. Drinking rate was >2-fold higher in SW- than FW-acclimated fish and radio-tracer experiments showed anterior accumulation in FW and posterior buildup in SW intestines. Salinity had no effect on expression of *cldn15a,* while *cldn15b* was ~100-fold higher in FW than SW. Despite differences in transcript dynamics, Cldn15a and Cldn15b proteins were both similarly localized in the apical tight junctions of enterocytes, with no apparent difference in localization and abundance between FW and SW. The stability of Cldn15 protein suggests a physiological role in water transport in the medaka intestine.

5.2 Introduction

In fresh water (FW) fishes, the intestinal epithelium must limit excessive fluid absorption while securing dietary ion uptake (Madsen et al., 2015); in seawater (SW), imbibed water is absorbed in a solute-linked process (Whittamore 2012; Madsen et al., 2015). Functional plasticity of the enterocytic epithelium is therefore a critical factor in euryhaline fish capability of going

through salinity transitions. Elevated intestinal aquaporin (Aqp/*aqp*) abundance in eel (Aoki et al., 2003; Martinez et al., 2005;Cutler et al., 2009) and salmonids (Madsen et al., 2011) in response to SW-transfer have led to propose a transcellular water path in these species (Sundell and Sundh, 2012) however, in medaka a consistent downregulation of several intestinal Aqp/*aqp* isoforms after SW-transfer has challenged this model and suggests a major involvement of a paracellular pathway (Madsen et al., 2014).

Transepithelial water transport has been suggested to be mainly transcellular via Aqps but this matter is still under debate (Fischbarg, 2010; Laforenza, 2012). Thus, in leaky epithelia, like the intestine, fluid transport may primarily be paracellular as proposed based on a corneal model (Fischbarg, 2010) or include both components as proposed for marine fish (Whittamore 2012). Taking species differences into account it appears that the medaka intestine may be a choice comparative model to study paracellular fluid transport because a tight junction defined path seems central as suggested by Madsen et al., 2014.

Proteins belonging to the claudin (Cldn) superfamily are the main determinants of tight junction permeability properties and thus important regulators of paracellular transport (Günzel and Fromm, 2012; Günzel and Yu, 2013). Cldns are integral membrane proteins with 4 trans-membrane domains and two extracellular loops (ECL). The amino acid residues of the first ECL are critical for the permselectivity of the junction they create in homo- or hetero-dimeric and -tetrameric combination (Angelow and Yu, 2009; Li et al., 2013; Samanta et al., 2018; Alberini et al., 2018). There are 27 CLDNs paralogs described in mammals (Günzel and Yu, 2013); in the teleost lineage an extensive expansion of the claudin gene family due to gene duplications has led to a higher number with e.g. 56 in Fugu (Loh et al., 2004) and 54 in zebrafish (Baltzegar et al., 2013). The specific permselectivity has been investigated for several mammalian CLDN paralogs,

and there are many examples of barrier-forming as well as specific anion- and cation-pore forming CLDNs (Günzel and Yu, 2009). In addition, there are a few examples of claudins contributing to creating water permeable pores. This has been convincingly demonstrated for CLDN2 (Rosenthal et al., 2010), which has functional significance in the mammalian kidney, and most recently intestinal CLDN15 has also been assigned such a role (Rosenthal et al., 2019) in addition to the cation-pore forming properties of both CLDNs (Günzel and Yu, 2009). However, Na^+ and water fluxes through CLDN15 inhibit each other in functional contrast to CLDN2 (Rosenthal et al., 2019). Based on amino acid homology, especially in the first ECL, it is often assumed that fish Cldns give rise to the same permeability properties as mammalian orthologues, but only a few have been investigated thoroughly (Engelund et al., 2011; Kwong and Perry, 2013). Mutational analysis and MD simulations (Samanta et al., 2018; Alberini et al., 2018) based on the crystal structure (Suzuki et al., 2014) have shown that especially amino acid D55 is critical for CLDN15 pore formation. In support for a similar function in medaka to the mammalian orthologue is the conservation of this amino acid in both medaka Cldn15a and Cldn15b.

A given tissue often shows expression of several CLDN paralogs (Günzel and Yu, 2009). In the mammalian nephron, this is coupled to a highly segmental pattern of expression (Hou et al., 2013). In the mammalian intestine CLDN15 appears to be one of the most abundant CLDNs at least in the small intestine (Holmes et al., 2006; Lu et al., 2013;Garcia-Hernandez et al., 2017) and it plays a critical role in gut ontogeny of both mammals and fish (Bagnat et al., 2007; Tamura et al., 2008). In mice, CLDN15 mediated Na^+ back-flux into the intestinal lumen is essential for active glucose absorption through the Na^+/glucose cotransporter safeguarding monosaccharide uptake (Tamura et al., 2011). In fishes, Cldn15a paralogs have been found to be expressed specifically in the gastro-intestinal (GI) tract (salmon (Tipsmark et al., 2008; Tipsmark et al.,

2010), zebrafish (Clelland and Kelly, 2010), medaka (Bossus et al., 2015). In medaka, we previously identified an additional new paralog, Cldn15b, which is also primarily expressed in the intestine at levels several orders of magnitude higher than any other examined organs (Bossus et al., 2015).

To develop our knowledge about paracellular versus transcellular fluid transport it will be valuable to expand our understanding of water transport and enterocyte tight junctions in medaka. Furthermore, the functional plasticity of the intestine during salinity change in this euryhaline fish is useful when seeking to understand basic principles. The goals of this work were therefore to first study drinking behavior and water handling in response to changes in the osmotic environment, which are unknown in adult medaka. Secondly, we examined expression and localization of the two Cldn15 paralogs in relation to hypo- to hyperosmotic acclimation based on the assumption that intestinal Cldn15 is implicated in water transport, as seen in other models.

5.3 Materials and Methods

5.3.1 Fish and rearing conditions

The Japanese medaka (*Oryzias latipes*) used for this study came from two different sources. Fish (CAB strain) used for histological examinations, drinking rate and drinking-related experiments were purchased from the UMS AMAGEN (Centre national de la recherche scientifique, Gives-sur-Yvette, France) and held in tanks with biofiltered FW or 30 ppt at 24-26 $^{\circ}$C and exposed to 12:12 light:dark photoperiod. These fish were generally fed four times per day with TetraMin® flakes (Tetra GmbH, D-49324 Melle, Germany) and the food was withheld 2 days before any experimentation. The experimental procedures were approved by the Danish Animal Experiments Inspectorate in accordance with the European convention for the protection of

vertebrate animals used for experiments and other scientific purposes (#86/609/EØF). Long-term acclimated fish for transcriptional analysis were obtained from Aquatic Research Organisms, Inc. (Hampton, NH, USA; CAB strain) and held in biofiltered FW or 30 ppt SW and sampled after 1 month of acclimation. They were fed daily with TetraMin tropical flakes (Tetra, United Pet Group, Blacksburg, VA, USA), and food was withheld 2 days prior to any sampling. To investigate the early response to hyper-osmotic environments, 10 female and 10 male FW-acclimated medaka were transferred to both sham FW conditions and SW (30 ppt; Instant Ocean, Spectrum Brands, Blacksburg, VA, USA; N = 40) and sampled after 6, 24, and 168 h (n = 6 per group). All handling and experimental procedures were approved by the Animal Care and Use Committee of the University of Arkansas (IACUC 17091).

5.3.2 Drinking rate measurements

A series of experiments was performed to estimate the rate of drinking in FW- and SW-acclimated medaka. The gamma emitter 51-Cr-EDTA (PerkinElmer, NEZ147001MCNSA1, Waltham, MA) was used as a non-absorbable marker for these experiments. The tracer (5 MBq) was added to the water (1 L FW or 30 ppt SW) and the fish (N = 10-12) were then transferred to the experimental tank [35, 40]. They were allowed to drink for 3 h, after which they were transferred to clean water (1 L) for 3 min and transferred to another tank with clean water (1 L) for 30 min. The fish were then anaesthetized in 100 mg/L MS-222 (Tricaine methanesulfonate) and killed by cervical dislocation. Before dissection, the fish was blotted by a paper towel and weighed to the nearest mg. The intestine was carefully ligatured at anterior and posterior ends, removed from the body and transferred to a 5 mL scintillation vial. The head was separated from the body with remaining organs and transferred to separate scintillation vials. All samples were added 0.5 mL distilled water and counted on a PerkinElmer 1480 WizardTM 3” Automatic gamma

counter. The radioactivity of a 1.0 mL water sample was measured to estimate the specific radioactivity of the drinking water. Background radioactivity was counted on a 1.0 mL non-radioactive water sample. All samples were corrected for background and the specific drinking rate (μL/g/h) was calculated as DR = sa/(bw*time), DR = drinking rate, sa = background-corrected specific activity (counts/minute); bw = body weight; time = time in radioactive water. Prior to these experiments the accumulation of 51-Cr radioactivity was investigated and found to be linear in excess of 3 h.

5.3.3 Water passage through the GI-tract

Medaka are agastric fish meaning that the esophagus is directly connected to the anterior part of the tube-like intestine. In order to trace the passage of imbibed water in FW and SW-acclimated fish, two fish were allowed to drink for 3 h in water which had been added 51-Cr-EDTA, as described above. After this the fish were anaesthetized in MS-222, killed by cervical dislocation and the complete GI tract was ligatured at both ends and removed from the fish. Segments of 5-6 mm were then ligatured and carefully dissected into scintillation vials, to estimate the longitudinal distribution of radioactivity. The counting and calculations were done according to the above methodology and the data were graphed in percent of total radioactivity as a function of longitudinal position.

5.3.4 Single photon emission computed tomography (SPECT) - Computed tomography (CT) scanning

In order to visualize the intestinal passage of imbibed water, a series of experiments was done in which fish were allowed to drink water with added non-absorbable marker 99-Tc-DTPA (Technetium-99mTc-diethylene-triamine-pentaacetic acid). This short-lived gamma emitter ($T_{1/2}$

= 6.0067 h) is a widely used clinical radio-phamaceutical for renal diagnosis and functioning. Subsequently, the fish were analyzed by SPECT-CT scanning. SPECT scanning is used for 3-dimensional analysis of the radiochemical, CT-scanning creates a 3-dimensional x-ray image, and when the two images are merged, a high-resolution image localizing the radiochemical to internal structures is obtained. All SPECT/CT scans were performed on a Siemens INVEON multimodality pre-clinical scanner (Siemens pre-clinical solutions, Knoxville, TN, USA).

Three fish were used for experiments in FW and SW, respectively, with imaging time-points at 1 h, 4 h and 6 h for each group. For each salinity, two fish were transferred to a container with 100 mL water with the addition of 3.5 GBq Tc-99-DTPA, and one fish was transferred to a container with 100 mL water with the addition of 5 GBq Tc-99-DTPA. Due to the short half-life of 99-Tc isotope a relatively high specific activity in the water is needed in order to obtain a good signal-noise ratio for visualization, thus a higher activity was required for the late imaging group. All fish were allowed to drink in the labelled water for 1 h. Then they were transferred to separate containers with 1 L of clean water for 5 min, followed by transfer to a second container with 1 L of clean water to rid the external surface for radioactivity. For each salinity, one fish was then euthanized in an overdose of MS-222 after a total of 1, 4, and 6 h after transfer to clean water and analyzed by SPECT-CT scanning in order to analyze the progressive movement of imbibed isotope through the GI tract. After euthanasia each fish was wrapped in plastic to avoid dehydration during the following imaging. The fish was placed in a lateral position on a dedicated SPECT/CT pre-clinical bed (25 mm).

CT scans were performed with the following settings; 360° rotation with 360 projections and 2x2 bin. The magnification was set at medium, yielding an isotropic pixel size of 40.00 μm and a trans-axial field view of 42 mm. Tube voltage was set to 80 kV, current was 500 μA and each

projection was exposed for 1000 ms. CT scans were reconstructed using Feldkamp algorithm, with Sheep-Logan filter and slight noise reduction. SPECT images were acquired using mouse high resolution single pinhole collimators. A full 360° rotation with 60 projections and fixed radius of 25 mm yielded a reconstructed of 28 mm trans-axial field of view. A 20% energy window centered around the energy peak of 99mTc at 140 keV was used. Acquisition duration was set to 100 sec/projection. CT and SPECT images were co-registered using a transformation matrix and SPECT data was reconstructed using Siemens MAP3D algorithm (matrix 128x128, 0.5 mm pixels, 16 iterations and 6 subsets).

5.3.5 RNA isolation, cDNA synthesis, and qPCR

RNA isolation was conducted according to the manufacturer's protocol (TRI Reagent®; Sigma Aldrich). All samples were homogenized using a Power Max 200 rotating knife homogenizer (Advanced Homogenizing System; Manufactured by PRO Scientific for Henry Troemner LLC, Thorofare, NJ, USA). 500 ng of total RNA was used for cDNA synthesis using the Applied Biosystems High Capacity cDNA Reverse Transcription kit (Thermo Fisher). Used primers were previously validated and published in Bossus et al. [34] and Madsen et al. [6]. Elongation Factor 1 alpha (*ef1α*), beta actin (*βact*), and ribosomal protein L7 (*rpl7*) were analyzed as normalization genes in all experiments. Quantitative PCR was run on a Bio-Rad CFX96 platform (BioRad, Hercules, CA, USA) using SYBR® Green JumpStart (Sigma Aldrich). qPCR cycling was conducted using the following protocol: a denaturation/activation step (94 °C) for 3 min, 40 cycles of a 15 s denaturation step (94 °C) followed by an annealing/elongation step for 60 s (60 °C), and finally a melting curve analysis at an interval of 5 s per degree from 55 to 94 °C. The absence of primer–dimer association was verified with no template controls (NTC). As an alternative to DNAse treatment, the absence of significant genomic DNA amplification was

confirmed using total RNA samples instead of cDNA in a no reverse transcriptase control (NRT). Primer amplification efficiency was analyzed using a standard curve method with dilutions of the primers from 2 to 16 times. Amplification efficiency was used to calculate the relative copy numbers of the individual targets. Relative copy numbers were calculated by $E_a^{\Delta Ct}$, where Ct is the threshold cycle number and E_a is the amplification efficiency. Data were normalized to the geometric mean of the three normalization genes.

5.3.6 Immunofluorescence, confocal and Stimulated Emission Depletion (STED) microscopy

Preparation of medaka intestines for immunofluorescence microscopy followed the procedures described previously (Engelund et al., 2015). Sections (0.5 cm) from the middle part of the intestines from medaka acclimated to FW and 30 ppt SW were sampled and fixed overnight in 4% buffered paraformaldehyde at 4 °C. After rinsing several times in 70% EtOH the tissues were dehydrated overnight through graded series of EtOH and xylene followed by embedding in 60 °C paraffin. Five-micron thick transversal sections were cut on a microtome and sections were placed on Superfrost plus (Gerhard Menzel GmbH, Braunschweig, Germany) slides before being dried overnight at 55 °C. The tissue sections were then hydrated through washes in xylene, 99, 96 and 70 % EtOH and finally Na-citrate (10 mM Na-citrate, pH 6.0). Antigen retrieval was performed by boiling the sections in the citrate solution for 5 min in a microwave oven and leaving them in the warm citrate solution for 30 min before being washed in 1x PBS (in mmol L^{-1}: 137 NaCl, 2.7 KCl, 1.5 KH_2PO_4, 4.3 Na_2HPO_4, pH 7.3). Representative sections were then blocked by incubation in 2% goat serum and 2% bovine serum albumin in 1x PBS for 1 h at room temperature. This was followed by dual labelling with a cocktail of an affinity purified polyclonal rabbit antibody against medaka Cldn15a or Cldn15b, respectively, in combination with the monoclonal mouse α5 antibody, which recognizes alpha-subunit of the Na^+,K^+-ATPase in all vertebrates (The

Developmental Studies Hybridoma Bank developed under auspices of the National Institute of Child Health Development and maintained by The University of Iowa, Department of Biological Sciences, Iowa City, IA, USA). Primary antibodies were diluted in 2% goat serum and 2% bovine serum albumin in PBS and incubated overnight at 4 °C. The polyclonal claudin antibodies were custom made in rabbits by Genscript (Piscataway, NJ, USA) against the following epitopes near the C-termini: Japanese medaka Cldn15a PAPTRSVVASTYGR, GenBank accession XP_004079873.1; Japanese medaka Cldn15b SHAAPSNYDRNAYV, GenBank accession XP_004076514.1). They were used at the concentrations 0.5 µg/mL (Cldn15a) and 0.6 µg/mL (Cldn15b). The α5 antibody was used at 0.2 µg/mL.

For immunofluorescence and confocal microscopy, the following secondary antibodies were used for visualization: Alexa Flour® 568 Donkey Anti-Rabbit IgG (H+L) at 1 ug/mL and Oregon Green® 488 Goat Anti-Mouse IgG (H+L) at 2ug/mL (InvitrogenTM Molecular ProbesTM, Carlsbad, USA). Incubation time was 1 h at 37 °C for the secondary antibody. Sections were then washed repeatedly in PBS and coverslips were mounted using ProLong Gold antifade reagent (Invitrogen).

For STED-microscopy we used higher claudin antibody concentrations: 0.7 µg/mL (Cldn15a), 0.9 µg/mL (Cldn15b). The secondary antibodies used for STED were: goat-anti-rabbit Abberior® STAR 488 and goat-anti-mouse Abberior® STAR 440SX (Sigma-Aldrich) at 1:200 and 1:1000 dilution, respectively. Negative control incubations with 2% BSA in PBS instead of primary antibodies were made routinely. The fluorescence was inspected on a Leica HC microscope (Manheim, Germany) and pictures of representative areas were captured using a Leica DC200 camera. Confocal images were taken on a Zeiss LSM510 META confocal microscope (CarlZeiss, Oberkochen, Germany) using a 63x objective with oil immersion. STED images were recorded

using a Leica TSC SP8 STED setup. The excitation was done at 500 nm using a white light laser for Abberior STAR 488 and at 458 using an Argon laser for Abberior STAR 440SXP. The depletion laser (STED laser) was a 592 nm CW for both channels. The emission was recorded at 510-560 nm using the gated hybrid detector (0.3 ns) in counting mode for the Abberior STAR 488 and at 500-550 nm using the non-gated hybrid detector in counting mode for the Abberior STAR 440SXP. The images were cross-talk corrected and deconvoluted using Huygens™ (Hilversum, Netherland). The deconvolution was done to further increase the resolution of the images and decrease the background.

5.3.7 Statistical Analyses

All data analysis was conducted using GraphPad Prism 8.0 software (San Diego, CA, USA). Data from the salinity transfer experiments where analyzed using Bonferroni adjusted two-tailed Student's t-test in experiments with two groups and two-way ANOVA followed by Bonferroni's multiple comparisons test of time-matched groups in experiments with more groups. Drinking rates were analyzed using two-tailed Student's t-test. When required, data were log or square root transformed to meet the ANOVA assumption of homogeneity of variances as tested with Bartlett's test. Significant differences were accepted when $P < 0.05$.

5.4 Results

5.4.1 Drinking rate and intestinal handling of imbibed water

In preliminary experiments using both FW- and SW-acclimated fish, it was assured that intestinal accumulation of radioactivity in fish continued linearly in excess of 3 h, thus gut-passage time after drinking was well in excess of 3 h (data not shown). Thus, drinking rate estimation was

based on a 3 h incubation in 51-Cr-EDTA containing water. Drinking rate was relatively high in FW-acclimated medaka (5 µL/g/h) but was doubled in fish acclimated to SW (figure. 5.1). Drinking rate measurements were based on counting radioactivity in the GI-tract after incubation and a 1 h rinsing period in clean water.

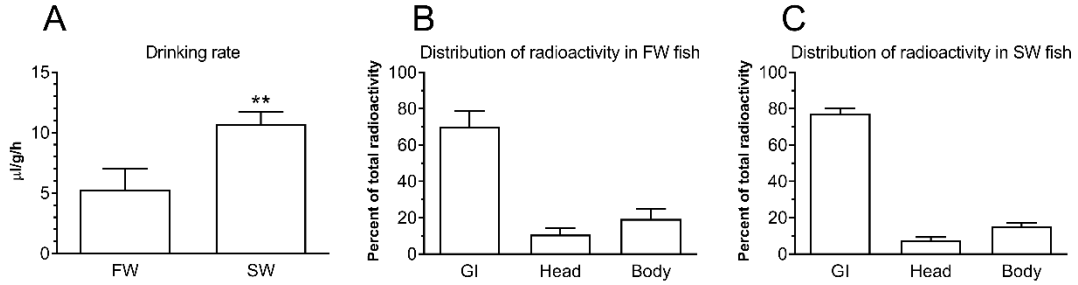

Figure 5.1 A) Drinking rate (µL/g/h) in FW and SW-acclimated medaka estimated by radioactivity in the entire gastro-intestinal tract after incubation in 51-Cr-EDTA traced FW or SW for 3 h followed by rinsing in clean water for 1 h. ** $P < 0.01$. In B (FW) and C (SW) the radioactivity content of the gastro-intestinal tract (GI, imbibed) is compared to radioactivity absorbed to the head and remaining body parts.

The head and body carcass where counted separately after the experiment, and the radioactivity content in these parts amounted to 8-10% and 15-20%, respectively, of the total radioactivity of the fish (figure 5.1B, C). It is assumed that this is mainly due to attachment to the external mucus layer in these body parts, as Cr-EDTA has been shown to be a non-absorbable marker, which means that it does not cross the intestinal epithelium (Usher et al., 1988).

When dissected intestines were carefully fragmented into 0.5 cm segments and analyzed, it was found that radioactivity was evenly distributed but with a trend of showing higher levels at the anterior end of the FW intestine (figure 5.2A). In the SW-acclimated fish, the radioactivity clearly accumulated toward the posterior end of the intestine (figure 5.2B).

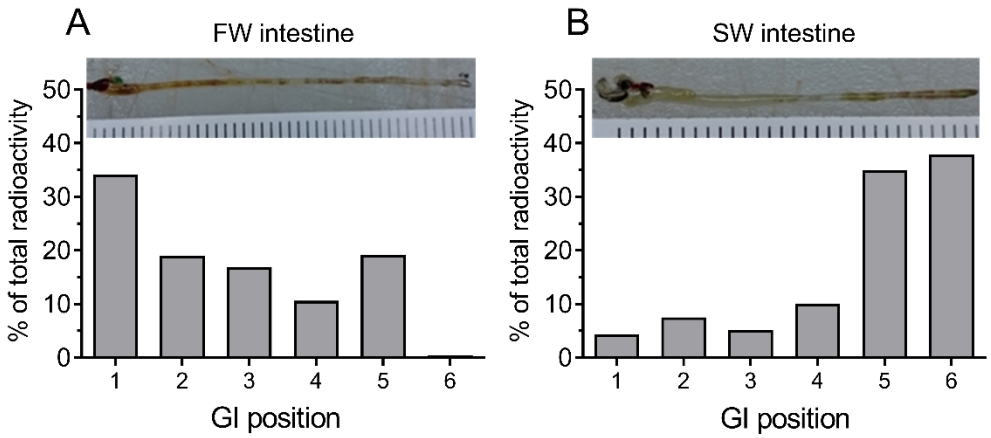

Figure 5.2 Distribution of radioactivity longitudinally in the gastro-intestinal (GI) tract of fish allowed to drink 51-Cr-EDTA traced FW (A) or SW (B) water for 3 h. After incubation, the entire GI-tract was ligatured into 0.5 cm segments and each segment was then transferred to a scintillation vial and scanned for radioactive content. The entire intestine was approximately 3 cm in length as shown in the inserted photographs.

The progressive movement of imbibed water along the intestine was followed in a more direct way by a series of SPECT-CT scans of intact, euthanized fish after incubation times in 99-Tc-DTPA- traced water (figure 5.3). The imaging series showed an initial high intensity of tracer in the esophageal end of the GI-tract with a more posterior distribution as incubation time was increased. Precipitation of mineral salts (Mg- and Ca-carbonates) could be seen in the CT-images of SW-acclimated fish ca 2/3 down the intestine (white arrowhead in figure 5.3D).

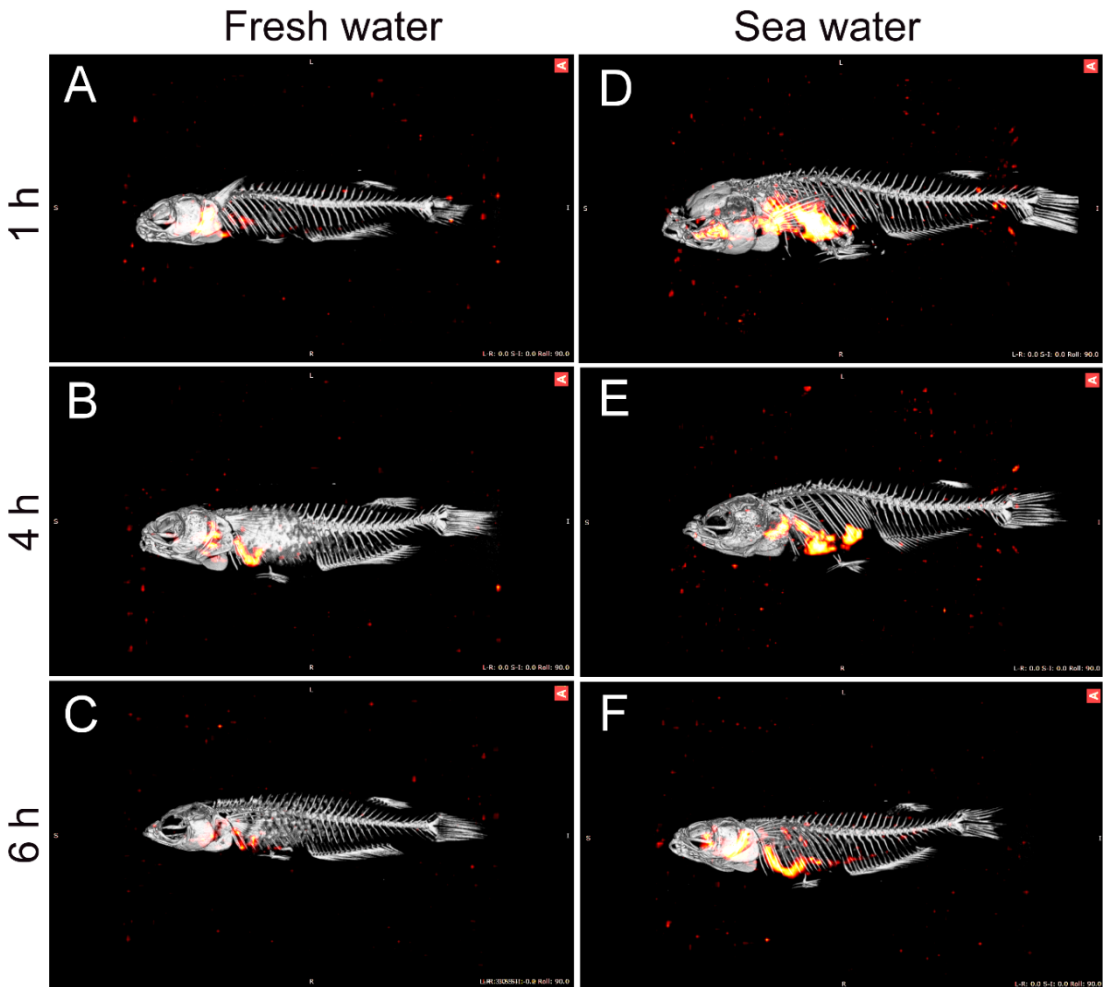

Figure 5.3 Visualization of the movement of imbibed water along the gastro-intestinal tract of medaka acclimated to FW (A, B, C) or SW (D, E, F). Images are merged from SPECT (red intensity layer) and CT (gray) scans of fish which had been incubated in 99-Tc-DTPA traced FW or SW for 1 h followed transfer to non-radioactive FW or SW for 1 h (A, D), 4 h (B, E) or 6 h (C, F). The SPECT layer visualizes the localization (and intensity) of imbibed isotope-labelled water, the CT layer visualizes mineralized structures (skeleton and mineral precipitates in the SW intestines, white arrowhead in D). Note that 99-Tc has a short half-life (6 h), which influences the apparent intensities of the imbibed isotope.

5.4.2 Transcript levels and response to salinity

The transcript levels of selected targets were analyzed in intestines from medaka long-term acclimated to FW and SW (figure 5.4). The absorptive Na^+, K^+,$2Cl^-$ cotransporter (*nkcc2*) level was several-fold higher in SW than FW fish, whereas *cldn15b*, *aqp1a* and *aqp8ab* levels were significantly reduced in SW compared to FW fish. *cldn15a* was unaffected by long-term salinity

acclimation. The salinity-induced changes in transcript levels observed in long-term acclimated fish were fully reproduced in a 7-day time course experiment (figure 5.5), with *nkcc2*, *cldn15b*, *aqp1a* and *aqp8ab* all being significantly affected by both salinity and time (2-way-ANOVA). *cldn15a* was unaffected by salinity during the 7-day time course experiment, as observed in long-term acclimated fish.

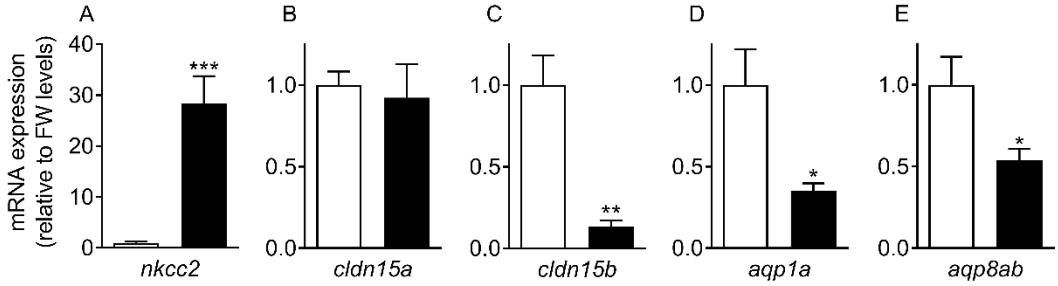

Figure 5.4 Transcript levels of nkcc2 (A), cldn15a (B), cldn15b (C), aqp1a (D) and aqp8ab (E) in intestine from medaka acclimated to fresh water (FW, white bars) or seawater (SW, black bars). Fish were acclimated to the respective salinities for over one month prior to sampling (n = 8). Expression levels represent the mean value ± SEM relative to FW levels. Asterisks indicate a significant difference from FW expression (*P < 0.05, **P < 0.011).

.

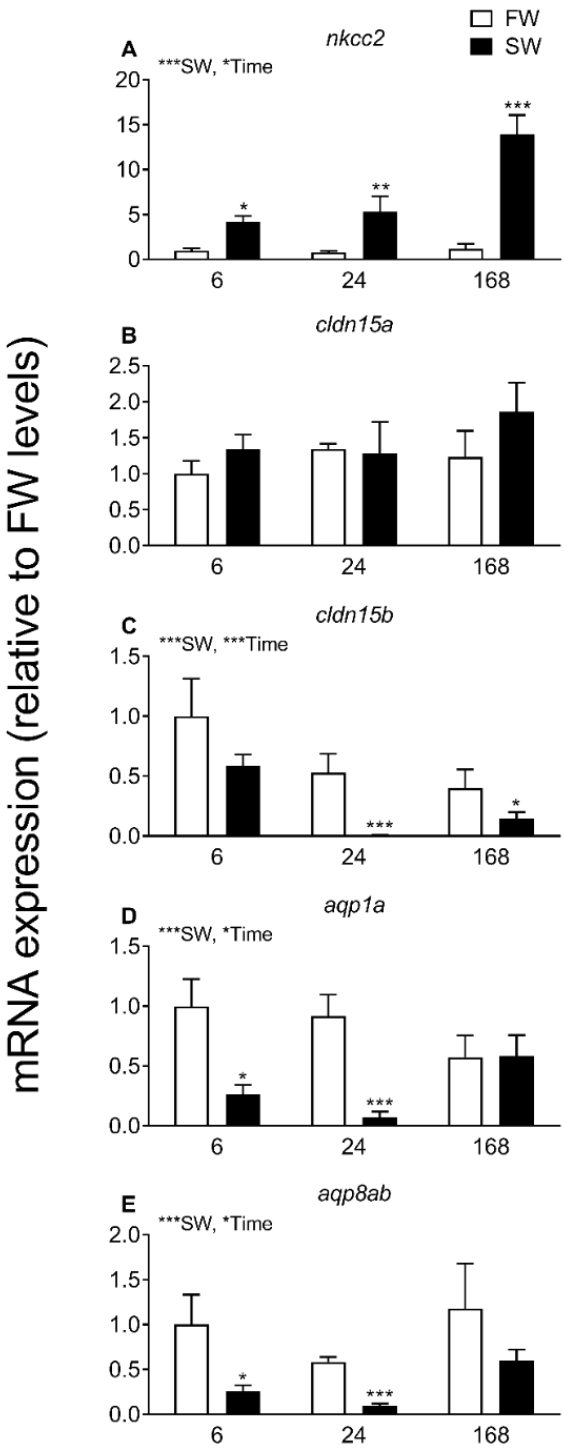

Figure 5.5 Effect of FW-to-SW transfer on intestinal transcript levels of *nkcc2* (A), *cldn15a* (B), *cldn15b* (C), *aqp1a* (D) and *aqp8ab* (E). Fish were transferred from FW-to-SW (black bars) or FW-to-FW (white bars) as a control and sampled at 6, 24 and 168 h

($N = 6$). Expression levels represent the mean value ± SEM relative to the 6 h-FW group. Asterisks next to *SW* and *Time* refers to overall effects of a factor with two-way ANOVA. When interaction between factors was significant, differences between time matched groups were analyzed with Bonferroni multiple comparisons test (*$P < 0.05$, **$P < 0.01$, ***$P < 0.001$).

5.4.3 Cldn15 localization in the intestinal epithelium

Cldn15a and Cldn15b showed similar localization in the intestinal epithelium. Immunoreactivity was confined to the apical area of enterocytes with distinct "hot spots" in the apical junction area between enterocytes (figure. 5.6 and 5.7). At lower magnification these hot spots were partly masked by non-specific staining of the brush-border area at variable intensity (figure 5.6A and C).

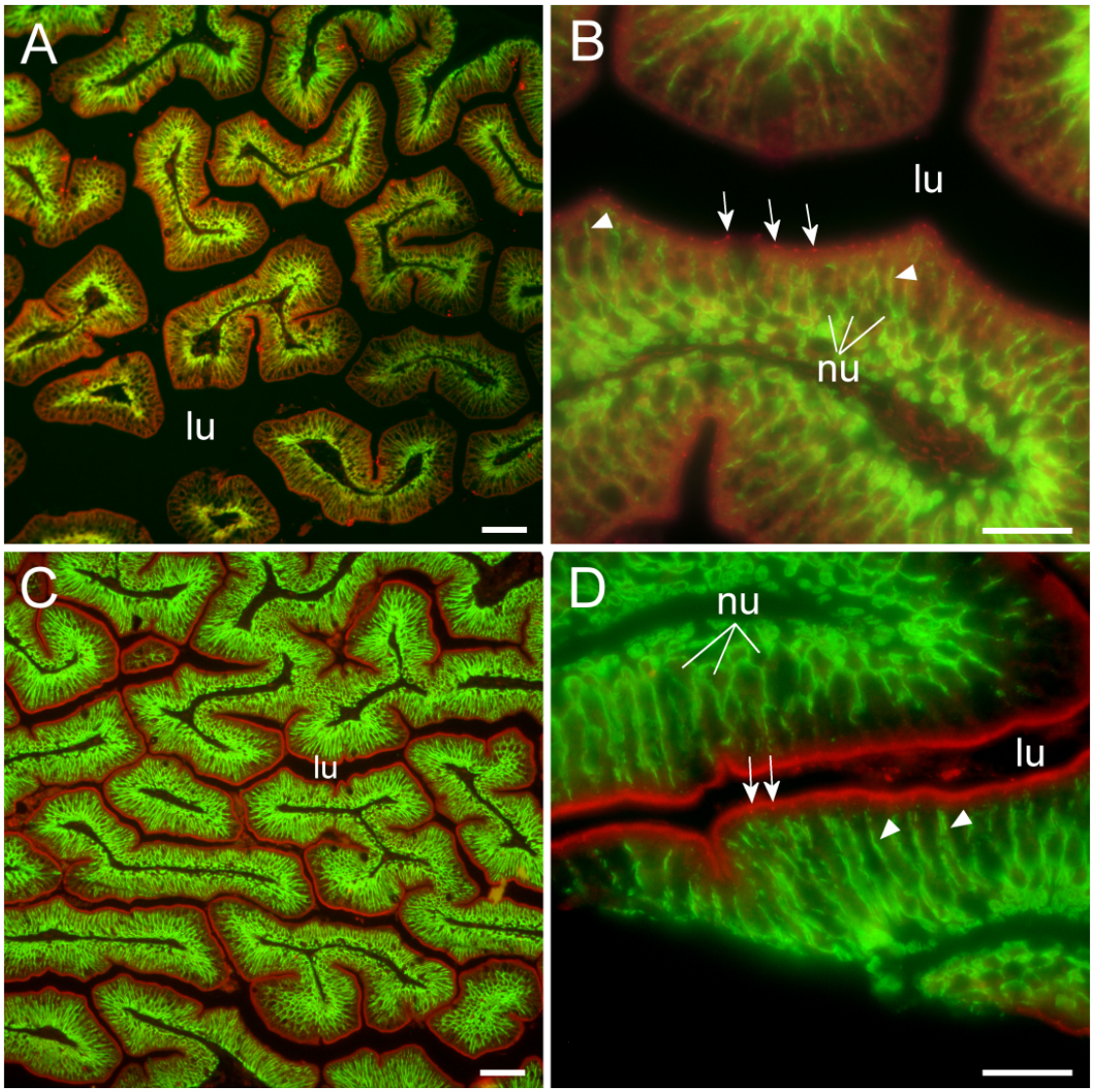

Figure 5.6 Immunofluorescence micrographs showing apical localization of Cldn15a (red, in A and B), and Cldn15b (red in C and D) and baso-lateral localization of Na^+,K^+-ATPase alpha subunit (green) in FW-acclimated medaka middle intestine. (A) and (C) are at 200x magnification, (B) and (D) are at 1000x magnification. lu = lumen, nu = nuclei; in (B) and (C) arrows point to claudin "hot spots" in the tight junction zones; arrowheads point to lateral membranes. Size bars indicate 50 µm (A, C) or 20 µm (B, D).

.

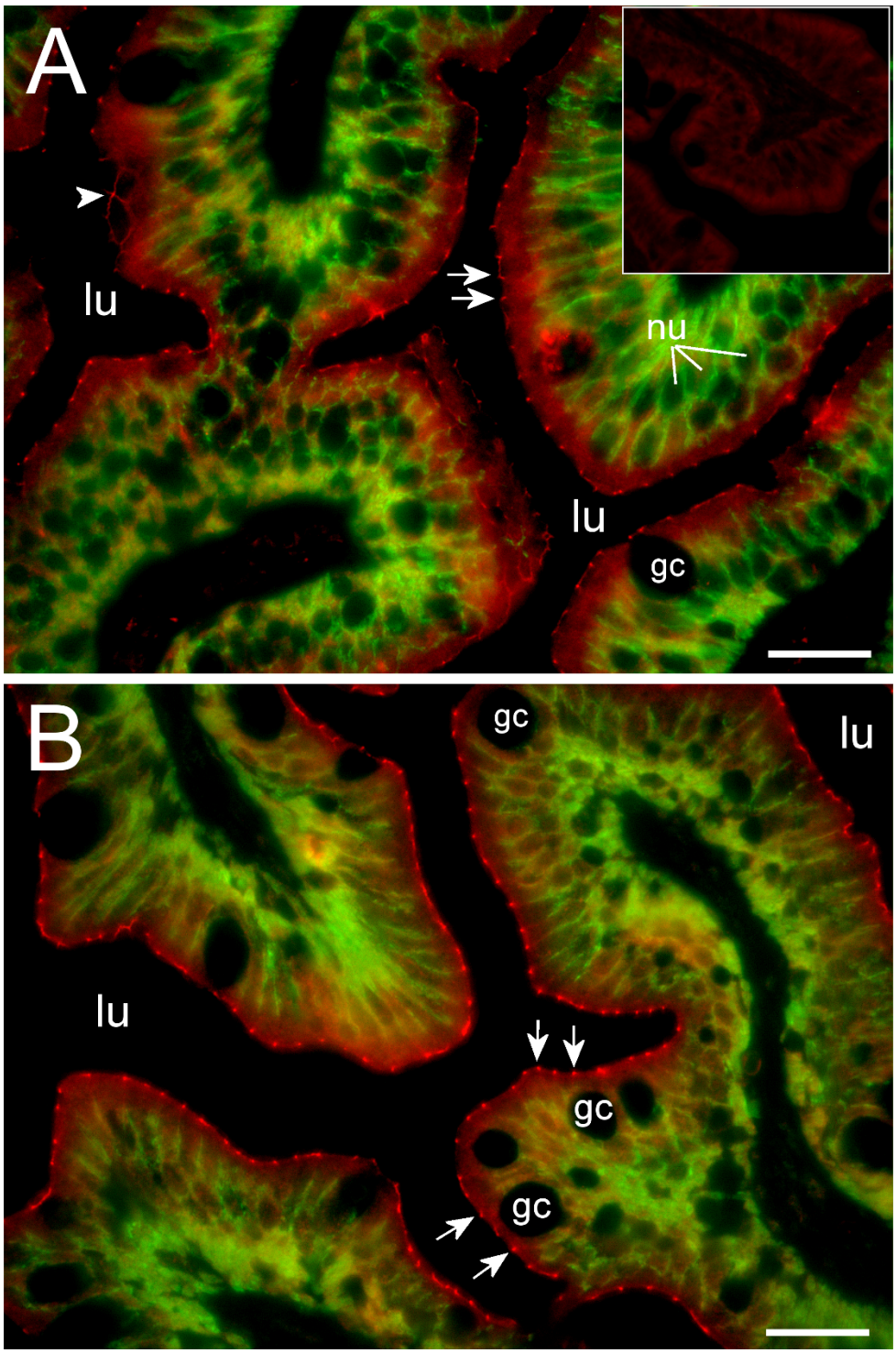

Figure 5.7 Immunofluorescence micrographs showing apical localization of Cldn15a (red in A) and Cldn15b (red in B) and baso-lateral localization of Na^+,K^+-ATPase alpha subunit (green) in SW-acclimated medaka middle intestine. Insert in upper left corner shows control without primary antibodies. Images are at 1000x magnification. lu = lumen,

gc = goblet cell, nu = nuclei; arrows point to "hot spots" in the tight junction zones; Size bars indicate 20 µm.

However, these “hot spots” became particularly evident at higher magnification (figure 5.6B, C, figure 5.7) and when inspecting the tissues with confocal and STED microscopy which has a much narrower z-plane focus (figure 5.8 and 5.9). Control incubation without primary cldn15 antibodies showed a very faint general fluorescence without the distinct “hot spots” (insert in figure 5.7A). Na^+,K^+-ATPase alpha subunit immunostaining revealed parallel lateral membranes, which were slightly spaced between neighboring cells, thus creating the lateral intercellular space (e.g. see figure 5.6D, 5.8A and 5.8B, marked with arrowheads). Near the basal borders, the membrane staining surrounded the nuclei, which appeared as circular dark "holes" in the images (marked "nu" in figure 5.6, 5.7 and 5.8). The distinct claudin staining was apical to the Na^+,K^+-ATPase staining, i.e. at the end of an axis extrapolated from the lateral membrane area. Thus, there was no co-localization of the two antibodies. This indicates that the two claudin 15 proteins are located in the tight junction zone.

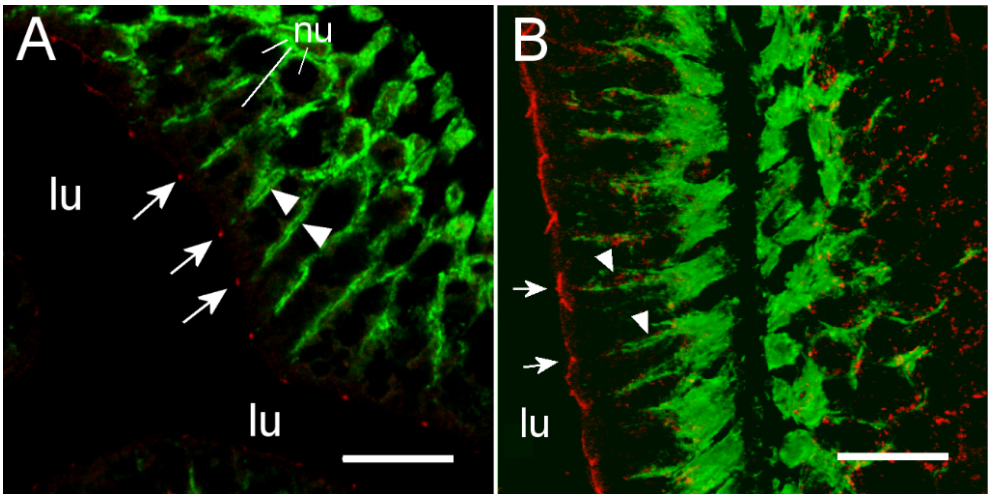

Figure 5.8 Confocal images showing apical localization of Cldn15a (red in A) and Cldn15b (red in B) and baso-lateral localization of Na^+,K^+-ATPase alpha subunit (green) in SW-acclimated medaka middle intestine. lu = lumen; arrows point to Cldn15 "hot spots" in the tight junction zones; arrowheads point to lateral membranes of enterocytes clearly separating the intercellular space. Size bars indicate 10 µm.

Occasionally, the section plane was slightly tilted and therefore made it possible to obtain a zoomed view of the apical junction area just below the brush border zone (figure 5.9). In these cases, confocal STED microscopy showed a beautiful polygonal staining revealing the 3-dimensional junction zone surrounding the individual enterocytes. These polygons varied from simple tetragons to heptagons in shape, indicating enterocytes surrounded by 4-7 neighboring cells.

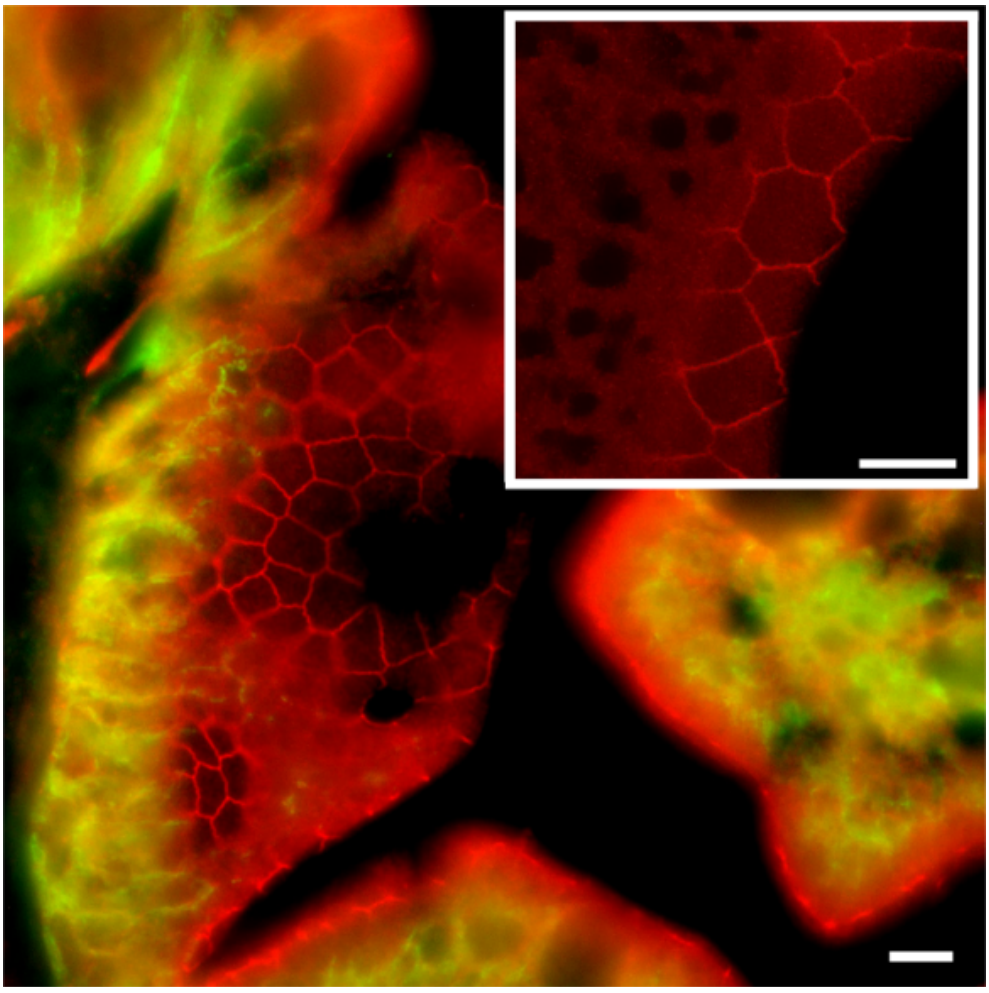

Figure 5.9 Confocal STED images showing apical localization of Cldn15b (red) in SW-acclimated medaka middle intestine. Large image shows double staining with anti-Na^+,K^+-ATPase alpha subunit (green). Na^+,K^+-ATPase is localized in baso-lateral membranes as shown in Figureures 6-8, and is absent in the apical area, where the tight junctions are located. Thus, the mosaic like pattern of Cldn15b is without green overlay.

Subfigureure shows a subsection of the apical area focusing on the tight junction area. Size bars indicate 5 μm.

5.5 Discussion

Japanese medaka can move between FW and SW while maintaining osmotic homeostasis. Based on our knowledge from several other teleosts, this requires high functional plasticity in e.g. the intestine, which in FW contributes to maintain ion-balance and in SW switches to fluid absorption to compensate for dehydration (Marshall and Grosell 2006). Fluid absorption in fishes is driven by solute-transport and is generally assumed to occur mainly through a transcellular pathway (Whittamore 2012; Sundell et al., 2012). Accordingly, intestinal aquaporin expression is elevated during hyper-osmotic exposure in order to develop the trans-cellular pathway (Cerdá and Finn, 2010; Tipsmark et al., 2010B). This paradigm was challenged in previous studies, where we and others showed that in medaka *spp*., unlike other species studied, intestinal aquaporin expression is *down*-regulated at both transcript and protein levels when fish are exposed to hyper-osmotic conditions (Kim et al., 2014; Madsen et al., 2014). This paradox suggests that the paracellular pathway may be of higher importance, at least in the medaka. The recent report that the mammalian tight junction CLDN15 may create intestinal water channels (Rosenthal et al., 2010), led us to investigate the role of the medaka orthologues in relation to fluid absorption. With limited knowledge about medaka drinking behavior and intestinal water handling, we set out by examining salinity effects on drinking behavior and water handling and then address the specific expression of *cldn15*. If involved in paracellular fluid absorption, our expectation was that *cldn15* expression would increase after SW-exposure.

5.5.1 Drinking rate and intestinal handling of imbibed water

After transition to SW drinking rates and fluid absorption in the intestine increase in most examined fish species (Marshall and Grosell, 2006). In order to understand intestinal function using the adult medaka model we had to describe its drinking behavior and water handling, which was until now unknown. We demonstrated that drinking rate was 5 μL/g/h and 10 μL/g/h in FW and SW medaka, respectively (figure 5.1); thus, SW-transfer doubled oral water intake, presumably due to the need to compensate for osmotic water loss in the concentrated environment. This is similar to what has been observed in other euryhaline fish (Usher et al., 1988; Perrott et al., 1992; Fuentes et al., 1996) including Japanese medaka larvae (Kaneko and Hasegawa, 1999), and rates are comparable to other studies albeit on the high side (Fuentes and Eddy, 1997). Drinking rate is inversely related to body mass (Fuentes and Eddy, 1997) and probably related to surface-to-volume ratio aspects, and most fishes examined up to now were larger fish (5-800 g). Medaka used in these experiments are small (0.4-0.6 g) and the smaller SW fish examined so far have comparable drinking rates [*Pholis gunnelus*, 2-10 g: 12 μL/g/h; *Aphanius dispar*, 0.4-1 g: 10 μL/g/h; see Fuentes and Eddy, 1997]. It is often assumed that FW fish should keep oral water intake to a minimum in order to not put excessive strain on the kidney in a hypo-tonic environment (Marshall and Grozell, 2006). This is certainly the case in some FW teleosts [e.g. 0.4 μL/g/h in 0.1-2.5 g *Platichthys flesus*: (Hutchinson and Hawkins, 1990). However, there are also reports of significant drinking in FW teleosts in the μL/g/h-range (Tytler et al., 1990; Fuentes et al., 1999; Lin et al., 2001) and this also seems to be the case in FW medaka. We do not have any physiological explanation why FW drinking rates were so relatively high compared to other studies. Feeding events could possibly be accompanied by swallowing of small amounts of water, but normally, including the present study, fish are unfed during drinking rate measurements. Stress

is another factor that may affect drinking and water turnover, but the fish were left undisturbed during the whole experiment, so we must assume that it is negligible. It has been speculated that drinking in FW may be a source of divalent ions such as Ca^{2+} (Tytler et al., 1990) but the significance of this was rejected by Lin et al. 2001 based on quantitative analyses in tilapia.

When analyzing the segmental distribution of 51-Cr-EDTA-traced water in the intestine (figure 5.2), our data showed that in FW fish, 51-Cr-EDTA was for the most part located anteriorly in contrast with a more posterior accumulation in SW fish. This is in perfect agreement with Kaneko and Hasegawa's 1999 observations in medaka larvae, using a laser scanning technique to visualize intestinal water handling. This suggests that imbibed water in FW fish is taken up by osmosis in the anterior intestine were the tracers accumulate, and the volume regulatory problem associated must then be corrected by the kidney. While it is difficult to get reliable measurements of luminal fluid in small medaka, a study on FW tilapia showed that anterior, middle and posterior luminal osmolality is close to plasma levels (Grosell 2007). This corroborates an equilibration of the luminal fluid (FW) with plasma in the anterior intestine. In SW, after initial desalination in the esophagus luminal fluid osmolality in tilapia is similar all along the intestine and is higher than plasma osmolality (Grosell 2007). Water uptake must therefore rely on solute-driven transport into the lateral intercellular space in the anterior parts of the intestine (Madsen et al., 2014) in combination with $CaCO_3$ precipitation in the posterior end to increase the concentration of free water molecules (Whittamore 2012; Marshall and Grosell, 2006). Therefore, continuous water flow along the intestine means that 51-Cr-EDTA tend to accumulate in the posterior section in SW fish. The accumulation of the non-absorbable tracer, 99-Tc-DTPA, at the posterior end indirectly supports the progressive absorption of water. This was further supported by the SPECT/CT imaging, in which the progress of water movement in the intestine was visualized directly in live

fish (figure 5.3). In SW fish, CT scans further revealed mineral precipitation in the posterior intestine, suggesting bicarbonate secretion which induces Mg- and Ca-carbonate precipitation that helps drive osmotic water transport across the intestinal epithelium (Whittamore 2012).

5.5.2 Transcript levels and response to salinity

The progress of SW-acclimation was followed by transcript analyses of a few selected targets representing intestinal NaCl uptake (*nkcc2*), which is needed to establish solute-driven water absorption and a possible transcellular water uptake pathway (*aqp1a, aqp8ab*) (figure 5.4 and 5.5). As expected, there was a steep increase in *nkcc2* in SW, suggesting increased NaCl transport across the apical enterocytic brush-border membrane. The data also confirmed the paradoxical drop in *aqp1a* and *aqp8ab* expression found in previous studies [*O. latipes*: 8; *O. dancena*: Kim et al., 2014]. Thus, based on aquaporin dynamics, transcellular water transport is not supported in SW medaka; and it remains puzzling, why aquaporin expression is kept higher in the FW condition.

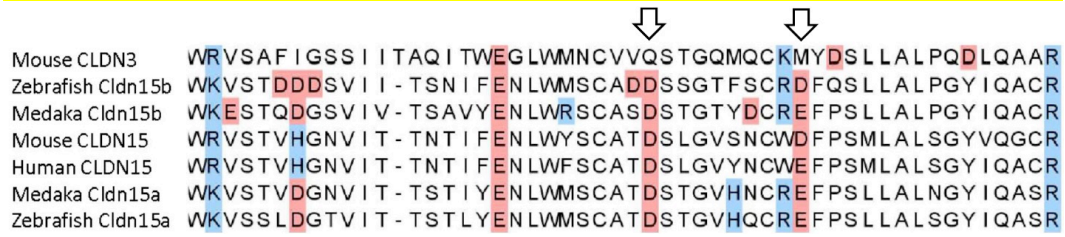

Figure 5.10 Alignment of the first extracellular loop of CLDN15 from human and mouse, and the orthologues from Japanese medaka and zebrafish shows that the residues critical to pore formation (D55 and D64) are found in both teleost Cldn15 paralogues. There are also differences from mammalian CLDN15, for example both medaka Cldn15a and Cldn15b have an R63 residue and Cldn15a an added H60. Amino acids are highlighted in red when acidic and in blue when basic. Arrows marks aspartic acids (D55 and D64), found to be important for cation and water pore function of CLDN15 (Günzel and Fromm, 2012; Günzel and Yu, 2013; Alberini et al., 2018; Samanta et al., 2018). Mouse CLDN3 has been classified as a barrier protein and included as a reference. Sequences used: Human CLDN15: Acc. No. NP_001172009; Mouse CLDN15: Acc. No. NP_068365; Mouse CLDN3: NP_034032; Medaka Cldn15a: XP_004079873; Medaka Cldn15b: XP_004076514; Zebrafish Cldn15a: NP_956698; Zebrafish Cldn15b: NP_001035404.

Based on the similarities to mammalian CLDN15 shown in Figure. 6.10, we hypothesized that the two medaka orthologs, *cldn15a* and *cldn15b,* share functional properties in terms of forming cation- and water pores and therefore may contribute to paracellular water absorption in SW medaka. In fishes (medaka (Bossus et al., 2015); salmon (Tipsmark et al., 2008; Tipsmark et al., 2010); zebrafish (Clelland and Kelly, 2010) and mammals (see Günzel and Yu, 2013) CLDN15 is expressed especially, but not exclusively, in the GI-tract. In Atlantic salmon, SW-acclimation was shown to induce elevated intestinal *cldn15a* mRNA expression (Tipsmark et al., 2010, and a different study in the same species documented higher transepithelial resistance in SW than FW intestine measured *ex vivo* (Sundell et al., 2003). Taken together, this seems counterintuitive if teleost Cldn15 paralogs like the mammalian orthologue form cation selective pores and thereby theoretically should *decrease* epithelial resistance rather than increase it. We did not find any effect of salinity on *cldn15a* mRNA levels in medaka. However, Na^+ and water fluxes through human CLDN15 was recently shown to inhibit each other and it is possible that physiological significance depends on the local chemical conditions which may be very different in FW and SW intestines. We found a roughly 100-fold decrease of the *cldn15b* paralog when fish are acclimated to SW which based on an expected possible role in creating a water-pore is somewhat surprising. The high FW expression level of this paralog suggests a specific role in the FW intestine, maybe related to Na^+/glucose cotransport or K^+ uptake from the diet. The interpretation of claudin data is not straightforward, because Cldn15 may interact with other proteins and Cldn paralogs when co-expressed in enterocytes (Garcia-Hernandez et al., 2017) and the properties and physiological significance may change depending on salinity and intestinal location. Expression of other intestinal Cldns should therefore be investigated in future studies.

5.5.3 Claudin-15 localization in the intestinal epithelium

To our knowledge this is the first study showing enterocyte tight junction claudin localization in a teleost fish. By using high-resolution fluorescence microscopy (figure 5.6, 5.7, 5.8, 5.9) we were able to demonstrate that Cldn15a and Cldn15b showed similar localization in the intestinal epithelium regardless of salinity. The use of Na^+,K^+-ATPase immunostaining to visualize baso-lateral membranes showed that parallel lateral membranes were slightly spaced between neighboring cells, thus creating the lateral intercellular space possibly involved in solvent drag (Sundell and Sundh, 2012). Discrete Cldn15 immunoreaction was seen apically to Na^+,K^+-ATPase immunoreaction, demarcating apical and baso-lateral membranes with no co-localization of the two antibodies. The antibodies gave some apparent non-specific staining of the brush border zone which had variable intensity between sections. It is possible that this is created by non-specific adsorption to the mucus layer in this area. Nonetheless, specific immunoreaction of both Cldn15 antibodies was restricted to a very narrow apical-most zone, below the brush-border and in direct extension from membranes bordering the lateral intercellular space. In cellular cross-sections at high resolution this appeared as an apical dot-like staining, and when viewed from above in a frontal section the pattern appeared as a circumcellular polygonal pattern, characteristic of epithelial tight junctions. This became particularly evident at higher magnification when using high-resolution STED microscopy. The localization is identical to that of CLDN-15 throughout the mouse intestine (Fujita et al., 2006) and that of occludin in the goldfish intestine (Chasiotis and Kelly, 2008) and strongly suggests its role as a tight junction protein. Despite their classification as tight-junction proteins, several other intestinal CLDNs (e.g. CLDN-1, -3, -4, -5 and -7) are localized further away from the apical zone in lateral and baso-lateral membranes in mammals (see Garcia-Hernandez et al., 2017). Based on the mRNA analyses, we expected to see

a significant down-regulation of *cldn15b* after SW-exposure, but we did not find any significant change in the localization and immunoreactivity of neither Cldn15 paralog. There was a trend that the "hot-spots" of claudin staining appeared more intense in SW-specimens, but it was not possible to quantify this (compare figure 5.6B, D with figure 5.7A, B). Unfortunately, the antibodies did not function for Western blots and further quantification efforts are not possible at present. Thus we conclude, that the Cldn15-based apical tight junction component is resilient to changes in salinity, suggesting that it may contribute to paracellular fluid transport.

5.6 Conclusion and perspectives

Drinking rate in FW medaka is exceptionally high though still increasing when fish are challenged with hyper-osmotic conditions. This suggests that the need for fluid absorption increases as dehydration threatens osmotic homeostasis. Several aquaporin isoforms are expressed in the medaka intestine (Madsen et al., 2014) but paradoxically the most abundant forms (Aqp1a, Aqp8ab and Aqp10 (Madsen et al., 2014)) are significantly down-regulated in SW, in parallel with the increased demand for fluid uptake. This led us to hypothesize that in medaka the paracellular pathway may be more important when fish move into a hyperosmotic environment. The present data does not reject this hypothesis but does not provide strong support either. Cldn15 paralogs make a significant constituent of the apical tight junction complex and may thereby create a paracellular water (and Na^+) leak pathway. However, there are no signs that this is reinforced during SW-acclimation.

The present study leaves behind a couple of questions: 1) What is the physiological significance of drinking in FW and is this water really absorbed in the intestine? 2) What is the significance of uncoupled transcript and protein dynamics with regard to the Cldn15b paralog? We have attempted to analyze unidirectional water fluxes across isolated gut segments *ex vivo* using

tritiated water as a tracer in an Ussing chamber setup, but so far, the data are inconclusive due to the fragility of the tissue. Future research in this area should pursue the functional aspects of water transport in this species by including *vivo* knock-down technology as well as analyses of luminal fluid chemical composition.

5.7 References

Alberini, G.; Benfenati, F.; Maragliano, L. Molecular dynamics simulations of ion selectivity in a claudin-15 paracellular channel. *J. Phys. Chem. B*. 2018, *122*, 10783-10792. DOI: 10.1021/acs.jpcb.8b06484

Angelow, S; Yu, A.S.L. Structure-function studies of claudin extracellular domains by cysteine-scanning mutagenesis. *J. Biol. Chem.* 2009, *284*, 29205-29217. DOI: 10.1074/jbc.M109.043752

Aoki, M.; Kaneko, T.; Katoh, F.; Hasegawa S.; Tsutsui, N.; Aida, K. Intestinal water absorption through aquaporin 1 expressed in the apical membrane of mucosal epithelial cells in seawater-adapted Japanese eel. *J. Exp. Biol.* 2003, *206*, 3495-3505. DOI: 10.1242/jeb.00579

Bagnat, M., Cheung, I.D., Mostov, K.E., Stainier, D.Y. Genetic control of single lumen formation in the zebrafish gut. *Nat. Cell Biol.* 2007, *9*, 954-960. DOI: 10.1038/ncb1621

Baltzegar, D.A.; Reading, B.J.; Brune, E.S.; Borski, R.J. Phylogenetic revision of the claudin gene family. *Mar. Genomics.* 2013, *11*, 17–26. DOI: 10.1016/j.margen.2013.05.001

Bossus, M.C.; Madsen, S.S.; Tipsmark, C.K. Functional dynamics of claudin expression in Japanese medaka (*Oryzias latipes*): Response to environmental salinity. *Comp. Biochem. Physiol.* 2015, *187A*, 74-85. DOI: 10.1016/j.cbpa.2015.04.017

Cerdá, J.; Finn, R.N. Piscine aquaporins: an overview of recent advances. *J. Exp. Zool.* 2010, *313A*, 623-650. DOI: 10.1002/jez.634

Chasiotis, H.; Kelly, S.P. Occludin immunolocalization and protein expression in goldfish. *J. Exp. Biol.* 2008, *211*, 1524-1534. DOI: 10.1242/jeb.014894

Clelland, E.S.; Kelly, S.P. Tight junction proteins in zebrafish ovarian follicles: stage specific mRNA abundance and response to 17-beta-estradiol, human chorionic gonadotropin, and maturation inducing hormone. *Gen. Comp. Endocrinol.* 2010, *168*, 388-400. DOI: 10.1016/j.ygcen.2010.05.011

Cutler, C.P.; Philips, C.; Hazon, N.; Cramb, G. Aquaporin 8 (AQP8) intestinal mRNA expression increases in response to salinity acclimation in yellow and silver European eels (*Anguilla anguilla*). *Comp. Biochem. Physiol.* 2009, *153A*, S78. DOI: 10.1016/j.cbpa.2009.04.047

Engelund, M.B.; Yu, A.S.L.; Li, J.; Madsen, S.S.; Færgeman, N.J.; Tipsmark, C.K. Functional characterization and localization of a gill-secific claudin isoform in Atlantic salmon. *Am. J. Physiol.* 2011, *302*, R300-R322. DOI: 10.1152/ajpregu.00286.2011

Engelund, M.B.; Madsen, S.S. Tubular localization and expressional dynamics of aquaporins in the kidney of seawater-challenged Atlantic salmon. *J. Comp. Physiol. B* 2015, *185B*, 207-223. DOI: 10.1007/s00360-014-0878-0

Fischbarg, J. Fluid transport across leaky epithelia: central role of the tight junction and supporting role of aquaporins. *Physiol. Rev.* 2010, *90*, 1271-1290. DOI: 10.1152/physrev.00025.2009

Fuentes, J.; Bury, N.R.; Carroll,S.; Eddy, F.B. Drinking in Atlantic salmon presmolts (*Salmo salar* L.) and juvenile rainbow trout (*Oncorhynchus mykiss* Walbaum) in response to cortisol and sea water challenge. *Aquaculture* 1996, *141*, 129-137. DOI: 10.1016/0044-8486(95)01222-2

Fuentes, J., Eddy, F.B. Drinking in marine, euryhaline and freshwater teleost fish. In *Ionic Regulation in Animals: A Tribute to Professor W.T.W. Potts;* Hazon, N.; Eddy, F.B., Flik G., Eds.; Springer, Berlin, Heidelberg. 1997, pp. 136-149.

Fujita, H.; Chiba, H.; Yokozaki, H.; Sakai, N.; Sugimoto, K.; Wada, T. Kojima, T.; Yamashita, T.; Sawada, N. Differential expression and subcellular localization of claudin-7, -8, -12, -13, and -15 along the mouse intestine. *J. Histochem. Cytochem.* 2006, *54*, 933-944. DOI: 10.1369/jhc.6A6944.2006

Garcia-Hernandez, V.; Quiros, M.; Nusrat, A. Intestinal epithelial claudins: expression and regulation in homeostasis and inflammation. *Ann. N.Y. Acad. Sci*. 2017, *1397*, 66-79. DOI: 10.1111/nyas.13360

Günzel, D.; Fromm, M. Claudins and other tight junction proteins. *Compr. Physiol*. 2012, *2*, 1819-1852. DOI: 10.1002/cphy.c110045

Günzel, D.; Yu, A.S.L. Claudins and the modulation of tight junction permeability. *Physiol. Rev.* 2013, *93*, 525-569. DOI: 10.1152/physrev.00019.2012

Grosell, M. Intestinal transport processes in marine fish osmoregulation. In: *Fish Osmoregulation*. Baldisserotto, B.; Mancera, J.M.; Kapoor B.G. (Eds.); Science Publishers, Enfield, New Hampshire. 2007, pp. 333-357.

Holmes, J.L., Van Itallie, C.M.; Rasmussen, J.E.; Anderson, J.M. Claudin profiling in the mouse during postnatal intestinal development and along the gastrointestinal tract reveals complex

expression patterns. *Gene Expr. Patterns* 2006, *6*, 581-588. DOI: 10.1016/j.modgep.2005.12.001

Hou, J.; Rajagopal, M.; Yu, A.S.L. Claudins and the kidney. *Annu. Rev. Physiol*. 2013, *75*, 479-501. DOI: 10.1681/ASN.2014030284

Hutchinson, S.; Hawkins, L.E. The influence of salinity on water balance in 0-group flounders, *Platichthys flesus* (L). *J. Fish Biol.* 1990, *36*, 751-764. DOI: 10.1111/j.1095-8649.1990.tb04329.x

Kaneko, T.; Hasegawa, S. Application of laser scanning microscopy to morphological observations on drinking in freshwater medaka larvae and those exposed to 80% seawater. *Fish. Sci*. 1999, *65*, 492-493. DOI: 10.2331/fishsci.65.492

Kim, Y.K.; Lee, S.Y.; Kim, B.S.; Kim, D.S.; Nam, Y.K. Isolation and mRNA expression analysis of aquaporin isoforms in marine medaka *Oryzias dancena*, a euryhaline teleost. *Comp. Biochem. Physiol.* 2014, *171A*, 1-8. DOI: 10.1016/j.cbpa.2014.01.012

Kwong, R.W.M.; Perry, S.F. The tight junction protein claudin-b regulates epithelial permeability and sodium handling in larval zebrafish, *Danio rerio*. *Am. J. Physiol.* 2013, *304*, R504–R513. DOI: 10.1152/ajpregu.00385.2012

Laforenza, U. Water channel proteins in the gastrointestinal tract. *Mol. Aspects of Med.* 2012, *33*, 642-650. DOI: 10.1016/j.mam.2012.03.001

Li, J.; Angelow, S.; Linge, A.; Zhuo, M.; Yu, A.S. Claudin-2 pore function requires an intramolecular disulfide bond between two conserved extracellular cysteines. *Am. J. Physiol.* 2013, *305*, C190-C196. DOI: 10.1152/ajpcell.00074.2013

Lin, L.Y.; Weng, C.F.; Hwang, P.P. Regulation of drinking rate in euryhaline tilapia larvae (Oreochromis mossambicus) during salinity challenges. *Physiol. Biochem. Zool.* 2001, *74*, 171-177. doi: 10.1086/319670

Loh, Y.H.; Christoffels, A.; Brenner, S.; Hunziker, W.; Venkatesh, B. Extensive expansion of the claudin gene family in the teleost fish, *Fugu rubripes*. *Genome Res.* 2004, *14*, 1248-1257. DOI: 10.1101/gr.2400004

Lu, Z.; Ding, L.; Lu, Q.; Chen, Y.H. Claudins in intestines. *Tissue Barriers* 2013, *1*, e24978. DOI: 10.4161/tisb.24978

Madsen, S.S.; Olesen, J.H.; Bedal, K.; Engelund, M.B.; Velasco-Santamaria, Y.M.; Tipsmark, C.K. Functional characterization of water transport and cellular localization of three aquaporin paralogs in the salmonid intestine. *Front. Physiol.* 2011, *2*, 56. DOI: 10.3389/fphys.2011.00056

Madsen, S.S.; Engelund, M.B.; Cutler, C.P. Water transport and functional dynamics of aquaporins in osmoregulatory organs of fishes. *Biol. Bull.* 2015, *229*, 70-92. DOI: 10.1086/BBLv229n1p70

Whittamore, J.M. Osmoregulation and epithelial water transport: lessons from the intestine of marine teleost fish. *J. Comp. Physiol.* 2012, *182B*, 1-39. DOI: 10.1007/s00360-011-0601-3

Madsen, S.S.; Bujak, J.; Tipsmark, C.K. Aquaporin expression in the Japanese medaka (*Oryzias latipes*) in freshwater and seawater: challenging the paradigm of intestinal water transport? *J. Exp. Biol.* 2014, *217*, 3108-3121. DOI: 10.1242/jeb.105098

Marshall, W.S.; Grosell, M. Ion transport, osmoregulation, and acid-base regulation. In *The Physiology of Fishes*; Evans, D.H., Clairborne, J.B., Eds.; Taylor and Francis Group: Boca Raton, FL, USA, 2006, pp. 177-210.

Martinez, A. S.; Cutler, C.P.; Wilson, G.D.; Phillips, C.; Hazon, N.; Cramb, G. Cloning and expression of three aquaporin homologues from the European eel (*Anguilla anguilla*): effects of seawater acclimation and cortisol treatment on renal expression. *Biol. Cell.* 2005, *97*, 615-627. DOI: 10.1042/BC20040111

Perrott, M.N.; Grierson, C.E.; Hazon, N.; Balment, R.J. Drinking behaviour in sea water and fresh water teleosts, the role of the renin-angiotensin system. *Fish Physiol. Biochem*. 1992, *10*, 161-168. DOI: 10.1007/BF00004527

Rosenthal, R.; Milatz, S.; Krug, S.M.; et al. Claudin-2, a component of the tight junction, forms a paracellular water channel. *J. Cell Sci*. 2010, *123*, 1913-1921. DOI: 10.1242/jcs.060665

Rosenthal, R.; Gunzel, D., Piontek, J.; et al. Claudin-15 forms a water channel through the tight junction with distinct function compared to claudin-2. *Acta Physiol. (Oxf)*. 2019, *12*, e13334. DOI: 10.1111/apha.13334

Samanta, P.; Wang, Y., Fuladi, S., et al. Molecular determination of claudin-15 organization and channel selectivity. *J. Gen. Physiol*. 2018, *150*, 949-968. DOI: 10.1085/jgp.201711868

Sundell, K.; Jutfelt, F.; Agustsson, T.; Olsen, R.E.; Sandblom, E.; Hansen, T.; Bjornsson, B.T. Intestinal transport mechanisms and plasma cortisol levels during normal and out-of-season parr–smolt transformation of Atlantic salmon, *Salmo salar*. *Aquaculture* 2003, *222*, 265-285. DOI: 10.1016/S0044-8486(03)00127-3

Sundell, K.S.; Sundh, H. Intestinal fluid absorption in anadromous salmonids: importance of tight junctions and aquaporins. *Front. Physiol.* 2012, *3*, 388. DOI: 10.3389/fphys.2012.00388

Suzuki, H., Nishizawa, T., Tani, K., et al. Crystal structure of a claudin provides insight into the architecture of tight junctions. *Science*. 2014, *344*, 304-307. DOI: 10.1126/science.1248571

Tamura, A.; Kitano, Y., Hatam M., et al. Megaintestine in claudin-15 deficient mice. *Gastroenterology* 2008, *134*, 523-534. DOI: 10.1053/j.gastro.2007.11.040

Tamura, A.; Hayashi, H.; Imasato, M.; et al. Loss of claudin-15, but not claudin-2, causes Na+ deficiency and glucose malabsorption in mouse small intestine. *Gastroenterology* 2011, *140*, 913-923. DOI: 10.1053/j.gastro.2010.08.006

Tipsmark, C.K.; Kiilerich, P.; Nilsen, T.O.; Ebbesson, L.O.E.; Stefansson, S.O.; Madsen, S.S. Branchial expression patterns of claudin isoforms in Atlantic salmon during seawater acclimation and smoltification. *Am. J. Physiol.* 2008, *294*, R1563-R1574. DOI: 10.1152/ajpregu.00915.2007

Tipsmark, C.K.; Sørensen, K.J.; Hulgard, K.; Madsen, S.S. Claudin-15 and-25b expression in the intestinal tract of Atlantic salmon in response to seawater acclimation, smoltification and hormone treatment. *Comp. Biochem. Physiol.* 2010, *155A*, 361-370. DOI: 10.1016/j.cbpa.2009.11.025

Tipsmark, C.K.; Sørensen, K.J.; Madsen, S.S. Aquaporin expression dynamics in osmoregulatory tissues of Atlantic salmon during smoltification and seawater acclimation. *J. Exp. Biol.* 2010B, *213*, 368-379. DOI: 10.1242/jeb.034785

Tytler, P.; Tatner M.; Findlay, C. The ontogeny of drinking in the rainbow trout, *Oncorhychus mykiss*. *J. Fish Biol.* 1990, 36, 867-875. DOI: 10.1111/j.1095-8649.1990.tb05634.x

Usher, M.L.; Talbot, C.; Eddy, F.B. Drinking in Atlantic salmon smolts transferred to seawater and the relationship between drinking and feeding. *Aquaculture* 1988, *73*, 237-246. DOI: 10.1016/0044-8486(88)90058-0

Chapter 6 Appendix

MEMORANDUM

TO: Dr. Christian Tipsmark

FROM: Craig N. Coon, Chairman
Institutional Animal Care and Use Committee

DATE: June 26, 2014

SUBJECT: IACUC APPROVAL
Expiration date: June 25, 2017

The Institutional Animal Care and Use Committee (IACUC) has APPROVED your protocol 14042: "Regulation of Epithelial Transport in Japanese Medaka".

In granting its approval, the IACUC has approved only the information provided. Should there be any further changes to the protocol during the research, please notify the IACUC in writing(via the Modification form) prior to initiating the changes. If the study period is expected to extend beyond June 25, 2017 you must submit a new protocol. By policy the IACUC cannot approve a study for more than 3 years at a time.

The IACUC appreciates your cooperation in complying with University and Federal guidelines involving animal subjects.

CNC/aem

cc: Animal Welfare Veterinarian

UNIVERSITY OF ARKANSAS

Office of Research Compliance

To:	Christian Tipsmark
Fr:	Craig Coon
Date:	September 5th, 2017
Subject:	IACUC Approval
Expiration Date:	December 31st, 1969

The Institutional Animal Care and Use Committee (IACUC) has APPROVED your protocol # **17091:** *Regulation of epithelial transport function in Japanese medaka*.

In granting its approval, the IACUC has approved only the information provided. Should there be any further changes to the protocol during the research, please notify the IACUC in writing (via the Modification form) prior to initiating the changes. If the study period is expected to extend beyond December 31st, 1969 you can submit a modification to extend project up to 3 years, or submit a new protocol. By policy the IACUC cannot approve a study for more than 3 years at a time.

The following individuals are approved to work on this study: Christian Tipsmark, Laura Ellis, Rebecca Bollinger, Julie Stanley, Hannah Weber, and Saxyam Gautam. Please submit personnel additions to this protocol via the modification form prior to their start of work.

The IACUC appreciates your cooperation in complying with University and Federal guidelines involving animal subjects.

CNC/tmp